ABSTRACT

IKIZ, YUKSEL. Fiber Length Measurement by Image Processing. (Under the direction of Dr. Jon P. Rust.)

This research studied the accuracy and feasibility of cotton fiber length measurement by image processing as an alternative to existing systems. Current systems have some weaknesses especially in Short Fiber Content (SFC) determination, which is becoming an important length parameter in industry.

Seventy-two treatments of five factors were analyzed for length and time measurements by our own computer program. The factors are: Sample preparation (without fiber crossover and with fiber crossover), lighting (backlighting and frontlighting), resolution (37-micron, 57-micron, 106-micron, and 185-micron), preprocessing (4-neighborhood and 8-neighborhood), and processing (outlining, thinning, and adding broken skeletons).

The best results in terms of accuracy, precision and analysis time for images without fiber crossovers were: 106-micron resolution with frontlighting using an 8-neighborhood thresholding algorithm and using an outline algorithm for length determination. With fiber crossovers, 57-micron resolution with backlighting using an 8-neighborhood thresholding algorithm and using a thinning algorithm combined with an adding algorithm for combining broken skeletons. Using the above conditions, 1775 cm^2 area can be analyzed using our current equipment in 15 seconds. In the case of images with crossovers, only 117 cm^2 can be analyzed in 15 seconds.

This research demonstrates that successful sample preparation without fiber crossovers would create the best fiber length measurement technique, however with fiber crossovers the system efficiency has been proven as well.

Fiber Length Measurement

by Image Processing

by

Yuksel Ikiz

A dissertation submitted to the Graduate Faculty of
North Carolina State University
in partial fulfillment of the
requirements for the Degree of
Doctor of Philosophy

FIBER AND POLYMER SCIENCE

Raleigh

2000

APPROVED BY:

_____ _____

_____ _____

Chair of Advisory Committee

DEDICATION

Canlarim, sevgili anneme ve babama

BIOGRAPHY

Yuksel Ikiz, the third child of Bekir and Hacer Ikiz, was born in March, 1966 in Zagoriceno, Bulgaria. He migrated to his motherland Turkey in 1968. He earned a Bachelor of Science Degree in Textile Engineering at Uludag University, Bursa-Turkey. After teaching two years in Edirne Vocational High School, he was awarded with a government scholarship for language, Master and PhD education overseas. After receiving his Master of Science Degree in Textile Engineering at Philadelphia College of Textiles and Science (currently Philadelphia University), he enrolled in the PhD program of Fiber and Polymer Science at North Carolina State University in 1996. He was married to Jaruthip Sudhirakuljai from Bangkok-Thailand, on May 24, 1999. His future position will be in Pamukkale University, Denizli-Turkey as a researcher and teacher.

ACKNOWLEDGMENTS

I wish to express my deep appreciation to Dr. Rust, my major advisor, for his encouragement, guidance, and support throughout every phase of this research. Whenever I had a problem, his help was right there for me as an advisor and as a friend. I want to give special thanks to Dr. Trussell, my minor representative, for his valuable advice and determination. He read each sentence carefully and questioned each fuzzy point, which resulted in a better final product.

My sincere thanks to Dr. Barnhardt, former Dean of College of Textiles, for his genuine interest and advice. I am grateful to Dr. Jasper for his help, support and discussions. I also thank Dr. Pourdeyhimi for his advice and the use of his equipment.

Finally, my deepest thanks to my best friend and wife, Jaruthip, for her support, care, patience and love.

TABLE OF CONTENTS

LIST OF TABLES

LIST OF FIGURES

1. INTRODUCTION

Staple length is one of the most important properties of cotton fibers in both marketing and processing. A premium is paid for longer length. Length is related to other cotton fiber characteristics such as strength, fineness, maturity and evenness. Longer fibers are generally stronger, finer and more uniform than shorter fibers. A few parameters affected by staple length during spinning are production efficiency, amount of waste, fly generation and cleaning. Yarn quality parameters such as strength, elongation, hairiness, and evenness are strongly correlated to the length of cotton fibers. Therefore, it is very important for fiber producers, ginners and spinners to be able to accurately measure the length distribution of cotton fiber.

For practical reasons, a single number designation of staple length is desired to represent a whole population of fibers. However, a remarkably uniform length distribution in seed cotton becomes highly variable and impossible to represent with a single number after processing because of fiber breakage. Besides, yarn formation requires unique length distribution characteristics in different processes. The best drafting roller settings are closely related to the longest fibers. Shorter roller settings can cause excessive fiber breakage. On the other hand, longer roller settings can cause more unevenness in the yarn. Mean length is the best indicator of yarn evenness while short fiber content determines prominently the amount of waste.

Because different yarn characteristics and spinning parameters are affected by different aspects of the length distribution, a family of length parameters has been developed over the years. Classer Staple Length, Effective Length, Mean length (ML), Upper Half Mean Length (UHML), Upper Quartile Length (UQL), Span Length,

Uniformity Index (UI), Uniformity Ratio (UR), Short Fiber Content (SFC) are the most common length distribution parameters.

Until recently, short fiber content (SFC) was ignored. The quantity of SFC was not indicated in length measurements and was not considered in machine settings. Research has shown that a high SFC could cause appreciable increase in waste, excessive unevenness in roving, more ends-down in spinning and weaker yarns. The weight of SFC is not nearly as significant as the number of short fibers, therefore, most length measurement values which depend on weight are insensitive to the relative importance of SFC. Now the industry is becoming more concerned about SFC and often demands to see SFC as an independent measured parameter.

There are a number of commercial length measurement techniques, each with inherent advantages and disadvantages. The Suter-Webb fiber array method is considered the most accurate although it is slow and expensive. Fibrograph, Peyer, HVI and AFIS systems have been developed for fast measurements, but they are not as accurate as Suter-Webb. Considerable research has been conducted to test the accuracy of these methods and usually questions remain as to whether these systems are satisfactorily precise. In addition, industry is becoming more demanding in the desire to measure SFC, which is the weakest point of the existing systems. All methods have adapted a SFC measurement unit, still, the problem remains that none are accurate enough to satisfy industry. Simply, existing systems cannot accurately and reproducibly measure SFC.

Technological developments in image capturing and image analysis, and computer processing speeds open new horizons for measurement techniques. Many fiber

properties can be measured by image processing such as color, yellowness, trash content, diameter, and maturity. However, fiber length measurement has not been implemented yet. The hypothesis for this work is that current vision and computing technology is mature enough to accomplish this task. The subject of this study is “measurement of fiber length distribution using image analysis”.

2. LITERATURE REVIEW

2.1. INTRODUCTION OF LENGTH

2.1.1. Variability

In a bale of cotton there are approximately 65 billion fibers in the range of 1/32 inch to 2 inches in length. Relatively little variation in seed cotton fiber length becomes great after ginning because of fiber breakage. Mechanical ginning decreases the fiber mean length by several mm and the percentage of fibers shorter than 13 mm increases to 6 to 8 times the corresponding value for hand-ginned cotton [33]. Completely hand ginning cotton samples have approximately 4% by weight SFC [101]. Each broken fiber in ginning makes at least two short ones and, in the bale, the fiber length distribution becomes far more variable than the seed cotton. Excessive fiber length variation within a particular cotton sample tends to increase manufacturing waste and drop spinning efficiency while decreasing yarn quality. The coefficient of variation is a relative measure of the fiber length variation. The larger the value, the greater the variation in fiber lengths. USDA rates fiber length variation in cotton as follows:

Table 2.1: Cotton variability classification [49].

Array coefficient of length variation	Classification
<26	Very low variation
26-29	Low variation
30-33	Average variation
34-37	High variation
>37	Very high variation

To represent the fiber distribution accurately, many fiber measurements are required. Obviously, more measurements yield more accuracy, however, for practical reasons this number is limited. A minimum number of measurements for satisfactory accuracy can be determined by statistical methods. Koshal and Turner [55] tried to find

the satisfactory number of samples and the degree of reliability of the results obtained by individual fiber length measurements. They measured 3,000 single fibers and obtained a frequency distribution, which was practically symmetrical and approximately normal. They found the standard deviation (σ) to be 0.4986 and coefficient of variation to be 21% for 3,000 tests. Using a 50% confidence level they calculated the probable error of the mean as follows:

$$\text{Probable Error Of Mean} = 0.67449 \times \left(\frac{\sigma}{\sqrt{n}}\right) \qquad \textbf{Equation 2.1}$$

This equation can be adapted for percent error, using CV% (Coefficient of Variation which is the ratio of standard deviation to mean value), as follows:

$$\text{Percent Error} = Z \text{ x } \frac{\text{CV\%}}{\sqrt{n}} \qquad \textbf{Equation 2.2}$$

Using equation 2.2 percent error was calculated for different cottons. Table 2.2 shows percentage of errors of normal distribution for cottons of different length CV% for different confidence levels. It shows that the confidence interval for a sample of 1,000 fiber length measurements with a normal distribution and a 30% CV is +/-1.86 of the mean length for the 95% confidence level.

Table 2.2: Percentage errors of normal distribution.

	95% confidence level			99% confidence level			99.9% confidence level		
# of Fibers	CV% 20	CV% 30	CV% 40	CV% 20	CV% 30	CV% 40	CV% 20	CV% 30	CV% 40
200	2.772	4.158	5.544	3.649	5.474	7.298	4.653	6.980	9.306
400	1.960	2.940	3.920	2.580	3.870	5.160	3.290	4.935	6.580
600	1.600	2.400	3.200	2.160	3.159	4.212	2.686	4.029	5.372
800	1.386	2.079	2.772	1.824	2.736	3.648	2.326	3.489	4.652
1000	1.240	1.860	2.480	1.632	2.448	3.264	2.081	3.121	4.162
2000	0.876	1.314	1.752	1.154	1.731	2.308	1.471	2.206	2.942
3000	0.716	1.074	1.432	0.942	1.413	1.884	1.201	1.801	2.402
5000	0.554	0.831	1.108	0.730	1.095	1.460	0.930	1.395	1.860
10000	0.392	0.588	0.784	0.516	0.774	1.032	0.658	0.987	1.316

Z value is found for 95%, 99%, and 99.9% confidence level respectively 1.96, 2.58, and 3.29 [70]. According to Zurek, Bartos and Konecki [118], if the number of cotton fibers in the sample is greater than 200, the variation of linear mass does not exceed +/-5%. Precision depends on the number of specimens analyzed for each cotton sample and the number of fibers measured. The variance estimation depends on fiber-to-fiber and sample-to-sample variances and is calculated as follows [21]:

$$\sigma_s^2 = \frac{\sigma_B^2}{J} + \frac{\sigma_E^2}{JK} \qquad \textbf{Equation 2.3}$$

σ_s^2 = variance estimation

σ_E^2 = variance between fibers

σ_B^2 = variance between samples

J = number of specimens anaylzed per cotton

K = number of fibers analyzed per specimen

However, this variability is not only limited from fiber to fiber in a bale but practically, from bale to bale, too. Lord [69] studied the variability of cotton between bales and within bales. He found the CV% within bales for upper half mean length 1.2% and for SFC 15%; between bales he found CV% of upper half-mean 1.3% and for SFC 15.5%.

It is often assumed that an inter laboratory variation (CV) of 5% or less is required for a test to be internationally acceptable [50]. Lewicki, Faia, Fairley and Robles [67] investigated the inter-laboratory sources of variability and conducted an experiment to partition variability between the sources of laboratory, instrument and sample. They found that more than half of the variation for length and length uniformity originates within the sample.

Table 2.3: Percentages of length variances from full data set attributable to between lab, instrument and sample variability [67].

BALE	AVG.	% OF VARIABILITY		
		LAB	INSTR.	SAMPLE
1	0.959	1.08	29.38	69.54
2	1.163	0.00	44.96	55.04
3	1.021	31.52	17.32	51.16
4	1.075	25.35	14.18	60.48
5	1.116	22.02	25.01	52.97

Table 2.4: Percentages of uniformity variances from full data set attributable to between lab, instrument and sample variability [67].

BALE	AVG.	% OF VARIABILITY		
		LAB	INSTR.	SAMPLE
1	79.3	0.00	22.24	77.76
2	84.0	3.24	34.36	62.41
3	80.7	0.00	21.77	78.23
4	82.5	1.87	18.50	79.62
5	82.3	11.29	30.54	58.17

USDA conducted a project to indicate laboratory-to-laboratory reproducibility of fiber property measurements for the 1992 through 1995 crop years. For this reason, cooperators were sent random cotton samples by USDA and each cooperator used its own high volume instrument or instruments when conducting the testing and followed its own procedures for sample conditioning, instrument calibration and sample testing. Reproducibility percentages for each crop year were determined by single test and module average methods. Results were represented as in Figure 2.1 and Figure 2.2 [110]. This data shows that length reproducibility for a single test is only a little over 60% while for a module average it is close to 75%.

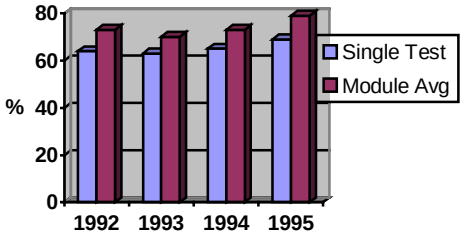

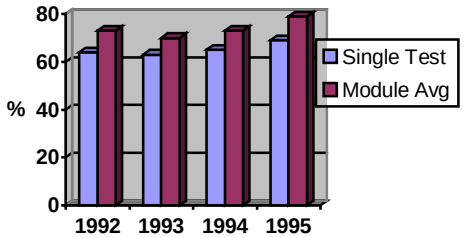

Figure 2.1: Length reproducibility (+/-0.02 inches) **Figure 2.2: Uniformity reproducibility (+/-1.0 %)**

Requirements for higher precision and lower standard deviations of test results have been established from time-to-time by the USDA. While requirements for precision have increased, the number of samples per bale has decreased with the same precision expectations (Table 2.5).

Table 2.5: USDA standard deviation requirements [36].

Property	1986	Tests per sample	1993	Tests per sample
Length (inch)	0.016	4	0.012	2
Uniformity (%)	1.1	4	0.80	2

2.1.2. Length Distribution

The length of a cotton sample can only be fully described by its fiber length distribution. To make comparisons, a number of different numerical parameters are derived from the length distribution. About ten parameters defined in the next chapter have practical applications and specific uses. If a sample of fibers is sorted into common length groups onto a velvet board, the velvet board shows the staple length distribution of the sample as in Figure 2.3.

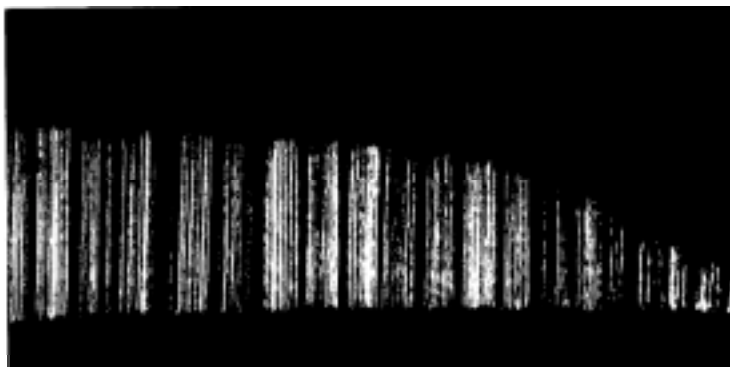

Figure 2.3: Staple diagram [106]

Since it is very difficult and time consuming to measure the length of each individual fiber, most test methods and instruments for fiber length analysis measure the length and weight of each group of fibers generally classified in 0.125 inch intervals.

Fiber length characteristics can then be obtained from the lengths and weights of the fiber groups. The weight fraction of each length group plotted against the length of the group gives a weight-length distribution. If, however, the number of fibers in each length group is determined by counting, and then the number fraction of each length group is plotted against length; a number-length distribution is obtained. This distribution may also be obtained directly from the weight-length distribution by multiplying the weight fraction by the fiber weight under the assumption of fiber length and fiber fineness independence. However, this assumption can cause a small amount of error in the results, because it is a well known fact that cotton containing immature short fibers has a lower percentage of short fibers by weight than one having the same length distribution of mature fibers. On the other hand, estimates of short fibers on a weight basis are necessarily less sensitive to real variation in short fiber content than estimates made on a number basis [82]. Figure 2.4 shows weight-length and number-length distributions of the given ASTM sample [3].

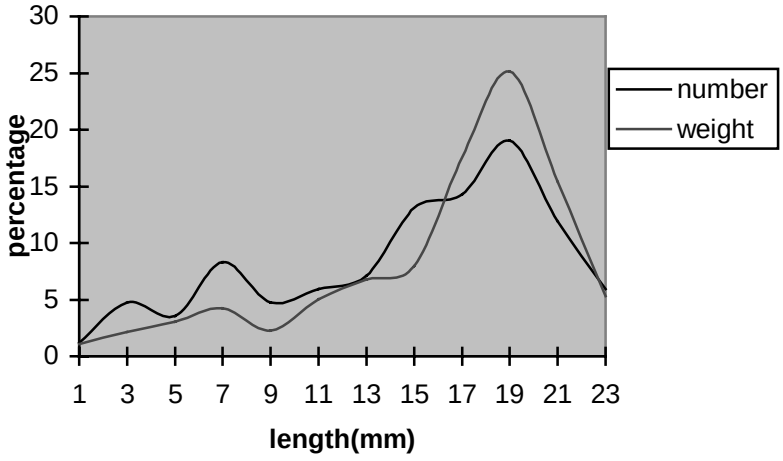

Figure 2.4: Weight-Length and Number-Length Distributions [3]

These functions are called frequency distribution functions and denoted $f_n(l)$ for Simple Numerical Frequency Function (number-length distribution) and $f_w(l)$ for

Frequency Function by Weight (weight-length distribution) [114]. It shows the probability that a fiber of a population has a length between l and $l + dl$. The cumulative distribution function or staple function or survivor diagram $S_n(l)$ is the integral of $f_n(l)$. It is the proportion of the number of fibers longer than x (equation 2.4).

$$S_n(x) = \int_x^{\infty} f_n(l)dl \qquad \textbf{Equation 2.4}$$

It has also a graphical interpretation. If the fibers of the population were laid horizontally and equally spaced with their left ends on the vertical axis and in order of their lengths, the right ends of the fibers would form the staple function. The same relationship can be derived for weight distributions (equation 2.5).

$$S_w(x) = \int_x^{\infty} f_w(l)dl \qquad \textbf{Equation 2.5}$$

If the randomly selected fibers are arranged with their catching points as in Figure 2.5, rather than their left ends, along the vertical axis, their right ends form the fibrogram function. The fibrogram is basically a representation of the various span lengths in a fiber population. The ordinate to a point on the Fibrogram (F(x)) gives the relative number of fibers spanning the distance represented by the abscissa of that point. This is the original theory of Hertel [46] developed for the Fibrograph optical instrument in 1940. In the original interpretation, the fibrogram's theoretical equivalent was denoted r(l).

$$r(l) = F(x) = \int_x^{\infty} S_n(l)dl \qquad \textbf{Equation 2.6}$$

This type of sample can be prepared by catching the fibers in a holding device, combing to remove unheld fibers and to make parallel the held fibers, and brushing to smooth the fiber specimen and remove crimp from the clamped fibers as in Figure 2.5.

Fibers are caught in the holding device in proportion to their relative lengths and in proportion to their relative numbers in the fiber mass. For example, a one-inch fiber is twice as likely to be caught in the holding device than is a one-half inch fiber.

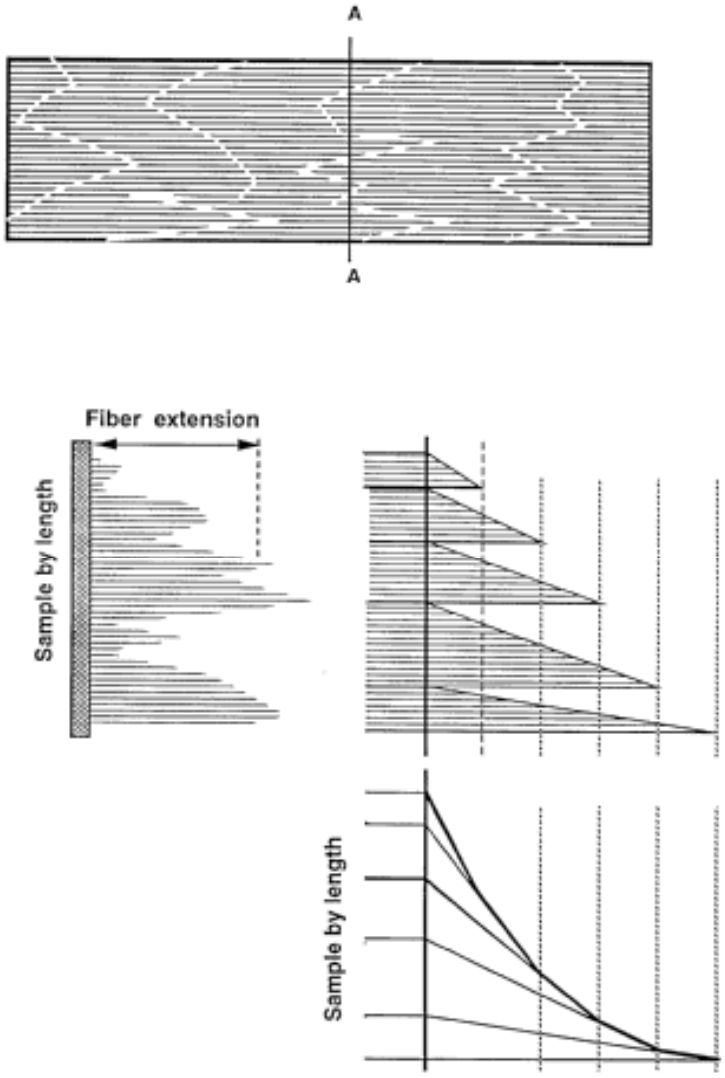

Figure 2.5: Random caught fibers and fibrogram curve [100].

The practical aspects of the fibrogram are revealed when it is recognized that, in converting fibers into yarn, at any instant of time those fibers caught by rollers or aprons and extending into machinery draft zones are in a fibrogram configuration as in Figure

2.6. Ideally, each fiber will extend a different distance away from the clamp line. Exposed fiber segments will have different lengths even if all fibers have the same end-to-end length. Consequently, expressions of fiber length and fiber length distribution extracted from the

fibrogram, in graphical form, are most useful in associating fiber length to fiber behavior in staple fiber yarn spinning processes.

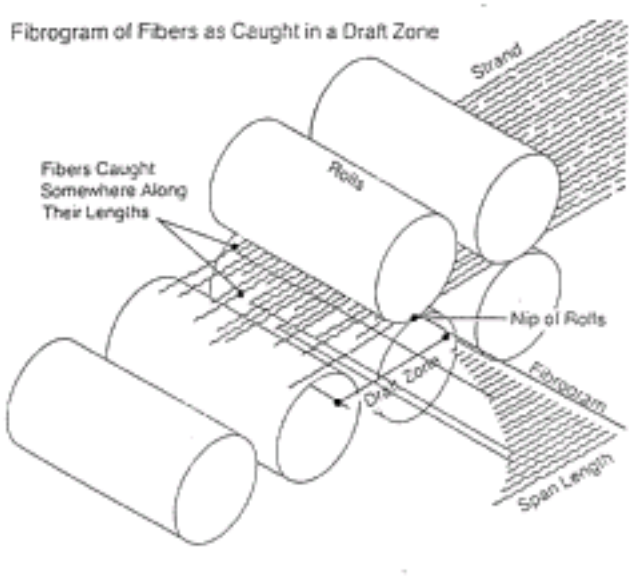

Figure 2.6: Fibrogram of fibers as caught in a draft zone [97].

Hertel [46] showed that by theory, a tangent from the origin of the vertical (amount) axis intercepted the horizontal (length) axis at the mean length. This must be true because the greatest ordinate of $F(x)$ is L, the mean length,

$$F(x) = \int_0^\infty S_n(l)dl = l(0) = L \qquad \textbf{Equation 2.7}$$

and since $dF/dl = -S(l)$ and $S(0)$ is unity, the tangent at $l = 0$ must have a slope of –1, and hence intercept the length axis at L.

Landstreet [65] described the basic ideas of fibrogram theory starting from a frequency diagram and establishing geometrical and probabilistic interpretations for single fiber length, two different fiber lengths, three different fiber lengths and multiple fiber length populations. Krowicki, Hemstreet and Duckett [62, 63] applied a new approach to generate the fibrogram from the length-array data similar to the Landstreet method. They assumed a random catching and holding of fibers within each of the length groups generating a triangular distribution by relative weight for each length group. They found that differences become negligible between the Landstreet method and the new method when the constants are carried to five significant digits during calculation and the new method simplifies fibrogram generation.

Krowicki and Duckett [57] reversed the Landstreet method and showed that, theoretically; the proportionate mass of fibers, the mean length by number, the proportionate number of fibers, the number probability array, the mass probability array, and the mean length by mass of a sample can be obtained from the fibrogram. Later, Krowicki, Thibodeaux and Duckett [60] practically generated these numbers from the fibrogram and concluded a minimum of four significant digits of fibrogram data is required for good estimations.

Prier and Sasser [83] discussed the feasibility of the Hertel's [46] r(L) value, which is the proportion of the area for fibers longer than a certain value to the total area. They offered proportionality by number instead of proportionality by weight to base the model when building the fibrogram. They also derived that the average length is equal to twice the area under the fibrogram curve by number. Later, Tallant and Pittman [104]

showed that the average length should be equal to twice the area under the fibrogram curve by weight.

Chu and Riley [22] investigated the length distribution of fibers sampled with the Fibrosampler and found it almost identical to that of the fibers in their original form. They concluded that fibers were sampled in clumps rather than individually and made an assumption that all fibers have an equal probability to be caught. Thus, the fiber length distributions will be the same for both the original fiber sample and the fiber beard.

The beard function, $B(x)$, is the integral of the fibrogram:

$$B(x) = \int_{x}^{\infty} F(l)dl \qquad \textbf{Equation 2.8}$$

These functions are used in practice both by number and weight. The beard function and fibrogram can be explained in non-dimensional forms called normalized functions by dividing each function by its initial value at x=0. Thus, the normalized fibrogram, $G(x)$, is defined as:

$$G(x) = \frac{F(x)}{F(0)} \qquad \textbf{Equation 2.9}$$

and the normalized beard function, $Z(x)$, is defined as:

$$Z(x) = \frac{B(x)}{B(0)} \qquad \textbf{Equation 2.10}$$

These four functions, $f(x)$, $S(x)$, $F(x)$ and $B(x)$ are different orders of distribution functions of the same type (Figure 2.7). Practical fiber length and length distribution values are derived from these functions using different orders for different systems.

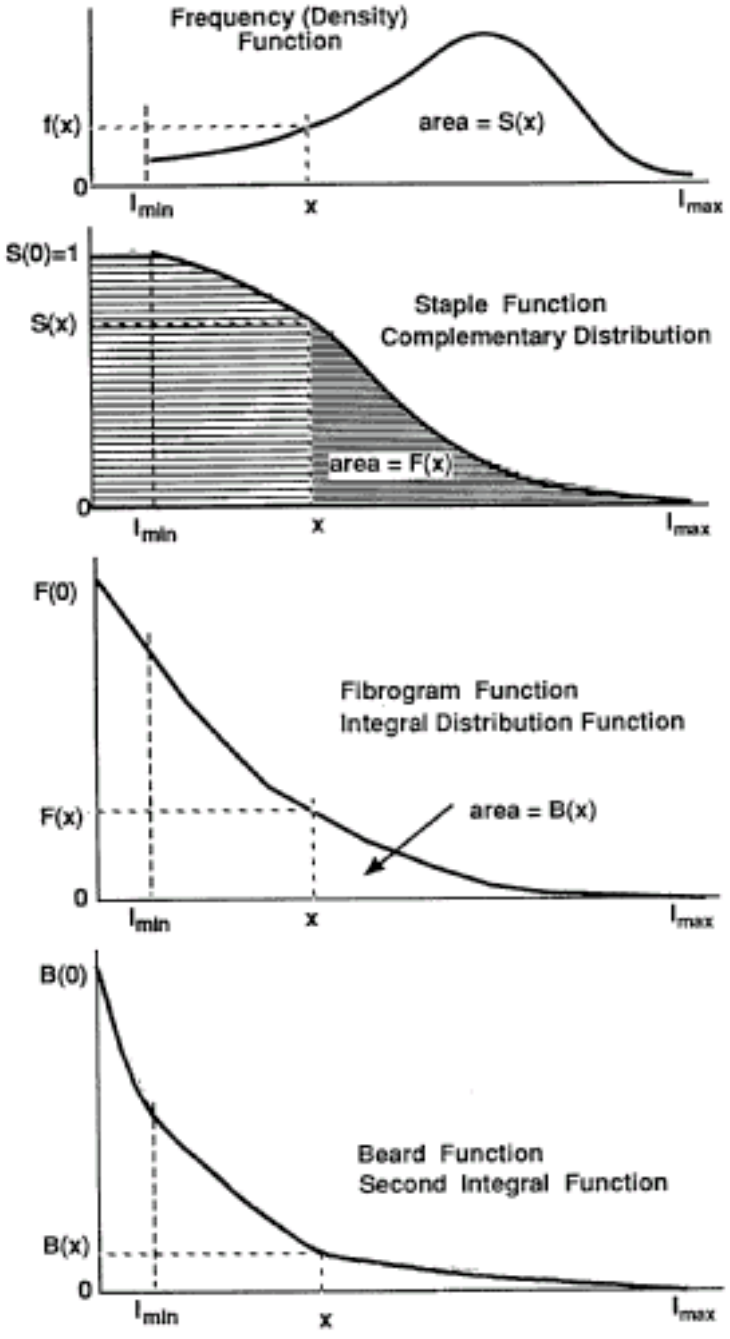

Figure 2.7: Frequency diagram, staple diagram, fibrogram, and beard diagram (Reproduced [100]).

2.1.3. Definitions

For practical reasons, a single number designation of fiber length and length distribution is desirable. The fact is that different aspects of a length distribution are important for different reasons. In addition, high sample variation and different

measurement techniques have the result that more than one parameter be desired from a length distribution. Most of the following parameters are being used practically in buying and processing cotton fibers.

2.1.3.1. Staple Length (STPL)

According to the USDA (United States Department of Agriculture), "The length of staple of any cotton shall be the normal length by measurement, without regard to quality or value, of a typical portion of its fibers under a relative humidity of the atmosphere of 65 percent and a temperature of 70° F [106]".

Staple length depends substantially on the nature of the long end of the fiber distribution and is influenced by other parameters. Up to the last 10 to 20 years, a subjective estimate of length was made by only hand and eye judgment. This is the length of a typical portion of the fibers in the sample as determined by the classer in comparison with official standards. The classer would pull a tuft of fibers from the sample and by a process of lapping, pulling, and discarding, would make parallel a typical portion of the fibers to compare with the standards. In the USA, the USDA office establishes these standards. The first official standards for staple length were promulgated in 1918 and revised and changed from time to time [106]. The classers were free to apply their own way for sampling as long as they were consistent with the standards, however, the most frequently used method is described in USDA publications [23, 106].

The staple length of a number of cottons and their physical description according to Hunter [49] is showing in Table 2.6.

Table 2.6: Cotton classification according to staple length [49].

Staple length		Description
(mm)	(inches)	
<20.6	<26/32	Short
20.6-25.4	26/32-32/32	Medium
26.2-27.8	33/32-35/32	Medium long
28.6-33.3	36/32-42/32	Long
>34.9	>44/32	Extra long

2.1.3.2. Mean Length (ML)

ASTM defines the mean length as "In testing of cotton fibers, the average length of all fibers in the test specimen based on weight-length data [2]." As an alternative, the mean length can be calculated by number-length data, too, and it is acknowledged to be the most important in engineering the yarn [118]. The mean length by number (ML_n) and by weight (ML_w) are calculated as shown in equations 2.11 and 2.12.

$$ML_n = \int_0^\infty l f_n(l) dl \qquad \textbf{Equation 2.11}$$

$$ML_w = \int_0^\infty l f_w(l) dl \qquad \textbf{Equation 2.12}$$

Depending on the type of cotton, there exist different relationships between these two lengths. The number-length data tend to emphasize the short fibers in the sample, whereas weight-length data tend to hide them. Cui, Calamari and Suh [27] statistically analyzed whether fiber length by weight and by number gives the same rank order when comparing cotton fiber length distributions. They showed that ML_w is always greater than ML_n with the assumption that fiber length and linear density are statistically independent. However, SFC and UQL by number and by weight may give opposite rank orders.

2.1.3.3. Upper-Quartile Length (UQL)

ASTM defines the Upper-Quartile length as "In testing of cotton fibers that length which is exceeded by 25% of the fibers by weight in the test specimen [2]". As we mentioned above, UQL by weight is not always greater than UQL by number. Cui, Calamari and Suh [27] found that 8.33% of measurements gave opposite ranks. $S_n(UQL_n)$ is the Upper-Quartile length by number and can be calculated as in equation 2.13. Similarly, $S_w(UQL_w)$ is the Upper-Quartile length by weight and can be calculated as in equation 2.14.

$$0.25 = S_n(UQL_n) = \int_{UQL_n}^{\infty} f_n(l)dl \qquad \textbf{Equation 2.13}$$

$$0.25 = S_w(UQL_w) = \int_{UQL_w}^{\infty} f_w(l)dl = \frac{1}{ML_n}\int_{UQL_w}^{\infty} lf_n(l)dl \qquad \textbf{Equation 2.14}$$

Table 2.7: Cotton classification according to UQL [49].

Upper quartile length	Classification
<27.9 mm	Short
27.9 mm to 31.5 mm	Medium
31.8 mm to 35.3 mm	Long
>35.3 mm	Extra long

2.1.3.4. Effective Length

Effective length is longer than the average length and is a measure of the length of the majority of the longer fibers in the sample [49]. Effective length may be defined statistically as the upper quartile of the fiber length distribution curtailed below the value equal to half the effective length [111]. Thus, the effective length is more independent of the tail of short fibers than is the upper quartile of the complete fiber. According to Woo [111] the effective length is equal to 0.859 of the maximum length in the sample.

Figure 2.8 shows a graphical representation of effective length where OQ is one half of OA, PP' is parallel and equal to OQ, OK is one quarter of OP, a parallel to OA from K to the staple diagram is KK'. KS is one half of KK', RR' is parallel and equal to KS, OL is one quarter of OR, and a parallel to OA from L to the staple diagram is LL' effective length.

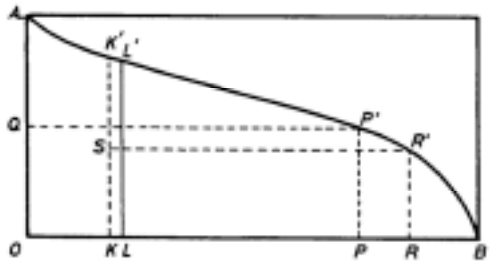

Figure 2.8: Effective length [14].

$$OQ = \frac{1}{2}OA = PP' \qquad OK = \frac{1}{4}OP$$

$$KS = \frac{1}{2}KK' = RR' \qquad OL = \frac{1}{4}OR \qquad LL' = \text{Effective Length}$$

2.1.3.5. Modal Length

Modal length is the length in a fiber length frequency diagram, which has the highest frequency of occurrence. The modal length for long staple cottons is more than the mean length because of the progressive increase in skewness of the fiber length distribution with increasing staple length.

2.1.3.6. Span Length (SL)

Span length is the distance spanned by a specified percentage of the fibers in the test beard, taking the amount reading at the starting point of the scanning as 100% [3]. There are an infinite number of reference points for span lengths. The 2.5% and 50% are the most commonly used by industry. The 2.5% SL is that length at which only 2.5% of the fibers are that long or longer. It references the shortest distance to which roller

drafting ratch settings can be adjusted so that few if any fibers are broken. Audivert and Castellar [7] found that the 2.5% span length was less variable than others and increasing span lengths tended to increase the coefficient of variation from 1% to 4%. The 2.5% SL also has been determined to be parameter which SL agrees best with the UHML by testing USA upland cottons [97]. On the other hand, Behery [14] proposed the 1-% span length as a best compromise in settings of machine parts. The 50% span length is more valuable as a potential measure of spinning performance and yarn quality [89]. Hertel and Craven [47] emphasized that the 67% span length was as good as mean length in describing the breaking strength of yarns.

2.1.3.7. Upper-Half-Mean Length (UHML)

The UHML is the average length by number of the longest one-half of the fibers when they are divided on a weight basis. The UHML was chosen because it was convenient for a technician to plot [97].

$$UHML = \frac{1}{S(ME_w)} \int_{ME_w}^{\infty} l f(l) dl \qquad \textbf{Equation 2.15}$$

where: $S(ME_w)$ is the proportion by number of the fibers longer than the weight type median.

2.1.3.8. Uniformity Index (UI)

UI is the ratio of the mean length divided by the upper half-mean length. It is a measure of the uniformity of fiber lengths in the sample expressed as a percent. Thus, this uniformity value is the ratio of the average length of all fibers to the average length of the longest one half. Table 2.8 shows the UI for a variety of cotton along with a qualitative description according to Sasser [91].

$$UI = \left(\frac{ML}{UHML} \right) \times 100 \qquad \textbf{Equation 2.16}$$

Table 2.8: U. S. Upland cotton uniformity index [91].

Length uniformity index	Description
Above 85	Very high
83-85	High
80-82	Average
77-79	Low
Below 77	Very low

2.1.3.9. Uniformity Ratio (UR)

Uniformity ratio (UR) is the ratio of the 50% span length to the 2.5% span length. It is a smaller value than the UI by a factor close to 1.8. Larger values indicate a more uniform fiber length distribution. Lower values tend to increase manufacturing waste, to make processing more difficult, and to lower the quality of the product. Table 2.9 shows the UR for a variety of cotton along with a qualitative description according to Sasser [89].

$$UR = \left(\frac{50\%\ SL}{2.5\%\ SL} \right) \times 100 \qquad \textbf{Equation 2.17}$$

Table 2.9: U. S. Upland cotton uniformity ratio [91].

Length uniformity ratio	Description
Above 48	Very high
47-48	High
44-46	Average
41-43	Low
Below 41	Very low

2.1.3.10. Short Fiber Content (SFC)

The percentage of fibers less than one half inch by weight is referred to as the short fiber content. Traditionally, the weight basis has been used for most spinning quality experiments concerning short fiber content. However, the number basis also has

been commonly used for comparisons, because it is believed that the number of short fibers is more important than their small weight fraction implies [108].

2.1.3.11. Floating Fiber Index (FFI)

Fibers in the drafting zone that are not clamped by either of the pairs of rollers of the drafting system are referred to as floating fibers [14]. The FFI was proposed as an alternative to SFC [85] and is calculated as in equation 2.18.

$$FFI = \left(\frac{UQL}{ML} - 1 \right) \times 100. \qquad \textbf{Equation 2.18}$$

FFI can also be calculated from the output of a fibrogram as

$$FFI = \left(\frac{UHML}{ML} - 1 \right) \times 100. \qquad \textbf{Equation 2.19}$$

2.1.4. Cross Examination of Different Lengths

Many authors have suggested relations to compare the different length parameters. Staple length, upper-half-mean length, upper quartile length, modal length, effective length and 2.5% span length represent the longer fibers in a sample and correlation is generally high among these parameters. Zurek [118] found the correlation to be 0.974 between staple length and mean length by number, and 0.985 between staple length and mean length by weight. The higher value between the staple length and mean length by weight is due to the insensitivity to variations in the number of short fibers in the test sample.

Staple length, upper-half mean length, and upper quartile length give values, which are about equal to the average length of fibers on the seed [108]. The 2.5% span length generally agrees with the seed cotton staple length to within one-millimeter [89].

The effective length is about 1.1 times the staple length [49, 111]. Table 2.10 shows correlations between various length parameters as found in the literature.

Table 2.10: Some correlation coefficients between different length measures.

Measures	Correlation coefficient	Source
STPL v. 2.5% SL	0.32	Woo [111]
STPL v. UQL	0.42	Woo [111]
UQL v. 2.5% SL	0.72	Woo [111]
STPL v. UHML	0.42	Woo [111]
STPL v. UQL	0.62	Woo [111]
STPL v. 3.0% SL	0.99	Woo [111]
UQL v. 3.1% SL	0.98	Woo [111]
UHML v. 3.1% SL	0.88	Woo [111]
UQL v. ML	0.89	Bargeron [13]
UHML v. UI	0.52	Zeidman [116]
UHML v. ML	0.97	Zeidman [116]
ML v. UI	0.72	Zeidman [116]
ML v. UI	0.615	Prakash [81]
SFC(n) v. UHML	0.59	Zeidman [116]
SFC(n) v. ML	0.66	Zeidman [116]
SFC(n) v. UI	0.75	Zeidman [116]
SFC(w) v. UHML	0.71	Zeidman [116]
SFC(w) v. ML	0.77	Zeidman [116]
SFC(w) v. UI	0.80	Zeidman [116]
SFC(w) v. UI	0.38	Bargeron [11]
SFC(w) v. UI	0.346	Sief [93]
SFC(w) v. UR	0.328	Sief [93]
SFC(n) v. UI	0.282	Sief [93]
SFC(n) v. UR	0.425	Sief [93]
SFC(w) v. HVI-UI	0.955	Ramey [85]
SFC(w) v. Fib.-UI	0.535	Ramey [85]
ML v. 2.5% SL	0.980	Prakash [81]
SFC(w) v. 2.5% SL	0.523	Prakash [81]

The measurement of individual fibers causes much of the trouble associated with sample preparation. Short fibers have a tendency to cluster, so that their number in the test sample is either too large or too small. Even severe fiber breakage has only a minor influence on staple length but a major effect on percent short fiber content. Tallant, Fiori, Alberson and Chapman [102] found that when various percentages of short fibers were added to a base sample, there was no appreciable decrease in upper quartile lengths and the change in the mean length was moderate. Hall [42] concluded that 50% span length does not provide an adequately precise estimate of SFC. Several algorithms to predict

SFC have been developed on the basis of length uniformity and controversial results have been found as can be seen from Table 2.10. The traditional Preysch formula derives SFC from HVI measurements of two span lengths (equation 2.20):

$$SFC\% = 39.4 + 1.3 \times (2.5\%SL) - 4.6 \times (50\%SL) \qquad \textbf{Equation 2.20}$$

Zeidman, Batra and Sasser [116] emphasized that Preysch predictions always exceed the experimental values. They derived new equations for SFC which depend on ML, UHML, and UI. The maximum coefficient of correlation was found to be 0.695. Using two span lengths as in Preysch they obtained equation 2.21.

$$SFC\% = 50.01 - 0.766 \times (2.5\%SL) - 81.48 \times (50\%SL) \qquad \textbf{Equation 2.21}$$

2.2. MEASUREMENT SYSTEMS

Fast and accurate single fiber measurements are desired characteristics of a reliable fiber length measurement method. Subjective measurement of fiber length is associated with inaccuracy especially when the classer is not familiar with the type of cotton. Lack of familiarity with standards is another important source of inaccurate results. One survey showed that there were wide differences in the assessment of length; in extreme cases this difference could go up as much as 3/8 inch to ½ inch between two classers [68].

Objective methods were designed to eliminate these personal differences in staple length determination. The comb sorter is one of the earliest designs of the semi-mechanical length measurement device. Baer Sorter and Suter-Webb devices are the best known types of the sorters. Suter-Webb was used in the US as a standard method. Hertel [46] introduced the Fibrograph in 1940. The most important device for cotton measurements, High Volume Instrumentation (HVI), was developed in 1980's. HVI is

the standard test method to officially measure all the US crop. The Spinlab-type HVI uses the same approach as the Fibrograph method to measure fiber length. The MCI-type HVI uses a pneumatic principle. The Peyer instrument is another important application of fiber length measurement scanning of the whole sample length distribution. In late 1980's, AFIS was introduced to measure the fiber length distribution and was the first to directly measure SFC. All systems have their own advantages and disadvantages. Let us look at these important systems more deeply.

2.2.1. Array Method

This method is acknowledged as the most accurate method available by ASTM [2], with the exception of individually measuring a very large number of single fibers. It has long been used to measure the complete fiber length distribution and the test results are used as reference values for other methods. However, it is extremely time consuming, costly, and requires skilled operators. It takes approximately 2-3 hours per sample [10, 9] and sampling, testing method and skill of the operator influence the results. Particularly for short fiber content, repeated measurements are necessary for satisfactory accuracy in many applications [82]. The USDA charges $137 for each sample using this method, while charging $38 for Peyer and $9.5 for Fibrograph [107].

In this method, a predetermined weight (75 mg) of fibers are sorted into common length groups onto a velvet board in 0.125-inch intervals. The velvet board shows the staple length distribution of the sample. Then, beginning with the longest group each length group is weighed. Weight data are used to calculate mean length, upper quartile length and other length measurements. A sample calculation is carried out by ASTM for Table 2.11 as follows:

Table 2.11: Fiber length array method [2].

Length, L	Lower limits (in.)	Group weights, W	Length squared, L^2	Sum of weights	Cumulative percentage of fibers
23	1.375	4.0	529	4.0	5.31
21	1.250	11.6	441	15.6	20.74
19	1.125	18.9	361	34.5	45.88
17	1.000	13.2	289	47.7	63.43
15	0.875	9.0	225	56.7	75.40
13	0.750	5.1	169	61.8	82.18
11	0.625	3.8	121	65.6	87.23
9	0.500	1.7	81	67.3	89.49
7	0.375	3.2	49	70.5	93.75
5	0.250	2.3	25	72.8	96.81
3	0.125	1.6	9	74.4	98.94
1	0.000	0.8	1	75.2	100.00
Totals	75.2				
$WL = 1217.0$		$WL^2 = 21583.2$			

A. Upper Quartile Length

1. Cumulative sum of longest group weights equal to or greater than quartile=34.5
2. Quartile $W/4$ ……=18.8
3. Difference (Line 1 minus Line2) ……=15.7
4. Correction=Diff.x0.125/weight group containing UQL=15.7x0.125/18.9 =0.1038 in.
5. Lower limit of group containing UQL ……=1.1250 in.
6. Upper Quartile Length (Line 4 plus Line 5)……..=1.2288 in.

B. Mean Length

Mean length $= WL/(W \times 16) = \dfrac{1217.0}{W \times 16} = \dfrac{1217.0}{1203.2} = 1.011469$ in.

C. Variance

1. $WL^2/(W \times 256) = \dfrac{21583.2}{W \times 256}$ ……=1.121135 in.
2. $(\text{Mean length})^2$ ……=1.023070 in.
3. Variance (Line 1 minus Line 2)……...=0.098065 in.

D. Standard Deviation

S.D.$= \sqrt{\text{Variance}}$ ……...=0.313 in.

E. Coefficient of Variation

$\dfrac{\text{S.D.} \times 100}{\text{Mean length}}$ ……=30.95%

F. SFC

100-Cumulative percentage of fibers in length group 9…….=100-89.49=10.51%

With weight-length arrays, such as those obtained from Suter-Webb sorter, it is common practice to calculate the average fiber length on a weight basis. This automatically reduces the effects of variation in short fiber content, and as such, weighted mean length varies more closely with staple length than mean length calculated on a number base. The coefficient of variation from a length array gives some indication of the relative amounts of long and short fibers present.

Zeidman, Suh, Batra and Sasser [117] emphasized that length groups are contaminated by other shorter or longer length groups during the segregation process. This affects the accuracy of all measurements, but especially the longest and shortest length range. Since other groups have two adjacent length groups, the errors are diluted. The shortest group has only one neighbor and after removing presumably all fibers longer than 0.125 in., the remaining fibers are all assumed shorter than 0.125 in.

ASTM carried out an interlaboratory test to evaluate the accuracy of this method. Table 2.12 shows the components of variance expressed as standard deviations.

Table 2.12: ASTM array interlaboratory test results [2].

Test item	Single operator	Within laboratory	Between laboratories
UQL, in.	0.01905	0.00140	0.00623
ML, in.	0.02196	0.00227	0.01307
CV%	1.450	0.361	1.173
SFC	1.441	0.033	1.162

For the components of variance in Table 2.12, the averages of observed values for both the three specimen and the two specimen tests should be considered significantly different at the 95% probability level if the differences equal or exceed the critical differences in Table 2.13.

Table 2.13: ASTM 95% confidence interval significant levels [2].

Number of specimens in test and item	Single operator	Within laboratory	Between laboratories
Three specimen test			
UQL, in.	0.030	0.031	0.035
ML, in.	0.035	0.036	0.051
CV%	2.3	2.5	4.1
SFC	2.3	2.3	4.0
Two specimen test			
UQL, in.	0.037	0.038	0.041
ML, in.	0.043	0.043	0.057
CV%	2.8	3.0	4.4
SFC	2.8	2.8	4.3

2.2.2. Fibrograph

The original idea of the Fibrograph was developed by Hertel and Zervigon [45] in 1936. It was intended to plot a seed cotton staple diagram by scanning the entire distribution of the sample. Hertel [46] developed the fibrogram theory that random caught fibers configure the fibrogram curve if they are arranged with their catching points along the vertical axis. Later the Fibrograph was digitized and added new features such as 2.5% SL, 50% SL and UR.

The Fibrograph simply scans caught fibers from the starting point to some maximum distance (no more fibers) while measuring the transmitted light intensity at each measurement point. Any variation in the number of fibers varies the amount of light detected. The 2.5% span length, 50% span length and uniformity ratio are derived from these data [3].

The Fibrograph is subject to a number of error sources. Krowicki and Thibodeaux [58], and Krowicki, Hemstreet and Duckett [61] reported important error sources to include: fiber crimp, lack of random clamping, starting of the scan relative to the fibers, lens width, fiber taper, and holding length. They calculated the average

holding length of the sampler as 4.06 mm. Taking the average start of scan as 3.81 mm and adding the average holding length, they found the actual beginning scan distance as 7.87 mm. Considering fiber crimp in addition to the combined effect of average holding length and beginning scan distance, they found an average ratio of 1.2 for the theoretical to measured length of upper half mean length and 2.5% span length.

Depending on the desired precision, two or four specimens from each subsample are tested. ASTM carried out an interlaboratory test in which two operators in each of three laboratories performed fiber length tests. The components of variance calculated from the results of these tests an expressed as standard deviations are listed in Table 2.14.

Table 2.14: Components of variance of Fibrograph calculated from two specimen test results and expressed as standard Deviations [3].

Test item	Single operator	Within laboratory	Between laboratories
2.5% SL, in. (mm)	0.01163(0.295402)	0.00003(0.000762)	0.00360(0.09144)
50% SL, in. (mm)	0.01028(0.261112)	0.00137(0.034798)	0.00834(0.211836)
50/2.5 UR, %	1.270	0.117	0.973

For the components of variance in Table 2.14, the averages of observed values for both the four specimen and the two specimen tests should be considered significantly different at the 95% probability level if the differences equal or exceed the critical differences in Table 2.15.

Table 2.15: Critical differences between two means in cotton fiber length tests [3].

Number of specimens in test and item	Single operator	Within laboratory	Between laboratories
Four specimen test			
2.5% SL, in. (mm)	0.016(0.4064)	0.016(0.4064)	0.019(0.4826)
50% SL, in. (mm)	0.014(0.3556)	0.015(0.381)	0.027(0.6858)
50/2.5 UR, %	1.8	1.8	3.2
Two specimen test			
2.5% SL, in. (mm)	0.023(0.5842)	0.023(0.5842)	0.025(0.635)
50% SL, in. (mm)	0.020(0.508)	0.021(0.5334)	0.031(0.7874)
50/2.5 UR, %	2.5	2.5	3.7

2.2.3. HVI-Spinlab

HVI-Spinlab uses the same principle of the Fibrograph for length measurement and includes other features, such as micronaire, strength, and elongation testing. It is the official USDA method that every bale in the US is measured by HVI. However, like all other methods they are subject to error.

Holding length is one of the important error sources whenever a holding device is used in scanning fibers to determine length parameters. Holding length is about 0.16 in. With the start of scan set point at 0.15 inch to 0.20 inch from the held point [87, 115], total unmeasured length is about 0.31 in. According to Zeidman and Batra [115] mostly short fibers are affected in this unmeasured area. On the other hand, the proportion of shorter fibers is smaller and that of longer fibers is larger in the sample than in the population. Thus, sampling error influences the short fiber content to a much higher degree than the long fibers.

A lens system that is about 0.125 inches wide scans caught fibers from the starting point to some maximum distance while measuring the transmitted light intensity [87]. The fibrogram is influenced by all fibers in the optical system. In the region of longer fibers, the rate of change is small and the actual optical reading approximates the mathematical average of the mass over the detector width of 0.125 inches. However, this is not true at the start of the fibrogram. This effect is referred to as lens broadening.

Palmer, Cooper, Pellow, McRae and Anderson [75] claimed that the Uniformity Index of Spinlab was similar to Fibrograph, while the mean length of Spinlab was consistently about one thirty-second of an inch shorter than Fibrograph measurements. Riley and Chu [88] found the correlation coefficient of Uniformity Index only 0.495

between Spinlab and Fibrograph and the correlation coefficient of the SFC 0.949 between Spinlab and Suter-Webb. Table 2.16 shows the components of variance and 95% probability level critical differences of ASTM test [4].

Table 2.16: Components of variance and critical differences of HVI-Spinlab [4].

	Standard deviations in indicated units		Critical differences in indicated units Two-specimen test	
	Within lab.	Between lab.	Within lab.	Between lab.
UHML, inch	0.013	0.030	0.035	0.091
UI, %	1.00	1.53	2.78	5.07

2.2.4. HVI-MCI

Brown [17] introduced the earlier version of pneumatic fiber length measurement. In this method, the length analyzer determines length parameters of the test beard by pneumatically scanning the specimen. Instead of using light, this system measures the air pressure drop across an orifice as the specimen is passed through the orifice. The pressure drop across the orifice is proportional to the total specific area of fibers in the orifice. Assuming that the fibers are uniform in cross section or specific area, the pressure drop is a measure of the number fibers in the air flow path. Therefore, as the specimen is being raised from the orifice, the pressure drop profile gives a measure of the number of fibers at each point along the length of the specimen. By scaling the output pressure from shortest distance to maximum distance, the specimen is converted into an internal representation of the percentage of the total number of fibers present at each length value.

Associated errors of the MCI method are similar to Spinlab. The average holding length is 0.11 inch and its start of scan is set at 0.20 inch so that the total unmeasured length is almost identical to Spinlab with 0.31-inch [59]. According to Krowicki,

Hemstreet and Thibodeaux [59], MCI measures all lengths 0.05 inch longer than Spinlab. The correlation coefficient of the Upper Half Mean Length, the Uniformity index and the Mean length of MCI and Suter-Webb array method have been found to be 0.914, 0.562, 0.871 respectively [117].

Gourlot, Vialle, Lassus, Duplan, Brunissen and Fallet [39] studied the effect of the pinch and universal sampling methods on accuracy. In the pinch sampler, a mechanical arm presses the pinch into the fiber mass. The pinch closes to hold the fibers which are then separated from the sample when the mechanical arm withdraws. In the universal sample, a comb removes fibers through perforations in a metal plate. A mechanical arm carrying the pinch presses it against the fiber mass. The pinch closes to hold the fibers which are then separated from the sample. Combing and brushing take place after pinching. Chanselme, Gourlot and Tamime [20] studied the universal and fibrosampling methods. In the Fibrosampler, fibers are combed before pinching. Results showed significant differences in the distribution and accuracy of length measurements. Table 2.17 shows components of variance and 95% probability level critical differences of ASTM test D 4604-95 for the HVI-MCI method [5].

Table 2.17: Components of variance and critical differences of HVI-MCI [5].

	Standard deviations in indicated units		Critical differences in indicated units Four-specimen test	
	Within lab.	Between lab.	Within lab.	Between lab.
UHML, inch	0.016	0.021	0.044	0.073
UI, %	0.87	0.89	2.41	3.44

2.2.5. Peyer ALmeter

The Peyer texlab system, developed for measuring the length of wool, appears to be an easy and relatively rapid way to determine the length distribution of cotton fibers.

The Peyer comprises two systems which sort and align a fiber bundle and measure its length distribution. The Fibroliner (FL-101) mechanically combs either sliver or ginned lint specimens into a parallel bundle or beard. The aligned fibers are placed between a pair of carrier films for measurement. The ALmeter (AL-101) scans the beard using capacitance measurements to produce an output signal that is proportional to the cumulative mass distribution. The capacitor scans the fibers of the test specimen every 0.125-mm (0.005-in.). The microprocessor can convert the mass distribution to a number distribution when the linear density of the fibers is assumed to be constant.

It takes about 15 minutes to test a sample on the Peyer ALmeter. The ALmeter can produce at least six different sets of array information from the raw data, including a fiber mass distribution, a number distribution, a fibrogram, and parametric values such as mean length and upper half mean length by weight and by number, the variance, and the 25% and 50% span lengths.

Hemstreet and Krowicki [44] measured the fiber length and length distributions for different staple length cottons using the Peyer system. Table 2.18 shows that the mean length by weight for the measured distributions appears shorter than the known distribution. The UHML and the UQL appears longer for the input than for the measured distribution. They observed that SFC by number is significantly lower than the known percentage. The weight loss that occurred in the samples ranged from 4 to 7% of the original sample. This percentage loss by number appears to increase with the length of the variety. Cui et al. [25] observed an average 1.20% short fiber loss and an average of 4.75% long fiber loss, and the ratio of short fiber loss to total loss was 23.60% for the Peyer method.

Table 2.18: Peyer length measurement comparison [44].

	Type I		Type II		Type III	
	known	Peyer	known	Peyer	Known	Peyer
ML(n), in.	0.757	0.753	0.810	0.815	0.928	0.970
UHML(n), in.	1.009	0.975	1.165	1.121	1.557	1.467
UI, %	75.0	77.2	69.5	72.7	59.6	66.1
SFC(n), %	17.7%	14.7%	23.3%	16.7%	25.3%	16.1%
ML(w), in.	0.862	0.822	0.971	0.920	1.223	1.160
UQL, in	1.016	0.990	1.175	1.139	1.573	1.496
SFC(w), %	5.9%	7.5%	7.8%	7.6%	6.6%	6.0%

Bargeron [11] compared the Peyer with the Suter-Webb array method. The average difference between the Peyer 25% and Suter-Webb UQL was -2.40 mm with a standard deviation of 0.86 mm. The linear correlation coefficient between the two was 0.99. The average difference in ML was –1.37 mm with a standard deviation of 1.02 mm. The linear correlation coefficient between the Suter-Webb ML and the Peyer was 0.99. SFC was greater than the Suter-Webb with an average difference of +1.70%, and a standard deviation of 2.40%. Ramey and Beaton [85] found a 0.961 correlation coefficient of SFC between the Peyer and Suter-Webb. Another analysis of Bargeron [13] showed 0.87 correlation coefficient of the ML between the Peyer and Suter-Webb. He explains the differences in the Suter-Webb and the Peyer distributions with the crimp factor. Table 2.19 gives the variance components of Peyer according to ASTM [6].

Table 2.19: Variance components of Peyer [6].

Test item	Within Laboratory	Between laboratories
ML, in. (mm)	0.0193(0.490)	0.0208(0.528)
UQL, in. (mm)	0.0224(0.569)	0.0244(0.620)
CV (%)	2.06	2.2071
SFC, %	2.20	2.4166

2.2.6. AFIS

The AFIS was designed for single fiber measurements which is distinguishable from the other methods. It is based on aeromechanical fiber processing, similar to

opening and carding, followed by electro-optical sensing. The fibers are separated from microdust and trash, and opened using specially designed pinned and perforated cylinders and stationary carding flats [1]. Airflow into the perforations of the cylinder allows efficient dust and trash removal by the combination of combing via the stationary carding flat and the airflow drawn through the cylinder[1]. Each of the components is transported in separate pneumatic paths to be analyzed electro-optically as in Figure 2.9.

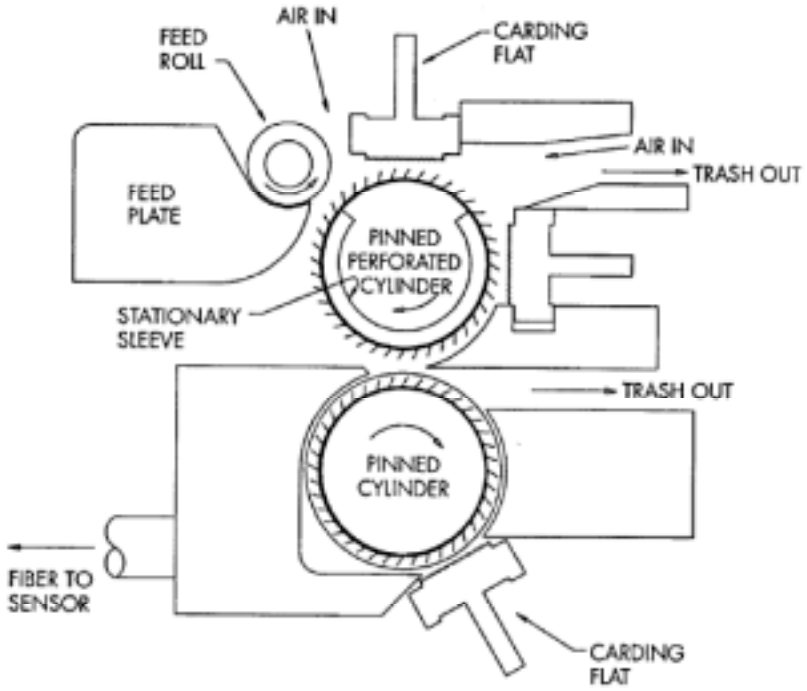

Figure 2.9: AFIS fiber individualizer [1].

The Electro-optical sensor consists of three basic elements: tapered entrance and exit nozzles, beam-forming and collecting optics, and the detection circuitry (Figure 2.10). Individual fibers are transported pneumatically from the fiber individualizer by a high-velocity air stream. As the material enters the tapered nozzle, it is accelerated and aligned by the airflow. As the fibers leave the entrance nozzle, they penetrate a

collimated beam of light. The fibers scatter and block that light in proportion to their mean optical diameter and in direct relation to their time of flight through the beam [1].

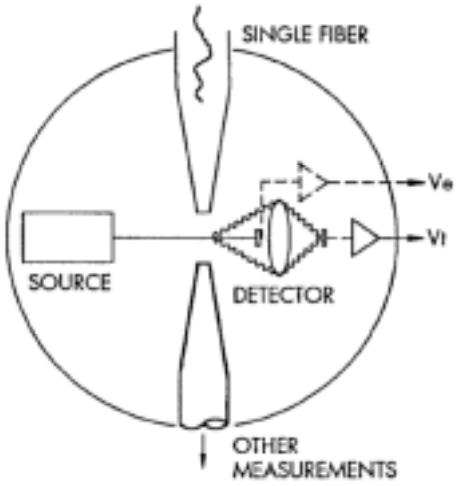

Figure 2.10: Electro-optical sensor [1].

There are a number of error sources in AFIS measurements. There are fiber breakages in the opening unit between 1% to 4% [26]. Fiber straightening, separation and alignments are questionable. Only between 9% to 33% of fibers are counted in the measurement unit [26], therefore there could be a bias for longer or shorter fiber lengths.

Cui, Calamari and Krowicki [26] established a test method to measure AFIS accuracy. The same number of different known lengths, 0.25, 0.50, 0.75, 1.00 and 1.25 inch, acrylic fibers were tested on AFIS. The percentage of each fiber length group was measured by AFIS as shown in Table 2.20. They also observed that lower sample density increased the percentage of fibers counted, while higher density reduced testing time. The length measured was not affected significantly based on the densities and samples used. The correlation coefficient between the results from the AFIS and HVI systems is 0.998. However, the level of AFIS is higher than HVI (interception = 0.05 inch).

Table 2.20: AFIS length accuracy test [26].

Cut length (in)	Measured length (in)	Percentage in Sample (%)	Percentage Counted (%)
0.25	0.28	20	19
0.50	0.57	20	23
0.75	0.80	20	25
1.00	1.04	20	18
1.25	1.18	20	15

Cecil [19] studied the repeatability and the variation from test to test within the AFIS. The AFIS has produced significant amount of variation from run to run. In this study there were larger variations from run to run than between gins and farmers, and this variation questions the ability of the AFIS to produce accurate results.

Table 2.21: AFIS measurement variability on SFC and UQL [19].

SFC (%)	Run# (10,000 fibers)	Min. Value	Max. Value
	1	4.8	7.4
	2	8.9	12.4
	3	10	13.4
UQL (in)	Run# (10,000 fibers)	Min. Value	Max. Value
	1	1.13	1.23
	2	1.17	1.27
	3	1.08	1.16

Cecil [19] conducted further tests with known 1.25-inch staple length polyester samples. The mean length by weight was measured to be 1.1 inches, and by length to be 1.03 inches. SFC values for the polyester samples averaged 0.6 percent by weight and 2.1 percent by number with a maximum of 4.4 percent by number for one sample tested. Over 70% (by weight) of the fibers were measured to be shorter than the 1.25 inch given polyester staple length. Cecil also found that sample density significantly affected SFC measurements on the AFIS.

On the other hand, other researchers found controversies regarding the accuracy of the AFIS as in Table 2.22 and Table 2.23. Cui , Calamari, Robert and Watson [25] found the repeatability of SFC of AFIS 0.745 for bales and 0.8399 for slivers.

Table 2.22: Some correlation coefficients of AFIS versus Suter-Webb.

Suter-Webb v. AFIS	Correlation coefficient	source
ML	0.96	Bragg [15]
UQL	0.96	Bragg [15]
SFC	0.89	Bragg [15]
ML	0.98	Ghorashi [38]
UQL	0.98	Ghorashi [38]
SFC	0.98	Ghorashi [38]

Table 2.23: 28 Staple length expected and measured values [87].

Length Data	Expected	Suter-Webb	AFIS
ML(w)	0.82	0.75	0.75
ML(w) CV%	23.7	29.9	32.7
SFC(w)	6.6	14.2	13.6
UQL(w)	0.96	0.92	0.89
ML(n)	0.75	0.63	0.64
ML(n) CV%	29.9	44.7	43.1
SFC(n)	14.2	31.6	28.7
UQL(n)	0.92	0.84	0.81

Guse, Scheffer, Tabibi and Tauber [41] added two new features to the AFIS principal measurement method, namely the fiber velocity tester and a multi-diode linear camera called ITV. Measured length depends not only on time but velocity, too. AFIS supposes that all fibers have the same velocity in the airstream. The multi-diode camera detects when two or more fibers appear simultaneously in the measuring window and omits them from measurement. The mean length measured on the basis of number of fibers were found to be 19.0 mm for 20-mm fibers, 13.5 mm for the 15-mm fibers, and 9.5 mm for 10-mm fibers. Additionally, they found that the ITV, AFIS and Peyer showed the same trend in mean fiber length, with the Almeter and the ITV giving about the same absolute values while the AFIS values were about 20% greater.

2.2.7. Conclusion

Each system has its own inherent advantages and disadvantages. Longer length measurement values are generally highly correlated to each other and usually satisfactory results can be obtained. However, short fiber content measurement is not satisfactory. None of the existing systems is able of measuring the short fiber content accurately. HVI and Fibrograph methods cannot scan lengths less than about 0.31 inch. The Peyer method losses many fibers in the opening unit resulting in a change in fiber length distribution. AFIS appears to be the ideal method with single fiber length measurement; however, there are considerable controversies about its accuracy and repeatability. More accurate measurement of cotton fiber length and length distribution is needed and recently being driven by the industry.

Table 2.24 compares UQL, ML, and SFC values as measured by Array, AFIS, Peyer and HVI length measurement systems on standard cotton types. Table 2.25 shows correlation coefficients between measurement systems according to Smith and Williams [94].

Table 2.24: UQL, ML, and SFC comparisons of length measurement systems [94].

Staple length	Array			AFIS			Peyer			HVI		
	UQL	ML	SFC	UQL	ML	SFC	UQL	ML	SFC	UQL	ML	SFC
26	0.84	0.66	24.7	0.84	0.70	18.2	0.84	0.67	26.2	0.83	0.63	19.3
28	0.92	0.72	20.6	0.89	0.74	14.2	0.87	0.71	19.2	0.88	0.68	17.3
29	0.94	0.72	22.5	0.90	0.76	13.7	0.89	0.72	21.2	0.90	0.70	16.0
30	0.98	0.76	20.1	0.94	0.78	13.7	0.94	0.75	19.4	0.94	0.75	13.6
31	1.02	0.79	17.0	0.98	0.80	14.1	0.95	0.77	17.0	0.98	0.78	11.9
32	1.08	0.88	12.1	1.02	0.85	10.1	0.98	0.82	10.9	1.01	0.82	11.0
33	1.11	0.88	13.8	1.05	0.86	11.4	1.03	0.83	13.3	1.05	0.86	8.9
34	1.15	0.94	10.1	1.11	0.92	7.6	1.06	0.88	8.3	1.08	0.89	8.0
35	1.17	0.92	14.3	1.14	0.92	11.2	1.10	0.90	9.6	1.08	0.90	7.5
36	1.23	1.00	10.6	1.19	0.97	7.8	1.13	0.94	7.2	1.12	0.94	6.4
37	1.27	1.06	7.6	1.21	1.03	6.8	1.18	1.00	4.9	1.18	1.00	4.1
38	1.31	1.08	7.7	1.26	1.05	6.3	1.22	1.02	5.4	1.21	1.03	3.2
39	1.36	1.11	8.2	1.31	1.08	6.1	1.26	1.06	5.0	1.25	1.07	1.8
40	1.35	1.12	6.9	1.34	1.11	5.3	1.26	1.07	3.6	1.29	1.11	1.1

Table 2.25: Correlation coefficients between measurement systems [94]

Fiber measure	staple	Array	AFIS	Peyer
Array UQL	0.994			
AFIS UQL	0.991	0.989		
Peyer UQL	0.986	0.988	0.993	
HVI UHML	0.992	0.988	0.989	0.986
Array ML	0.980			
AFIS ML	0.983	0.989		
Peyer ML	0.984	0.989	0.998	
HVI ML	0.994	0.978	0.990	0.989
Array SFC	0.896			
AFIS SFC	0.905	0.938		
Peyer SFC	0.932	0.972	0.950	
HVI SFC	0.992	0.915	0.895	0.931

Table 2.26 shows correlations between measurement systems for various length parameters as found in the literature. Table 2.27 shows measurement methods of the existing systems.

Table 2.26: Correlation coefficients between measurement systems.

Methods	Length type	Correlation coefficient	Source
AFIS v. Peyer	SFC(w)	0.2404	Cui [25]
AFIS v. HVI	SFC(w)	0.2550	Cui [25]
HVI v. Peyer	SFC(w)	0.2379	Cui [25]
AFIS v. Peyer	ML(w)	0.5981	Cui [25]
AFIS v. HVI	ML(w)	0.8822	Cui [25]
HVI v. Peyer	ML(w)	0.7045	Cui [25]
Array v. AFIS	SFC(w)	0.250-0.676	Sief [93]
Array v. Peyer	SFC(w)	0.580-0.033	Sief [93]
AFIS v. Peyer	SFC(w)	0.747-0.688	Sief [93]
AFIS v. Peyer	SFC(n)	0.640-0.731	Sief [93]

Table 2.27: Measurement methods of the existing systems [114].

METHOD		AFIS	Suter-Webb Array	ALmeter	HVI
Type of sample		By number			By length
Fiber formation		Individual fibers	Aligned array		Beard
Measuring procedure	Counting	$f(x)$ $f_w(x)$			
	Weighing Groups		$f_w(x)$		
	Differential Scanning			$S(x)$	$G(x)$
	Integral scanning			$G(x)$	$Z(x)$

2.3. IMPORTANCE OF FIBER LENGTH

1997/1998 worldwide cotton production was 91,167,000 bales each weighing approximately 480 LB [107]. Table 2.28 shows production and the economic impact of cotton on the US economy. The Schlafhorst Utility Value shows that staple length is the second most important price parameter behind clean cotton content [98]. Table 2.29 shows cotton prices depending on the staple length while other parameters remain constant.

Table 2.28: Production and value of cotton in US [107].

Year	Production 1,000 bales	Average price Cents	Value of production 1,000 dollars
1989	12,195.6	66.2	3,877,888
1990	15,506.4	68.2	5,075,826
1991	17,614.3	58.1	4,913,244
1992	16,218.5	54.9	4,273,935
1993	16,133.6	58.4	4,520,908
1994	19,662.0	72.0	6,796,654
1995	17,899.8	76.5	6,574,612
1996	18,942.0	70.5	6,408,144
1997	18,793.0	66.2	5,975,585
1998	13,796.2	65.3	4,321,585

Table 2.29: Span length effect on the cotton prices [107].

year								
	28	29	30	31	32	33	34	35
	Cents	Cents	Cents	Cents	Cents	Cents	Cents	Cents
1988	48.02	48.02	48.94	50.21	52.39	54.12	57.67	58.13
1989	59.78	59.78	60.74	62.93	64.89	66.63	69.78	70.23
1990	61.27	61.27	62.48	65.46	69.15	71.52	74.80	75.38
1991	47.93	47.93	50.12	52.37	53.23	54.15	56.68	57.06
1992	46.21	46.21	48.62	50.79	52.45	52.41	54.10	54.76
1993	59.39	59.39	61.38	62.84	64.17	64.16	66.12	66.76
1994	81.51	81.51	83.46	85.01	85.80	86.06	88.14	88.53
1995	76.00	76.00	77.82	79.49	79.99	81.06	83.03	83.58
1996	64.61	64.61	66.38	67.18	67.93	69.81	71.59	72.20
1997	60.97	60.97	62.65	63.48	64.56	66.07	67.79	68.39

Staple length has a great effect on price for many reasons. First it is closely associated with other fiber properties due to a complex inter-relationship between fiber

properties. Many machine settings in spinning processes are decided on the basis of fiber length. Spinning efficiency is mainly determined by fiber length and length distribution values, thus fiber length is particularly important to spinners. Depending on the yarn production system, fiber length may be greatly correlated to yarn quality parameters and indirectly to fabric parameters. Complete and accurate information of length and length distribution of cotton fibers and their contribution to the spinning efficiency is vitally important to spinners.

2.3.1. Length Related to Other Fiber Properties

Pillay and Shankaranarayana [77] researched the effect of fiber length to other cotton properties. They concluded that longer length groups are finer, stronger and more mature than the shorter length groups. They propose no significant difference in elongation at break but longer varieties generally have higher elongation than shorter varieties. Longer length groups are found to be stiffer and generally have a greater number of reversals.

Morlier, Orr and Grant [72] came to nearly the same conclusions as well. One exception is that they found elongation at break increases significantly with increasing fiber length. Further analysis showed that the ratio of elongation at break to breaking load decreases, and coefficients of variation for both breaking load and elongation at break decreases with increasing fiber lengths. The same result was observed by Rebenfeld and Polly [86]. Fiber toughness, defined as one-half the product of fiber breaking extension and breaking tenacity, was found to reach a maximum value above the mean length. They [86] also observed that breaking tenacity remains essentially constant up to the mean length and then rises significantly.

2.3.2. Length Related to Spinning Process and Yarn Quality

Raw material costs are approximately 50% of yarn production costs depending on spinning system and yarn count [30, 53]. Spinning performance is considerably influenced by the raw material quality. Longer staple is required for the manufacture of fine, strong yarns. These fibers also increase spinning efficiency. Therefore, fiber length is an essential part of the economical operation of a spinning mill and essential for maintaining yarn quality. Table 2.30 illustrates various reasons why fiber length is important.

Table 2.30: Parameters affected by fiber length [32].

Mill processing	Yarn quality	Fabric quality
Ends-down Cleanability Waste	Strength Elongation Uniformity hairiness	Strength Appearance

Wakeham [108] showed the effect of fiber length on quality and spinning processes. Cotton fibers processed with two different ginning conditions were used. One gin produced more SFC due to fiber breakage. Upper quartile lengths were measured and found to be 1.10 and 1.12 inches, and mean lengths were measured 0.91 and 0.96 inches, after ginning. In spinning, the shorter fiber distribution resulted in 21.4% more ends down and slightly more processing waste. For another pair of cottons, upper quartile lengths were measured as 1.19 and 1.23, and mean lengths were measured 0.97 and 0.99 inches. Shorter fiber due to fiber breakage resulted in 46% more ends down and 2.22% more waste. This shows the importance of SFC on processing efficiency.

When an assembly of fibers is stretched, an internal pressure directed to the core is developed. It is this pressure that generates friction between the fibers and causes them

to grip each other and thereby provide strength to the yarn. The pressure is at a low level on the surface and progressively increases to a relatively high level as the core is approached. If the frictional hold exerted on a fiber by adjoining fibers exceeds the fiber breaking strength, then the fiber will break and contribute fully to the breaking load of the yarn. If, on the other hand, the frictional hold is less than the breaking load, the fiber will slip rather than break and will not make its full contribution to the strength of the yarn. It is fiber slippage that is primarily responsible for strength loss in staple yarns especially at low twist. Obviously, it is the short fiber that will slip rather than the longer one. Inter fiber friction is dependent upon fiber length, specific surface area and surface characteristics of the fibers. Longer fibers will improve the frictional resistance because of increased area of contact that they have with adjoining fibers. Likewise finer fibers, because of their greater specific surface area, also offer more frictional resistance. Longer and finer cottons require less critical pressure to resist slippage. In other words, longer and finer cottons require less twist to arrest slippage.

At comparable twist densities, the minimum length of fiber contributing to tenacity lies between 6 and 8 mm for ring and between 8 and 10 mm for rotor yarn [89].

Gregory's equation [10] defines a critical pressure at which fibers start breaking:

$$P = \frac{8\lambda}{3L\mu S} \qquad \textbf{Equation 2.22}$$

λ = Breaking length of the fiber
μ = Coefficient of friction of fiber upon fiber
L = length biased mean length of fiber
S = surface per unit mass of fiber (sq. meter/gm).

Sullivan's equation [47] defines yarn strength with a similar approach:

$$\frac{F}{MT} = \frac{1-T}{LCSP} \qquad \textbf{Equation 2.23}$$

F = strength of a yarn
M = mass per unit length of yarn
T = tenacity of fibers
L = length of fibers
C = coefficient of friction
S = surface per unit mass of fibers
P = average pressure between fibers

El Mogahzy [31] found that length is the most important fiber criteria for ring spinning yarn quality, but only the third most important for open-end spinning yarn quality. He generated regression equations to conclude this result (Tables 2.31 and 2.32).

Table 2.31: Relative contribution of fiber properties to yarn SBF of ring spun [31].

Fiber property	Percent relative contribution %		
	8's	26's	Average
Fineness	11.1	18.7	14.85
Length	25.6	26.3	25.95
Uniformity	11.8	12.1	11.95
Strength	17.8	18.1	17.95

Table 2.32: Relative contribution of fiber properties to yarn SBF of open-end [31].

Fiber property	Percent relative contribution %		
	8's	26's	Average
Fineness	20.2	24.0	22.10
Length	12.6	15.9	14.25
Uniformity	13.0	12.1	12.55
Strength	23.6	16.6	20.10

Suh [99] theoretically explained irregularity of slivers related to staple length. He concluded that irregularity increases rapidly along with an increase in fiber length up to 1 in. followed by a much slower rise beyond 1 in.

2.4. SHORT FIBER CONTENT:

One reason that longer cotton is more valuable than shorter cotton is that longer cotton tends to have lower short fiber content. High SFC historically has been identified with unsatisfactory textile performance, but no practical method for measuring this

attribute for marketing purposes has been developed [16]. None of the known length measurement methods are sufficiently sophisticated to measure short fiber content; the analysis of subsections of fibers is not suitable for the measurement of short fibers. There is general agreement between cotton research workers, ginners and spinners that a quick and reliable method to estimate the troublesome SFC is needed.

SFC has a tremendous impact on yarn quality and processing efficiencies. These short fibers contribute yarn unevenness and weakness because they are not uniformly distributed along the yarn. In roller drafting, short fibers tend to lag behind the long ones until a group of the short fibers is carried through the front rolls. Thus, the shorter fibers are responsible for the alternating thick and thin places in the yarn, called drafting waves. As SFC increases, there is a significant increase in the number of thick and thin places. Table 2.33 shows the parameters affected by SFC.

Table 2.33: Parameters affected by SFC and UI [32].

Mill processing	Yarn quality	Fabric quality
Ends-down Fly Waste	Strength Elongation Uniformity Imperfections hairiness	Strength Appearance

Klein [53] assumed that fibers of under 4-5 mm will be lost in processing as waste and fly, fibers up to about 12-15 mm do not contribute to strength but only to fullness of yarn. Backe [9] compared the effect of SFC, number of bales per laydown, and span length and micronaire variability in ring spinning performance. He concluded that SFC has a much more significant effect on Uster CV% and thin places but only a slightly greater effect on break factor than the others do. Tallant, Fiori and Landstreet [101] found that a 1-% increase in SFC lowers the yarn strength more than 1%. They concluded that

the short fibers add useless bulk to the yarn and prevent the working fibers from performing at their maximum potential. Another paper by the same authors [102] showed that skein tenacity was lowered 2% to 3% for each 1-% increase in SFC. They also concluded that SFC decreased yarn elongation and yarn appearance, increased difficulty in spinning, and increased twist in the roving for constant hardness. Fine yarns are more sensitive than coarse yarns to SFC. SFC also increases waste levels, fly generation and nep counts [90]. Wakeham [108] and Tallant [103] have shown that a large number of short fibers in cotton causes poorer processing efficiency and lower end-product quality.

Sanderson and Hunter [90] declared that the inclusion of a measure of SFC generally improved the correlation coefficient and therefore the accuracy of prediction in the case of Classimat faults, neps, and ends down, tenacity, irregularity and hairiness. They found that Fibrograph values of 17 mm or 18 mm, or possibly 20 mm are the most useful short fiber numbers in predicting spinning performance and yarn properties.

Traditionally the weight basis has been used in most spinning quality experiments concerning short fiber content. Considering weight basis distribution has contributed to the failure of understanding the effects of SFC. The general attitude seems to be that short fibers in the sample, because they do not weigh much, are really not of much importance and hence can be ignored. Apparently they do matter much more than generally thought, much more than their small weight fraction implies [108].

The economic implications of SFC combined with the current inability to accurately and reproducibly measure it represent an opportunity to improve fiber length

measurement technology. Advances in vision and computing technology provide the vehicle for this forward step in fiber length determination.

2.5. IMAGE PROCESSING IN LENGTH MEASUREMENT

Even though image processing has been used to measure trash in cotton, it is fairly new concept to measure the fiber length. A CCD camera equipped with a microscope for high magnification or a scanner for low magnification generally captures fiber sample images. Xu and Ting [112] measured the length of three scanned wool staples by using the image processing techniques. They applied the skeletonization algorithm to obtain one pixel fiber width. Then, they connected broken skeletons by a tracing algorithm and measured the natural length and the extended length of the fibers by counting the pixels. Their results were in agreement with manual measurements with less than 5% variation.

Schneider, Rettig and Mussig [92] measured SFC using image analysis. They placed approximately 10,000 singled fibers on a 50x50-cm black velvet covered surface. Then, they digitized a small portion of surface in each measurement and transferred the data to the image analysis software. They found SFC by number to be higher than the HVI and AFIS systems.

Cotton fiber diameters range from 10-22 microns [23]. Detection of fibers requires high resolution for better accuracy. On the other hand, analysis of image data is a very time consuming process. Higher resolution gives better image quality but unnecessary data, too. Optimum resolution and correct image capturing techniques are essential to fast and accurate length distribution measurement. In addition, depending on

image quality, image preprocessing and processing techniques strongly affect the accuracy of the results and the time required completing the analysis.

2.5.1. Lighting

Correct lighting design and light sources can give an image with maximum information utility. The design should maximize the contrast between foreground and background. There are three principal methods, frontlighting, backlighting, and structured lighting [8, 18]. Structured lighting provides 3D-object information [18].

Frontlighting techniques are utilized when surface features are important rather than object outlines. Frontlighting is also used when backlighting is impractical. There are two varieties of frontlighting: diffuse and directional [8, 18]. Diffuse frontlighting is most often associated with requirements for shadowless lighting but can also be used to good effect in the lighting of objects with specular surfaces where glinting highlights may cause camera saturation [18]. A variation in the front lighting technique provides for the use of directional illumination to highlight surface texture. Figure 2.11 shows application of the diffuse frontlighting technique.

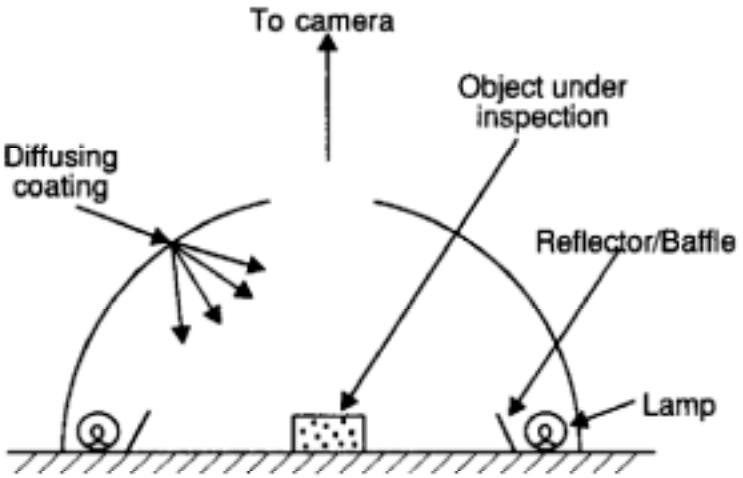

Figure 2.11: Diffuse frontlighting technique [18].

Backlighting provides the greatest scene contrast and highest lighting efficiency of any lighting technique [18]. The use of backlighting effectively produces a binary image directly. This technique is ideally suited for applications in which silhouettes of objects are sufficient for recognition [18]. A point-source of light produces sharp edges. In our application, only the outline of the fibers is needed, therefore, backlighting appears ideal. Pourdeyhimi and Dent [80] used backlighting in the measurement of fiber orientation and diameter in nonwovens. Figure 2.12 and Figure 2.13 shows applications of the backlighting technique.

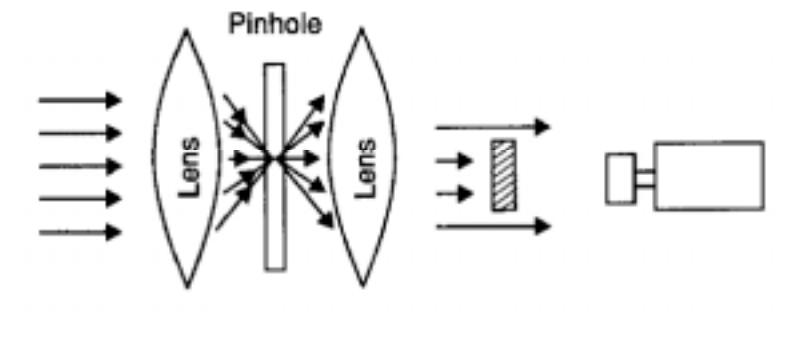

Figure 2.12: Collimated backlighting [18].

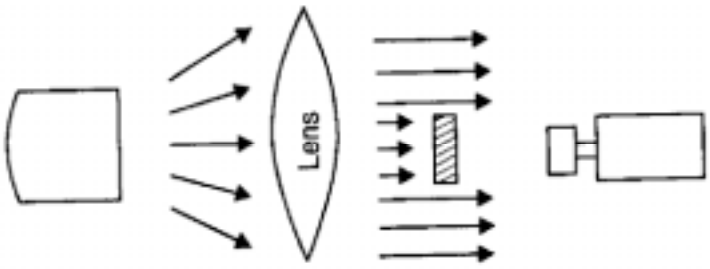

Figure 2.13: Backlighting with condenser lens [18].

2.5.2. Image Acquisition

The general aim of image acquisition is the transformation of optical image data into an array of numerical data. The conventional optical system will deliver a

continuous 2-D function. It is necessary that the continuous function should be *quantized* (*discretized* or *digitized*) so that it can be represented as an array of numbers. The sampling frequency determines the maximum spatial frequency that can be accurately resolved in the digitized image. As the number of samples per unit distance is reduced, the high spatial frequency content in the image is lost. A reduction in sampling rate may result in degradation of the final image. The Nyquist theorem states that to properly sample an image, the sampling frequency must be at least twice the maximum spatial frequency present.

Images are sampled by MxN discrete points. Each sample is called a *pixel* and must be assigned a numerical code which represents the intensity of the image function at that point. The resolution of the code is determined by the number of gray levels that are available between the extremes of intensity, namely black and white. There is a special case of intensity quantisation called *binarisation* where an image is generated with only two gray levels, black and white. Binary images are very simple to store and manipulate.

There are two fundamentally different mechanisms for the transduction of optical radiation into electrical signals: thermal detectors and quantum detectors [48]. In thermal detectors the absorption of photons causes a temperature rise which in turn produces the desired output. Quantum detection relies upon the energy of absorbed photons being used to promote electrons from their stable state to a higher state above an energy threshold.

There are several types of operation for quantum detectors. CCD (charge-coupled device) operation is the best known of them. Principles of CCD operation are discussed as follows by Holst [48]: "The basic building block of the CCD is the metal-oxide-

semiconductor capacitor. Applying a positive voltage to the gate causes the mobile positive holes in the p-type silicon to migrate toward the ground electrode since like charges repel. This region, which is void of positive charge, is the depletion region. If a photon whose energy is greater that the energy gap is absorbed in the depletion region, it produces an electron-hole pair. The electron stays within the depletion region whereas the hole moves to the ground electrode. The amount of negative charge that can be collected is proportional to the applied voltage, oxide thickness, and gate electrode area. The total number of electrons that can be stored is called the well capacity. As the wavelength increases, photons are absorbed at increasing depths. Very long wavelength photons may pass through the CCD and never be absorbed".

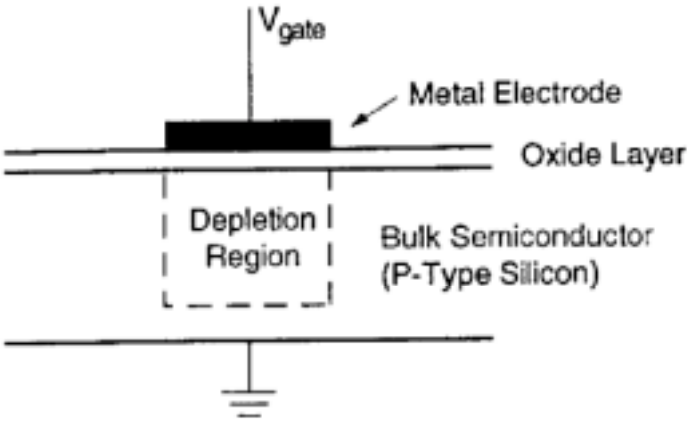

Figure 2.14: CCD operation [47].

There are many noise sources in these applications. Shot noise is due to the discrete nature of electrons. It occurs when photoelectrons are created and when dark current electrons are present. Reset noise is due to thermal noise generated by the resistance. The amplifier and quantization add additional noise. Although the origin of the noise sources is different, they all appear as variations in the image intensity.

2.5.3. Image Processing

Images are preprocessed to modify and prepare the pixel values for subsequent operations. There are two branches of image preprocessing namely image enhancement and image restoration [8]. Image enhancement attempts to improve the quality of the image or to emphasize particular aspects within the image. The aim of image restoration is to recover the original image after known effects such as geometric distortion within the camera system or blur caused by poor optics or subject or camera movement. These operations take the acquired image array as input and produce a modified array as output. Noise elimination is the common operation of image preprocessing.

If a continuous input signal $f(t)$ is applied to a system which produces an output signal $g(t)$, supposing the system as being linear and shift-invariant, the output can be defined mathematically as

$$g(t) = \int_{-\infty}^{\infty} f(\tau) h(t-\tau)\, d\tau \qquad \textbf{Equation 2.24}$$

where $h(t)$ is a function known as the impulse response and represents the output of that filter, and the term $h(t-\tau)$ identifies a version of $h(t)$ shifted by the amount τ. This integral is called the convolution integral and shows that filtering can be implemented in the time domain.

Fourier transforms can be used to convert data from the time domain to the frequency domain, and Inverse Fourier transforms do the reverse. The Fourier transform $F(\omega)$ of $f(t)$ is defined as

$$F(\omega) = \int_{-\infty}^{\infty} f(t) e^{-j2\pi\omega t}\, dt \qquad \textbf{Equation 2.25}$$

The Inverse Fourier Transform, transforming $F(\omega)$ back into $f(t)$, is defined as

$$f(t) = \int_{-\infty}^{\infty} F(\omega) e^{j2\pi\omega t}\, dt \qquad \textbf{Equation 2.26}$$

Multiplying the frequency domain by a low-pass filter that passes only frequencies below a certain value results in filtering. On the other hand, multiplication in the frequency domain corresponds to convolution in the time and the spatial domain [8, 51, 76]. Using a convolution mask over an image is much easier and faster than performing Fourier transforms and multiplication [76]. Low-pass filtering smoothes out sharp transitions in gray levels and removes noise. Table 2.34 shows 3x3 Low-pass filter convolution masks.

Table 2.34: Low-pass filter convolution masks [76].

0 1 0	1 1 1	1 1 1	1 2 1
1/6 * 1 2 1	1/9 * 1 1 1	1/10 * 1 2 1	1/16 * 2 4 2
0 1 0	1 1 1	1 1 1	1 2 1

Recognition of fibers on a surface is an application of edge detection operations in image processing. An edge is where the gray level of the image moves from an area of low values to high values or vice versa. High-pass filters amplify or enhance an edge. Table 2.35 shows some 3x3 high-pass filter convolution masks. High-pass filters generally have a peak at the center, negative values above, below, and sides of the center, and near zero at the corners [76, 109].

Table 2.35: High-pass filter convolution masks [76, 109].

0 -1 0	-1 -1 -1	1 -2 1	0 -1 0
-1 5 -1	-1 9 -1	-2 5 -2	-1 20 –1
0 -1 0	-1 -1 -1	1 -2 1	0 -1 0

Fiber detection on a surface appears to be an easy task since a large contrast between the fiber and the background can be created. However, uneven lighting can cause lower differentiation in gray levels between parts of images. Most edge detectors result in a strong edge in well-lit areas and a weak edge in poorly lit areas. Figure 2.15 and Figure 2.16 show the images of three cotton fibers with 4 and 256 gray levels respectively. Edge enhancement might be necessary in these conditions. The contrast-based edge detector defined by Phillips [76] helps take care of this problem. This contrast-based edge detector takes the result of any edge detector and divides it by the average value of the area. This division removes the effect of uneven lighting in the image.

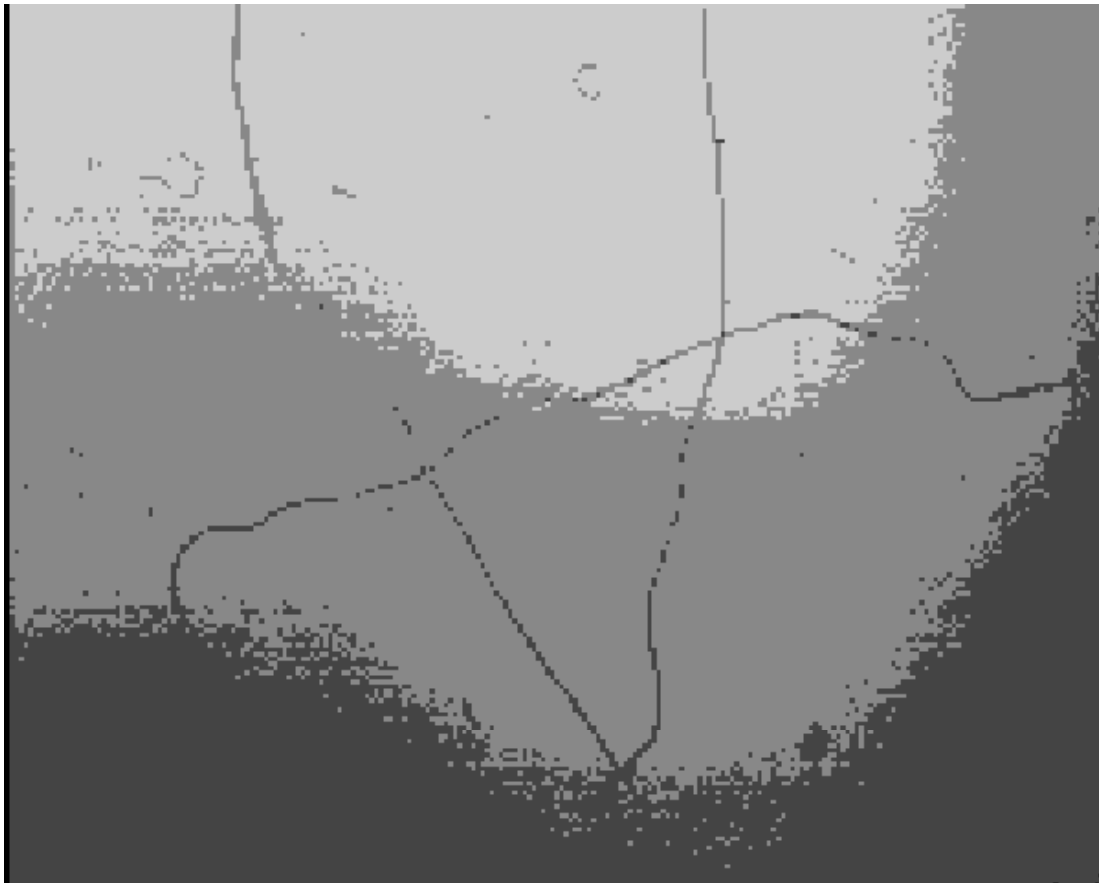

Figure 2.15: Image of three cotton fibers with 4 gray levels.

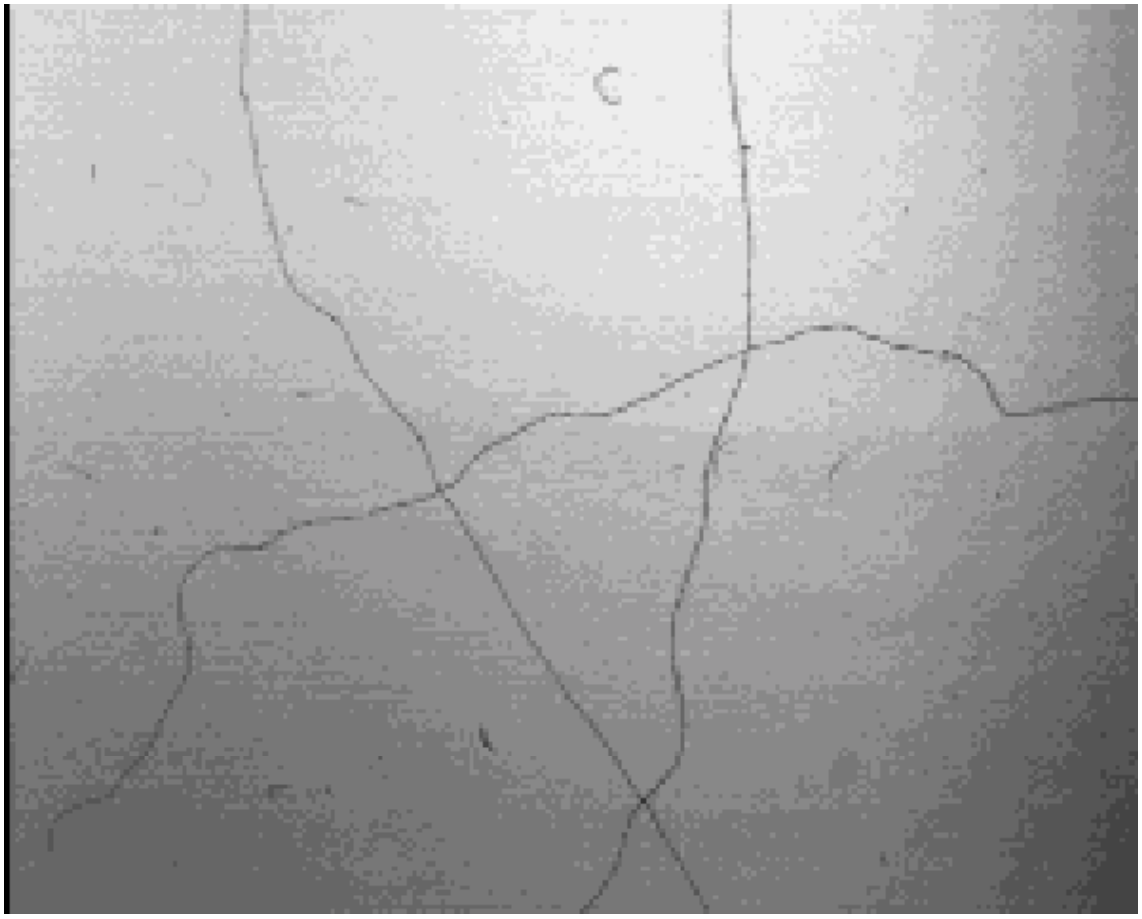

Figure 2.16: Image of three cotton fibers with 256 gray levels.

Thresholding and thinning or skeletonization are common algorithms used for line detection to prepare images for analysis. Thresholding reduces a gray-scale image to a binary image. Since our only concern is to know whether a pixel represents a fiber or background, binary images should work well for our application. If the pixel values of the fiber and the surface are consistent in their respective values over the entire image, then a single threshold value can be found for the image. This use of a single threshold is called *global thresholding.* However, it is possible that images will not have perfect illumination and, thus, will not yield a fixed threshold value for separation of fibers from a surface. In this case, adaptive thresholding can be used. Adaptive thresholding

requires the image to be analyzed locally to determine gray-level intensities at these various locations.

The skeleton of a line pattern is a pixel distribution that is one pixel in thickness and lies wholly within the original line. Ideally, the skeleton lies at the center of the line pattern from which it is derived. Skeletonization is generally done by iteratively removing edge pixels that can be deleted without destroying connectivity. On each iteration, every image pixel is inspected in a 3x3-neighborhood region. A pixel can be deleted if it has more than one and fewer than seven pixels as neighbors and is connected to only one region [76, 78]. Different decision criteria to delete a pixel may produce different results. Figure 2.17 shows the results of different algorithm [24] on letters that look very closely related to fiber crossovers in our application.

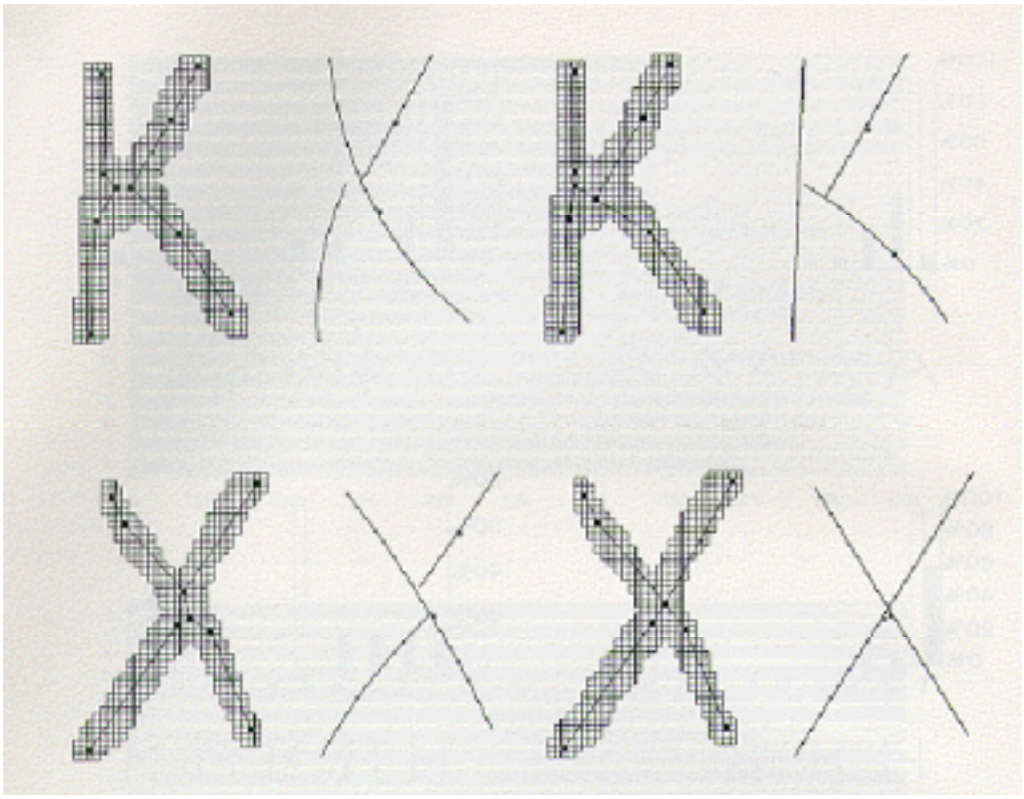

Figure 2.17: Application of different thinning algorithms [24].

Some noniterative thinning algorithms also have been developed to yield the result in a fixed number of steps. In these methods, skeletal points are estimated from distance measurements with respect to opposite boundary points of regions [74]. Some of these methods require joining line segments after thinning to restore connectivity. "In general, noniterative thinning methods are less regularly repetitive, not limited to local operations, and less able to be pipelined, compared to the iterative methods [74]".

A skeletonization algorithm may result in extraneous branches of the skeleton mainly due to noise pixels. A skeleton pruning algorithm [95] cleans extraneous skeleton branches removing the endpoints of an image. In Soille's [95] application all pixels belonging to a chain of the skeleton and lying within a distance of less than 20 pixels from an endpoint are removed.

There are many causes of broken skeletons in an image. Recognition of broken fibers and connection of appropriate pieces is closely related to line detection in related literature such as dashed lines [28, 51, 52, 54]. Estimation of maximum variation from the direction and estimation of maximum distance between broken segments are at the heart of the solution. Pourdeyhimi, Ramanathan and Dent [79] applied a tracking algorithm which assumes that fibers do not undergo severe disruptions or kinks or bends within one pixel distance. Therefore, the directions were limited to a range spanning +45 to –45 degrees relative to the previous direction. On the other hand, Figure 2.18 shows real images of polyester fibers that require 360 degrees of spanning to find appropriate pieces of broken skeletons. (Of course this is related to the magnification).

Random fiber sample preparation will cause many complicated fiber shapes. Crossovers will be the main interaction between and within the fibers. Appropriate

thinning algorithms, as discussed before, can help provide fast and accurate detection of fiber crossovers. Soille [95] introduced a solution to the separation of fiber crossovers. In this solution, a thinning algorithm was applied at the beginning. The skeleton pruning algorithm removed small skeleton branches. The skeleton of the intersection of two fibers generated two rather than a unique multiple point. Then, skeletal lines merged multiple points that were close to each other. The skeletal lines, which lie within the original image, separated the fibers.

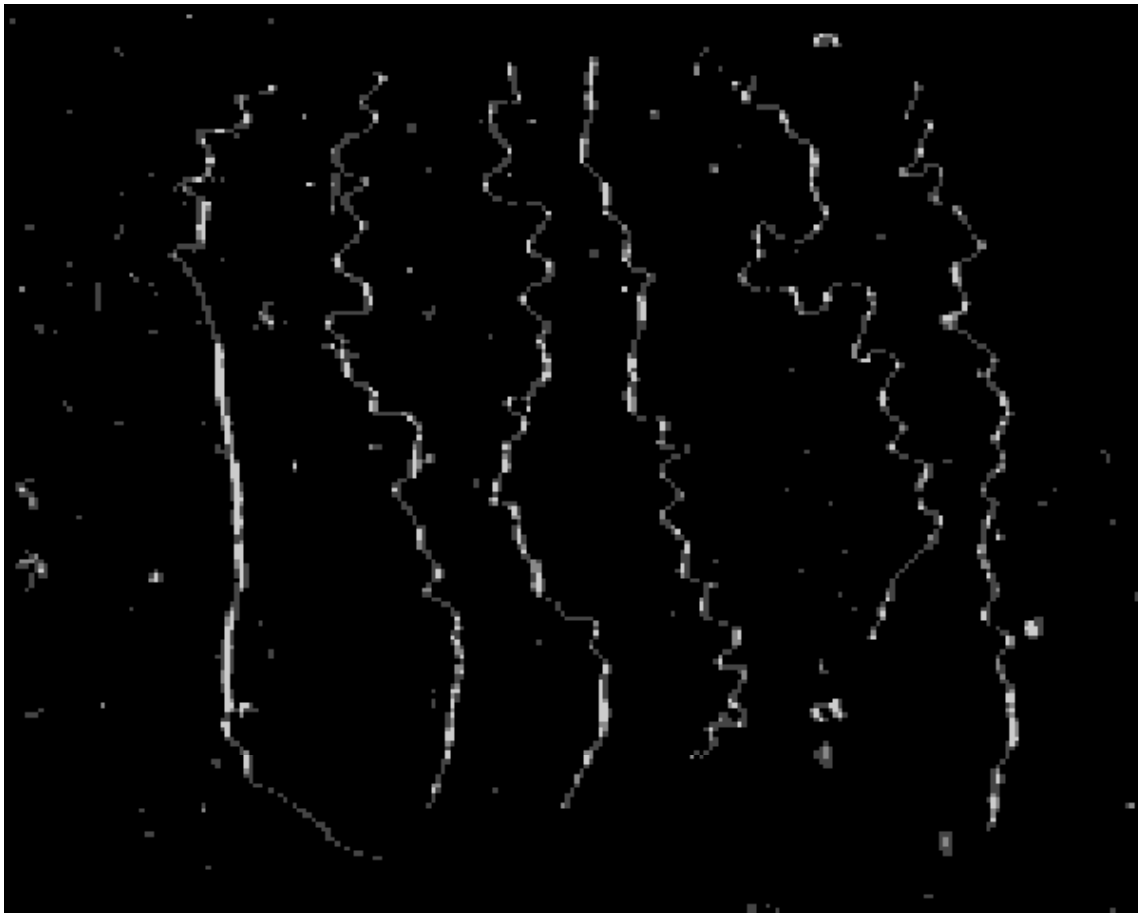

Figure 2.18: Image of 4 gray level polyester fibers with frontlighting technique.

3. RESEARCH APPROACH

Accuracy, precision and time are the main parameters to evaluate the success of a measurement technique. Better accuracy and precision require more analysis time and finding the optimum solution is crucial from an industrial standpoint. Since all the existing cotton length measurement techniques have some weaknesses, there is need for a new measurement technique, especially for the accurate determination of SFC which is desired by industry.

3.1. OBJECTIVE

The main objective of this study is to show that image processing could be an alternative method to the existing cotton fiber length measurement techniques, depending on following factors:

1. Sample preparation
2. Lighting technique
3. Resolution
4. Preprocessing algorithm
5. Processing algorithm

3.2. APPROACH

There are two main parts to this study. The first part is the implementation of length measurement techniques by capturing and analyzing images. Prepared samples were digitized for two lighting techniques and different resolutions. Then, our own software was applied to these images. The second part is the measurement of applied system accuracy, precision and analysis time. These parameters were analyzed and the

best condition was derived for a predetermined confidence interval for the following factors and each treatment.

1. **Sample preparation:** Fiber individualization is the prerequisite of a single fiber length measurement technique. Ideally, the fiber sample should be separated down to individual fibers. Open-end spinning and AFIS system opening units are two successful implementations of fiber individualization. Ulku, Acar, King and Ozipek [105]; and Lawrence and Chen [66], showed fiber individualization and alignment after the opening roller using high-speed photography. Cui, Calamari, Robert and Krowicki [26] found 1-4% fiber breakage in the AFIS system. However, because of natural crimp and waves, cotton fibers have a 3D form. Since our aim is to implement 2D image processing, fibers were brought in 2D form by sandwiching between two transparent surfaces.

   Increasing the number of fibers per given area will result in more interactions between fibers: namely crossovers. Up to a certain point, these interactions can be identified and fibers can be separated from others by image processing. However, in complex cases, it may result in large errors. For better alignment of fibers, patented electrostatic separation [43, 64, 73, 113] offers great application opportunities.

2. **Lighting:** Backlighting gives the highest contrast and is the ideal method to capture binary images. However, because of very small fiber diameters, high resolution is required which means only a relatively small area can be digitized for a given frame. By comparison frontlighting, with powerful light sources, can capture considerably larger areas per frame than backlighting applications with

lower resolution. Both lighting techniques were applied and results have been compared.

3. **Resolution:** High-resolution images give better image quality and also more data for the same number of fibers. However, since processing time is also one of our main concerns, increasing the amount of data does not always improve system performance. From very high to low resolution fiber images were analyzed to find the optimum resolution considering accuracy, precision and processing time.
4. **Preprocessing:** Some possible preprocessing algorithms include: masking, global thresholding, and local thresholding. Global thresholding is the best for its simplicity and efficiency. However, most of the time it does not work for many reasons. Instead, local thresholding and its derivatives often replace global thresholding as we have done in this work.
5. **Processing:** More advanced analysis with image processing algorithms results in more processing time. For example, crossover applications are extremely time consuming algorithms. Iterative thinning use considerable processing time as well. For a given time period, these algorithms can compute analysis of fewer frames of data than relatively simple algorithms such as outlining.

4. EXPERIMENTAL

We developed our own software to measure cotton fiber length and computer processing time and tested for variable measurement conditions to find the optimum processing methods and measurement conditions. Since cotton fibers are so variable and not easy to measure by hand, we used polyester fibers given by the producer to be 1.5-inch (38.1 mm) in length and 1.2-denier. The diameter of the polyester fibers can be calculated as follows:

$$d = \sqrt{\frac{4 \times 1.2g}{\pi \times 1.38 \, g/cm^3 \times 9x10^5 cm}} \times 10^4 = 11.09\mu \qquad \textbf{Equation 4.1}$$

This diameter is the finest range (10 micron) of cotton fibers that would be measured in practice. Even though polyester fiber has a cut length of 1.5 inches, still some variation occurs. For this reason, a skillful person has measured 30 individual polyester fibers by hand.

Differences between cotton and polyester fibers and the impact of these differences are as follows:

1. Cotton has an average length of about 26-mm while the polyester used in this study is about 38-mm.
2. Cotton fiber diameter ranges from 10-micron to 22-micron, while the diameter of these polyester fibers are relatively much more consistent at about 11-micron. It should be easy to detect the thicker cotton fibers if we are able to detect the polyester fibers.
3. Cotton fibers are much straighter than our polyester fibers. These polyester fibers have high crimp that, especially in low-resolution conditions, adds error to the

several algorithms by connecting the closest points of crimps causing loops and, as a result, errors in length measurement.

4. The smooth surface of polyester fibers cause glinting highlights in the frontlighting technique that leads to measurement errors and especially generates noisy images in crossover detection.

The lengths of these polyester fibers were measured with the most common existing methods namely HVI and AFIS . The main objective of these measurements was to show deviations and to prove that better results are necessary.

The Zellweger Uster SPINLAB 900 High Volume Fiber Test System was calibrated for man-made fiber length measurement. This is the method that scans light intensity for given intervals. SPINLAB Fibrosampler 192 was used for sampling. Two sets of data with five replications were collected.

The Uster AFIS Length Module Version 4.00 was calibrated for length measurement. This system is designed only for cotton length measurement; therefore polyester fiber length measurement might be quite variable. The collected data set has 3 replications with 3,000 fibers for a total of 9,000 fiber measurements.

A Kodak Ektapro Hi-Spec Motion Analyzer has been used for image acquisition. It is a CCD camera with 256 gray levels and 238x192 pixel resolution (about 25 micron pixel size) that can capture up to 1,000 frames per second. In our experiments we used only 50 frames per second for better image qualities. SNR (Signal to Noise Ratio) is not given by the producer, but we captured completely black images to inspect the camera sensitivity. Ideally, each pixel has to produce ‘0’ gray level value meaning no light detection. Unfortunately, some pixels produced a ‘10’ gray level value meaning highly

noisy images would be obtained with this camera. Signals from the camera are digitized in the processor and the digitized data are carried to the computer by National Instruments GPIB hardware and software. The data transfer rate of our camera is only 60 Kbytes per second barely more than one frame (46 Kbytes) of information can be carried through the camera to the computer in one second. This number is much improved in other cameras; in fact, latest developments have data transfer rates more than 1,000 times faster than ours.

Our experimental design included: a factorial design with five factors and 72 treatments. The factors are sample preparation, lighting, resolution, preprocessing and processing. For each treatment, length and time were analyzed. Sample size was chosen as 30 in order to have enough data to allow the type of distribution to be determined. Some images were eliminated from the measurements because of errors in image capturing. Table 4.1 shows the experimental design.

4.1. SAMPLE PREPARATION

Two levels of sample preparation are without fiber crossovers and with fiber crossovers. Sample preparation is beyond the goal of this project. However, it is the key issue of image processing success. The condition of fiber delivery will determine image-processing applications. Also, the condition of fibers being delivered to the camera will determine the processing requirements for the system and, therefore, the analysis time required. Well oriented fibers without crossovers can be processed more easily and quickly. Poorly oriented fibers and those with crossovers, require more analysis and therefore, more processing time. It is essential that fibers be individualized. We assumed successful fiber individualization and prepared fibers according to two conditions: with

Table 4.1: Experimental Design

EXPERIMENTAL DESIGN

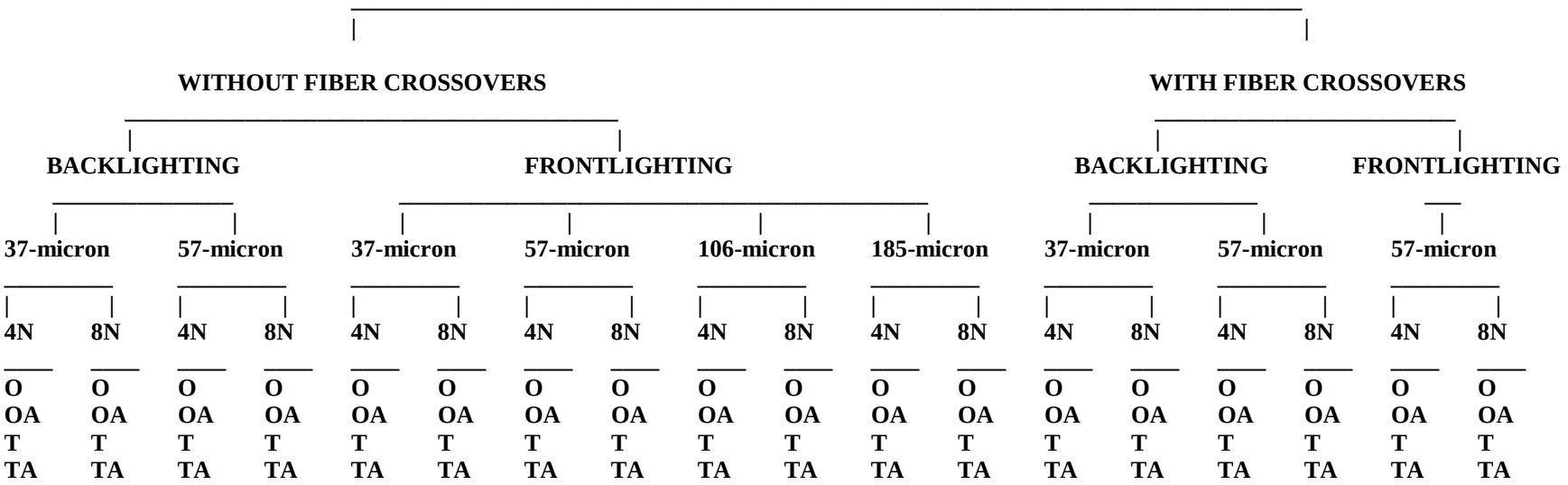

4N-4 Neighborhood thresholding
8N-8 Neighborhood thresholding
O-Outline algorithm for length determination
OA-Outline algorithm including an "Adding" algorithm for connecting broken skeletons
T-Thinning algorithm for length determination
TA-Thinning algorithm including the "adding" algorithm for connecting broken skeletons

and without crossovers. Individual polyester fibers were caught by tweezers and separated from the bundle. These fibers were laid down between two microscope slides in natural conditions if their width fit within the frame, otherwise they were oriented lengthwise without stretching or deforming the original length. For the first condition, images were taken as is. For the second condition, one cotton fiber was added to the surface crossing over the polyester fiber and creating a crossover. A hand-controlled ruler fed prepared microscope slides into the measurement area. Figure 4.3 shows an image with a fiber crossover while Figure 4.4, Figure 4.5 and Figure 4.6 show images without fiber crossovers.

4.2. LIGHTING

Two levels of lighting techniques are backlighting and frontlighting. These techniques create negative images. In backlighting, fibers block incident light creating a shadow on the image and fibers are seen darker on the bright background. In frontlighting, fibers reflect light from the surface creating bright points on the darker background.

A beamsplitter was used for the backlighting technique. Four fiber optic cables carried light from a Fostec 150 W DCR regulated light source to a diffuser. Diffused light was reflected from a beamsplitter, which is placed at 45° to the diffuser to the camera. Beamsplitters are coated material in which part of the light is transmitted and part of the light is reflected. The intensity ratio of the reflected and transmitted components is a function mainly of the difference in refractive index between the two materials in the beamsplitter and the angle of incidence. Only 45° incident light is aimed to reflect from the surface while the remainder of the incident light is allowed to transmit

through the beamsplitter and not interact with the sample. This creates parallel light beams while increasing the contrast and image quality. Higher contrast increases the best threshold selection eliminating noise from the images, eventually causing more accurate and precise measurements.

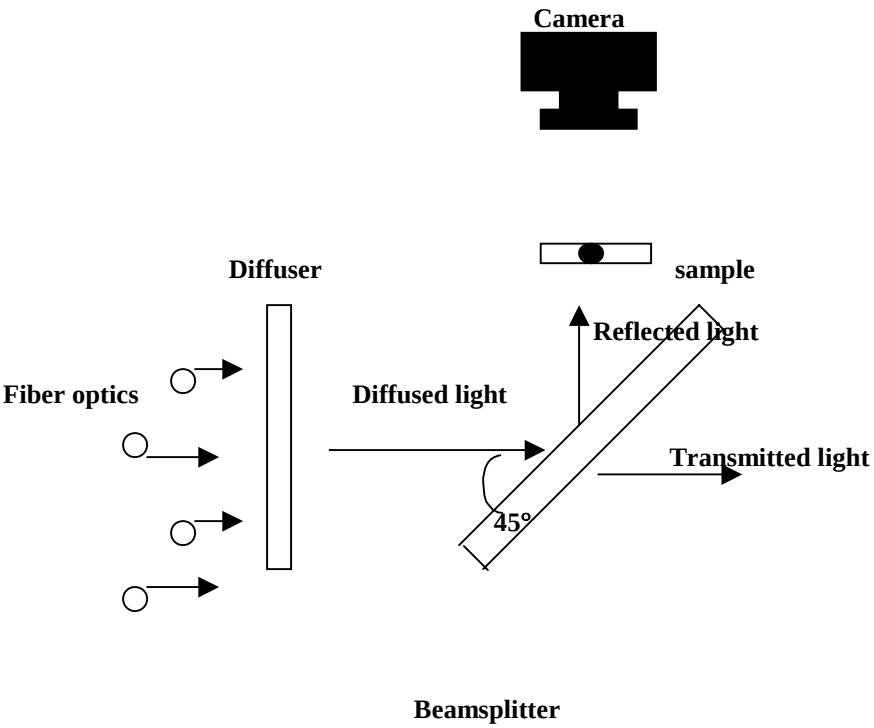

Figure 4.1: Backlighting

Light distribution for the obtained images is highly variable, however. Optic cables produce four bright spots with gradually decreasing lighting areas creating a wave effect on the images. Uneven lighting conditions causes three very important negative effects in analyzing the images:

1. The constructed image from multiple frames has to be treated frame by frame; otherwise uneven light distribution between frames creates long lines in the final image causing measurement errors.

2. Global thresholding cannot be used, causing more analysis time.
3. As contrast is reduced, so does image quality. To protect saturation, the brightest point on the image should be less than the maximum 255 gray level. In addition, a gradual decrease of gray level from the brightest point creates less contrast.

We also used a directional frontlighting technique. In this case, two 75 W narrow spot halogen light sources, perpendicular to each other, were mounted approximately 30 cm from the measurement surface. Our experiments showed that the best angular position of the light sources to the surface is about 10°.

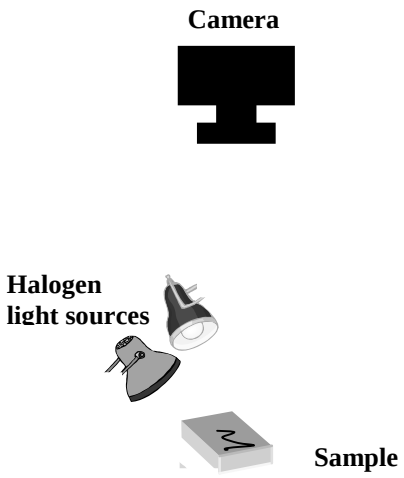

Figure 4.2: Directional frontlighting

The main advantage of this technique is that it is far less dependent on fiber diameter unlike backlighting. The bigger the distance between camera and sample, the stronger the light source we need. A small angle of incident light does not produce too much noise from the surface itself. However, small particles from the air like dust become very shiny points in the image that cause measurement errors. On the other hand, polyester fibers produce specular reflections (bright spots) because of the smooth surface characteristics. Even though frontlighting has relatively much more even light

distribution than backlighting, global thresholding does not work for every condition. Besides, the light intensity on the surface changes for many reasons that each change requires a new global thresholding value. Instead of looking for a global thresholding for every situation we applied local thresholding for frontlighting, too. Figure 4.3 is an example of backlighting image, while Figure 4.4, Figure 4.5 and Figure 4.6 are the examples of frontlighting images. Backlighting images were converted to frontlighting images taking the negatives of them (subtracting each pixel value from the maximum gray level value of 255). This allowed us to use same code for both techniques.

4.3. RESOLUTION

Changing distance between the camera and the sample changes the resolution. A shorter distance results in higher resolution. The highest resolution for our camera results in a pixel size of about 25-micron. For flexibility, we started our experiments at about 37-micron resolution. In this case, each frame captures about 9x7.5 mm area so that one polyester fiber length fits into approximately five frames as in Figure 4.3. Both lighting systems responded with high quality images in terms of fiber detection with this resolution. Next, we decreased the resolution to about 57-microns capturing an area about 14x11.5 mm so that one polyester fiber fits into three frames as in Figure 4.4. Again both systems responded with satisfactory image qualities. In third step, we decreased the resolution to 106-micron level capturing about 25x20 mm area as in Figure 4.5. Single polyester fibers fit into only one frame. And finally we decreased resolution to about 185 micron capturing 44x35 mm area as in Figure 4.6. Two polyester fibers fit into one frame very easily. This was the lowest resolution used for the length measurement.

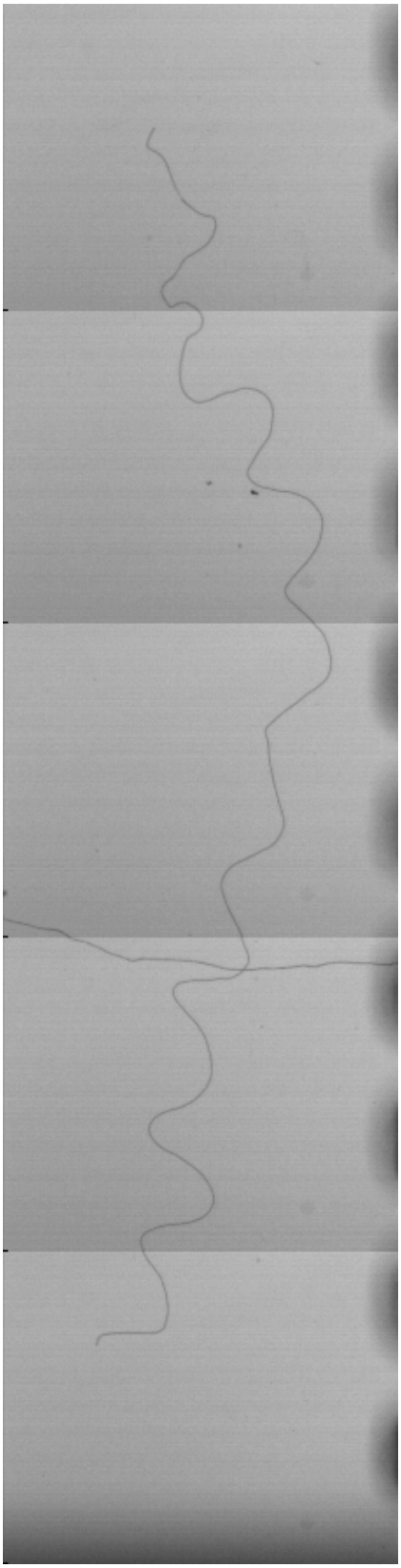

Figure 4.3: 226x884, 37-micron, backlighting

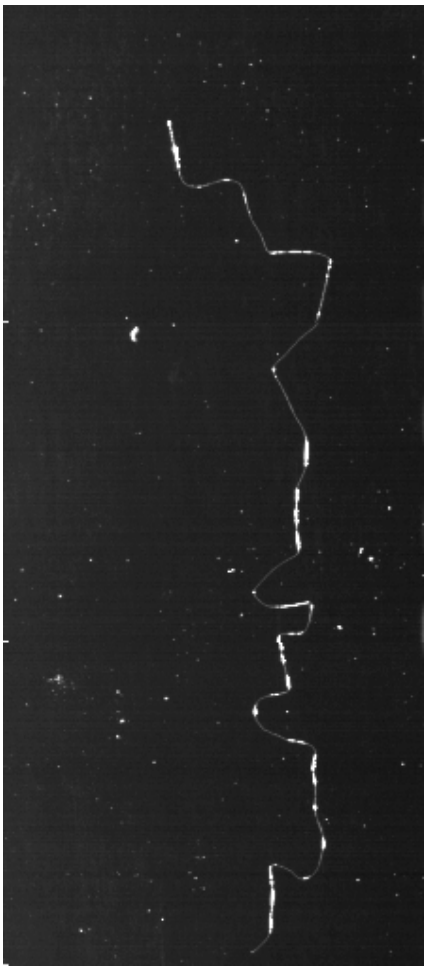

Figure 4.4: 223x508, 57-micron, frontlighting

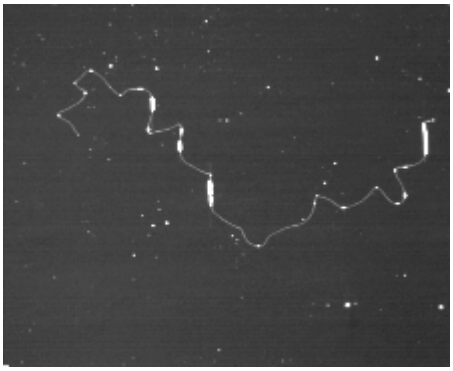

Figure 4.5: 223x189, 106-micron, frontlighting

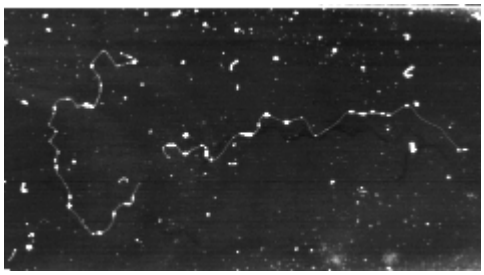

Figure 4.6: 238x133, 185-micron, frontlighting

4.4. PREPROCESSING

Ideally, global thresholding is the best for our application. Checking each pixel for lower or higher gray value than the predetermined threshold value, and assigning each pixel to be only black or white makes the program faster and easier. Unfortunately, as we discussed before, uneven lighting for both lighting conditions does not work for global thresholding. Instead we applied local thresholding. There are many local thresholding applications. Most of them average a 3x3 or 4x4 or bigger area and make the comparison of a specified pixel to this average value. In our case, a direct comparison of 4-neighborhood and 8-neighborhood local thresholding to the reference pixel was applied as in Figure 4.7 and Figure 4.8, respectively.

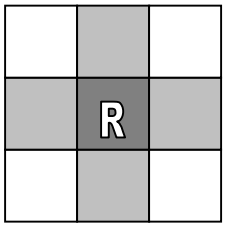

Figure 4.7: 4-neighborhood

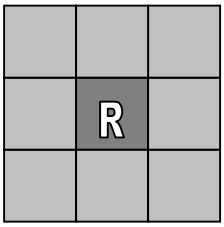

Figure 4.8: 8-neighborhood

A decision criterion is whether the reference pixel (R) has a higher gray level than the predetermined threshold value of one of the colored neighboring pixels. If this is the case, we make the reference pixel white representing the fiber, otherwise we make the

reference pixel black representing the background. Obviously, 4-neighborhood thresholding requires almost half the preprocessing time of 8-neighborhood thresholding. Besides, 8-neighborhood produces more noise thereby causing extra processing time in later stages. However, 8-neighborhood thresholding is safer than 4-neighborhood by means of fewer broken skeletons.

4.5. PROCESSING

Preprocessed images are treated under two conditions: in the first condition, it is assumed that single fibers are totally separated from each other. In the second condition, fibers are assumed to make random crossovers without being entangled. For each condition; outline, thinning and adding algorithms were applied to the images.

Each application has distinguishing characteristics, however, each application uses the chain code to calculate fiber length at the final stage in the same way: either by the outline or the thinning method. The chain code algorithm [8, 78] traces fiber outlines. When the first pixel is detected for a group of white pixels, this pixel location is assigned for the reference point and the reference pixel. While the reference point stays as constant, the reference pixel is relocated for the next connection pixel by inspecting the 8-pixel neighborhood in a clockwise direction as in Figure 4.9. The next connection pixel relative to the reference pixel is either diagonal to the reference pixel as in the directions of 1-3-5-7 or beside the reference pixel as in the directions of 0-2-4-6. Side pixels correspond to movements of unit pixel spacing, while diagonal pixels, being at directions of 45° to the principal axis, correspond to movements of $\sqrt{2}$ times the unit spacing. This search is continued throughout the entire group of white pixels until the reference point is hit again. Meanwhile the program counts all odd and even numbered

connections and assigns a value of 1 unit spacing to the even connections and a value of 1.41 times the unit spacing to the odd numbered connections. The final fiber length will be the total unit spacing times the spatial resolution of the pixels.

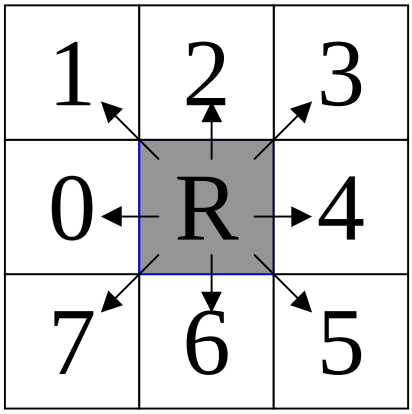

Figure 4.9: Chain code of neighbor pixels.

4.5.1. Outline

The outline procedure is the simplest and most straightforward analysis of the images for length measurement. It is also the fastest algorithm. It is simply a perimeter description of detected white points on the images. If a white pixel has a black neighbor pixel in the directions of 0-2-4-6 of Figure 4.9, this white pixel is assigned as one perimeter pixel of the group. Once the total perimeter length has been determined, it is halved to give the final resulting fiber length measurement. Figure 4.10 shows an outline algorithm applied to the image of Figure 4.5.

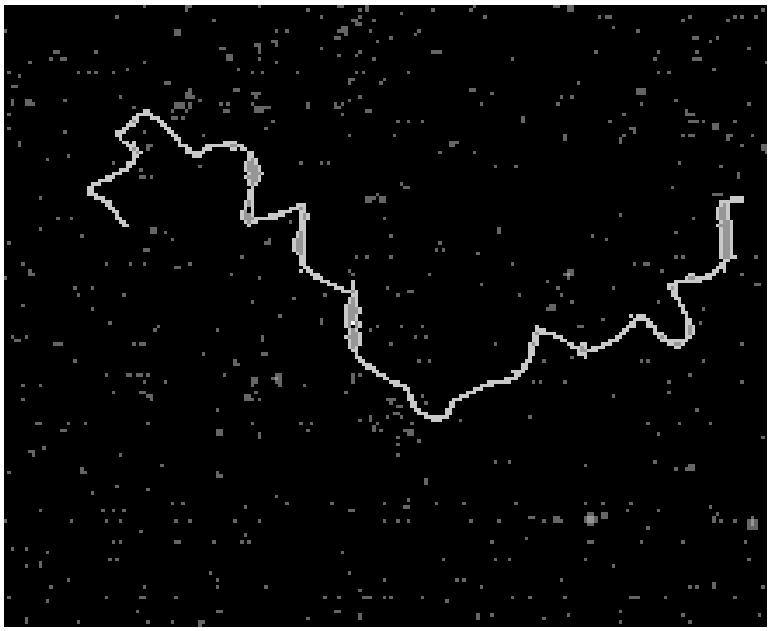

Figure 4.10: Outline applied image

4.5.2. Thinning

An iterative thinning algorithm has also been applied to the images. In the case of thinning, the final fiber image is one pixel in width. Counting the number of neighbors connected to the reference pixel is the first step of the thinning algorithm. If there is no neighbor to the reference pixel, the reference pixel is most likely noise, but it also might be the tracing pixel of a broken skeleton, which can be fixed by a dilation application. If there is only one neighbor to the reference pixel, it may be a true fiber end or, again, a false fiber end caused by a broken skeleton. For all other cases, where the reference pixel sees more than one neighboring pixel, we must inspect the pixel condition. The decision criteria to eliminate a pixel which has more than 1 and less than 7 connection pixels is whether this elimination will create two groups of distinct white pixels on the image.

Thinning produces some unwanted noise creating short branches on the image, which requires a cleaning algorithm to be applied. This algorithm eliminates these

branches from the main fiber image if they are less than five pixels long. For different applications, eliminated branch length could be adjusted shorter or longer. For high-resolution images, this number most likely will be higher. It is important to note that this creates an error possibility if the branch actually represents a fiber crossover. Figure 4.11 shows a resulting fiber image from a thinning algorithm application of Figure 4.5.

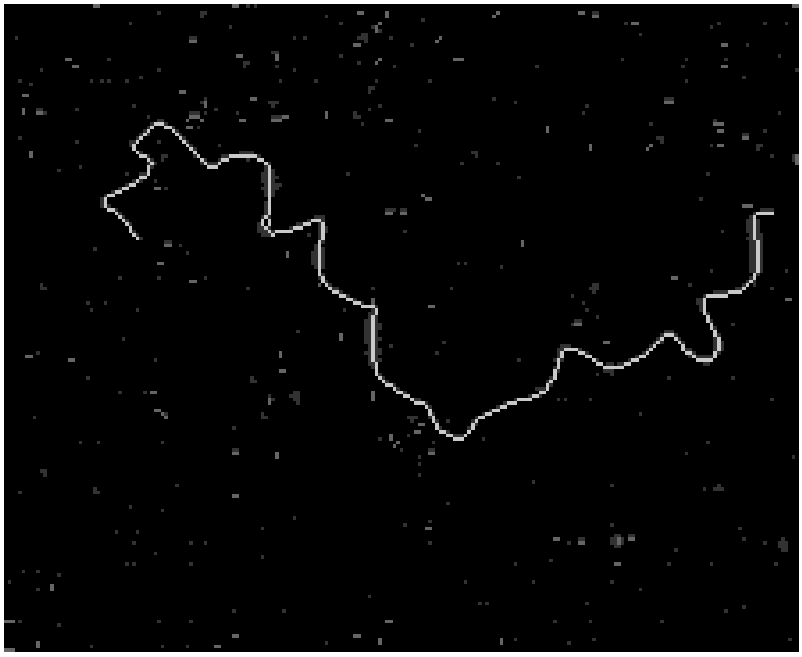

Figure 4.11: Thinning applied image

4.5.3. Erosion and Dilation

This is the connection algorithm for broken skeletons. White pixel groups are made to expand by adding an additional row of white pixels around the perimeter of the original image. After the process is repeated several times (dilation) the reverse process (erosion) is applied for an equal number of times. If two groups of white pixels are connected during dilation, the connection will be retained during erosion. The erosion algorithm works the same as the thinning algorithm.

In our application we applied dilation only once. This will connect two pixels differences between white groups. This number might be increased more which will definitely help to connect broken skeletons but will create more noise connections to the fibers and, in some cases, if two fibers come close to each other, they could be connected to form only one fiber. Resolution, noise production, and the number of fibers per given area are the main considerations to determine the number of pixels for dilation. Figure 4.12 shows an image resulting from the dilation application of Figure 4.5.

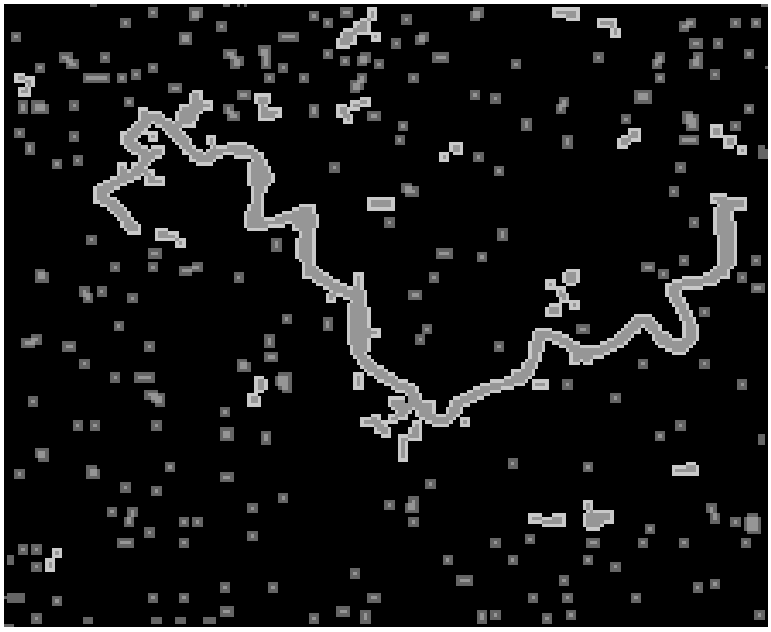

Figure 4.12: Dilation applied image

4.5.4. Crossovers

This is the most complicated algorithm and the most time-consuming for the computer. Many possible rules could be created to detect crossover points. We applied the following procedure:

Algorithm 1: Crossover Detection

Apply thresholding
Apply thinning process

Find white pixels that have more than two connections and assign them to gray level A
Find neighboring A gray level pixels (two A gray level pixels touching one another) and count total number of connections to these pixels
If total number of connections is three, assign gray level A to gray level B
If total number of connections is four, assign gray level A to gray level C
If total number of connections is more than four, assign gray level A to gray level D
Find remaining A gray level pixels and count number of connections and assign them to gray level B, C, and D as before
Starting from one pixel distance to ten pixels distance, match-up B gray level pixels and assign them and pixels between them to gray level C
Find remaining B gray level pixels and assign them to gray level D
Eliminate D gray level pixels and its connected neighborhood from length measurement
Start chain code
If chain code hits a C gray level pixel as a meaning of a crossover, skip next C gray level pixel and continue to search for next available C gray level pixel

Unfortunately, this algorithm is very noise sensitive. If we cannot find a match to a three connected pixel, we have to eliminate the whole set of white pixels from the length measurement or, even though it is a little bit risky, we can eliminate the shortest branch of the three connected pixels. In our application, we chose the elimination of a fiber, which contained unmatched three connection pixels unless a branch was fewer than 5 pixels long.

4.6. STATISTICAL ANALYSIS

Descriptive statistics was used to investigate the accuracy and time requirements of the applied algorithms. An analysis of variance (ANOVA) technique was used to investigate if the observed differences among some factors are statistically significant.

5. PRERESULTS AND PREDISCUSSION

This section is devoted to reporting some results taken from preliminary trials during system development and the discussion of some image processing applications that were not studied as factors in the main experimental design. These applications such as image construction, masking, and threshold selection may directly or indirectly have an important impact on the results. For the purpose of simplifying the text, we will refer to the various algorithms with a sort of shorthand notation. For instance, we will refer to the outlining length measurement algorithm with the adding algorithm (dilation and erosion) included, using a 4-neighborhood thresholding technique as: Outline-adding-4N.

5.1. IMAGE CONSTRUCTION

In high-resolution images, a single polyester fiber did not fit into one frame lengthwise. Multiple frames were captured and a complete fiber image was constructed as in Figure 5.1 and Figure 5.2. A ruler can be seen on the right side of Figure 5.1 which has 1.645 mm dark and light blocks. Each frame has six complete and two incomplete blocks one is at the top and the other one is at the bottom. These incomplete blocks represent the repeating parts of the frames that need to be eliminated. The construction algorithm detects the color change at the right side of the frames counting the number of blocks and eliminating incomplete blocks from the constructed image as in Figure 5.2.

A few problems arose in this application. First, feeding has to be perfectly parallel to the camera position. Otherwise, horizontal movements can cause broken skeletons. Second, detection of blocks on the row can vary one or two pixels because of poor lighting conditions or lack of focus on the image and this can cause horizontally oriented fiber segments to be detected as broken skeletons. The camera was focused on

the fibers and the ruler was one microscope slide thickness away from the focus point. This distance makes a difference in the high-resolution images by making the ruler edges slightly out of focus. Third, this process collects unnecessary repeated information: the parts of the image which are discarded. And finally, image capture and construction are time consuming processes.

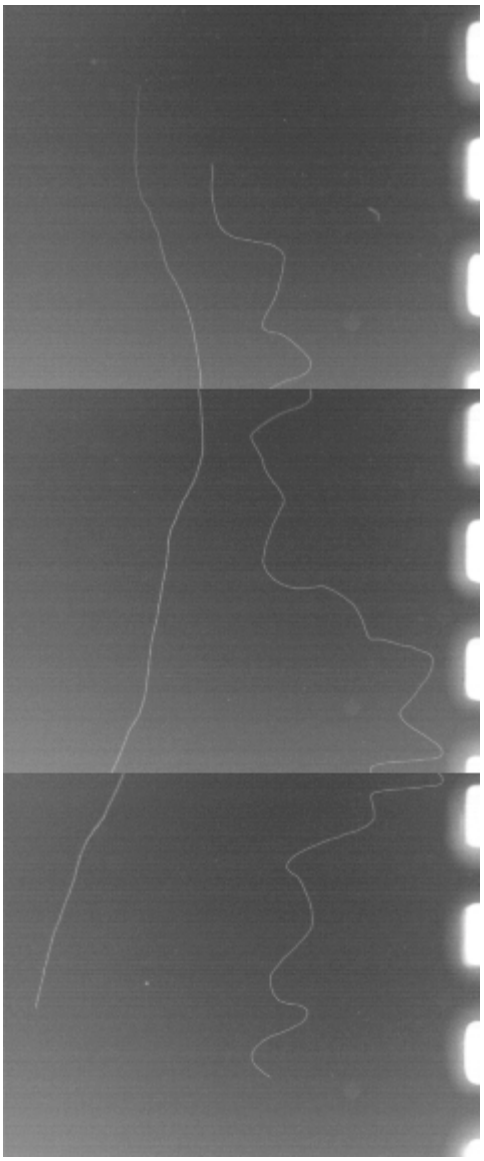

Figure 5.1: Original image from camera

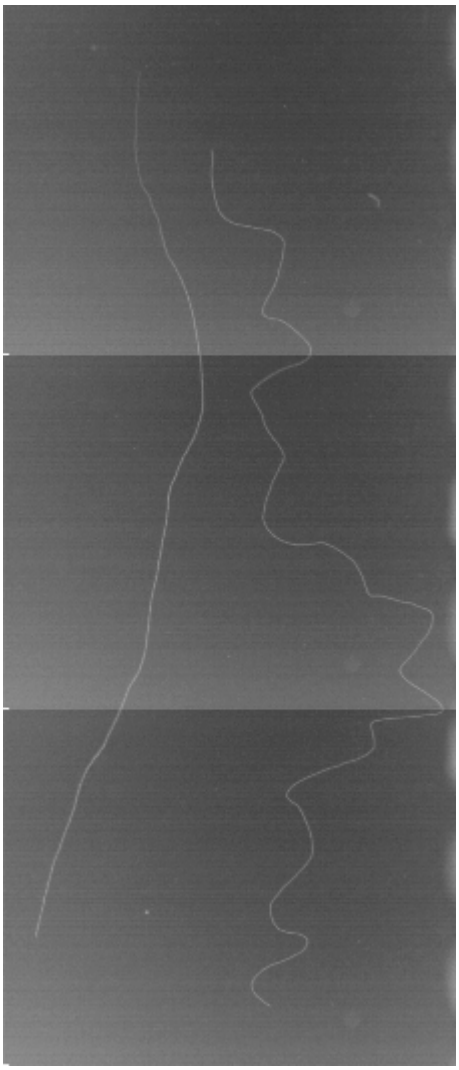

Figure 5.2: Constructed image

5.2. MASKING

Masking would be another preprocessing application. Basically, it involves the multiplication of the reference pixel gray level by its neighbors, which produces higher or lower contrast on the total image. Technically, masking can be seen as a high-pass or low-pass filter application. We thought that a high-pass filter could produce higher contrast and, as a result, better detection and better results. However, it did not turn out to give the desired results. Of course, it produced higher contrast on the image, but it also produced more broken skeletons. By contrast, a low-pass filter helped to connect broken skeletons to some point. However, it expanded the perimeter of fibers giving the result of added noise to the image which caused added measurement error. As a result, masking was not used in the study. Results of low-pass and high-pass filter applications to original Figure 4.5 are given in Figure 5.3 and Figure 5.4.

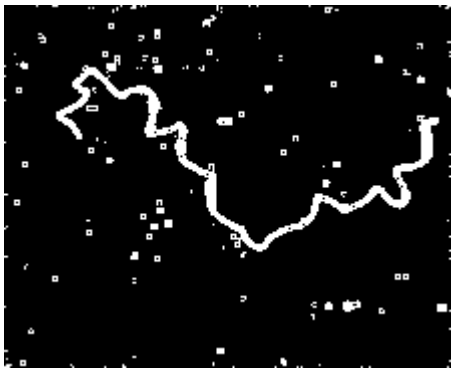

Figure 5.3: Low-pass filter applied

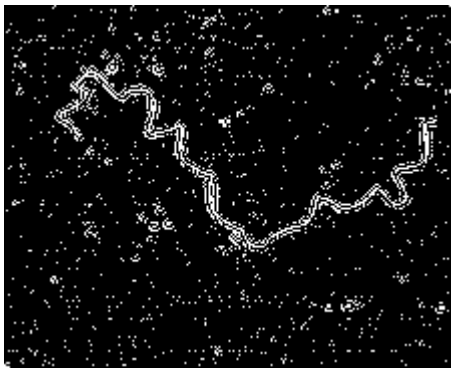

Figure 5.4: High-pass filter applied

5.3. THRESHOLD SELECTION

Thresholding is a process used to analyze a raw image and convert it to an image with only 2 gray levels: white and black. The threshold is a value used to make the decision of whether a given reference pixel should be white or black. Selection of the threshold value has a great impact on the resulting image. The threshold was not

considered as a factor in our applications, instead it was determined preliminarily according to which value gave the best results. It is important to know how sensitive the image is to the threshold value and what procedure we used to choose the best threshold.

For our purposes, 10 gradually increasing threshold values were applied to each image starting from the lowest thresholding value to the highest. The optional values changed for different algorithms and resolutions. For example, the lowest threshold value tested was 6 for the outline algorithm while it was 9 for the outline algorithm with adding. Appendix A shows descriptive statistics of selected length and time measurements of backlighting 37-micron resolution images in the order of Outline-4N, Outline-8N, Thinning-4N, Thinning-8N, Outline-adding-4N, Outline-adding-8N, Thinning-adding-4N, Thinning-adding-8N. Figures 5.5-5.10 show the influence of threshold value on the resulting image.

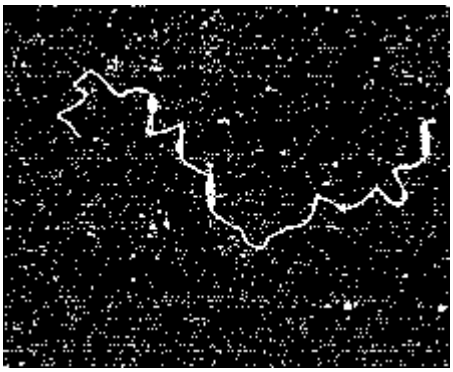

Figure 5.5: 4-neighborhood, threshold 6

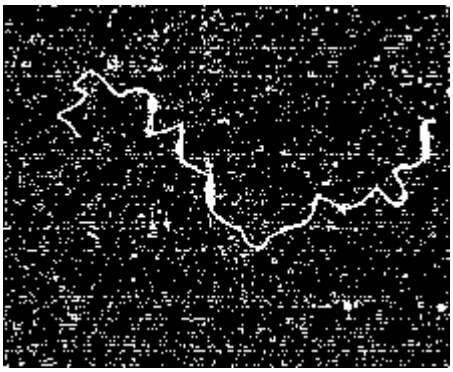

Figure 5.6: 8-neighborhood, threshold 6

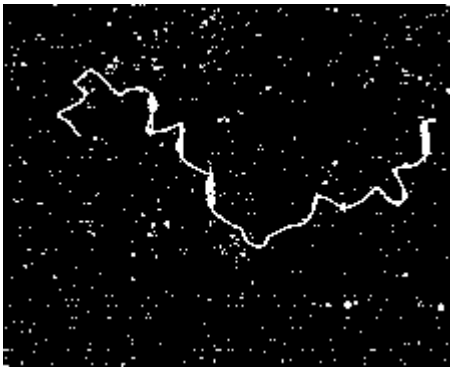

Figure 5.7: 4-neighborhood, threshold 8

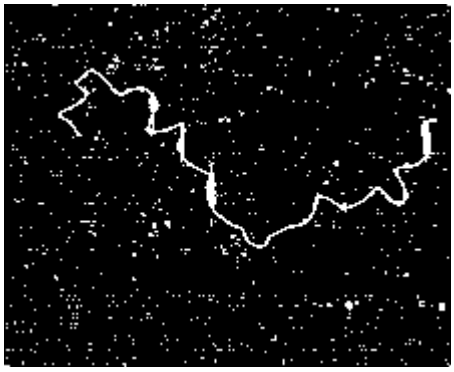

Figure 5.8: 8-neighborhood, threshold 8

Figure 5.9: 4-neighborhood, threshold 20

Figure 5.10: 8-neighborhood, threshold 20

Appendix A shows that when the threshold value was 6, 7 and 8, all images captured enough contrast to see the fibers as a whole for the outline and thinning algorithms. However, when the threshold value was increased to 9, two images out of 29 created broken skeletons measuring more than one fiber, which should have been one single fiber. When the threshold was 15, only two images out of 29 produced images without broken skeletons. Conclusively, lower threshold values reduced the risk of broken skeletons. On the other hand, lower threshold values caused longer length measurements due to added noise in the image which was sometimes added to the fiber image. The average length of twenty-nine measurements was about 50 mm for threshold 6, 45 mm for threshold 7, and finally 42.8 mm for threshold 8 using the outline application. Results show logarithmic function characteristics. For a given length of 38.1 mm, results show very significant variation. Threshold 6 produced results which were different than threshold 7, with statistical significance. The same was true for a comparison of threshold 7 and threshold 8. Standard deviation, standard error and confidence interval were also increased, proving variation increased when threshold gray value was reduced. Analysis time showed almost a proportional negative correlation with the chosen threshold value meaning lower threshold values required more analysis

time (Table A.2). The reason is: lower threshold values produced more noise and consequently, more white points, each of which, must be analyzed on the image.

As expected, 8N images produced more noise which resulted in more white points, greater analysis time, and longer length measurements than 4N images for the same threshold values (Table A.3). On the other hand, the best threshold value for 8N images was usually one gray level higher than the 4N images. This difference made the length measurements more or less the same for two different neighborhood thresholding applications. However, the 8N thresholding generally was more time consuming than 4N applications.

Appendix A shows that threshold values are not as critical for the outlining procedure as for the thinning procedure in terms of analysis time and length measurement, but still cause statistically significant differences in results (Table 9 and 10). As a conclusion, the highest threshold value that does not cause broken skeletons is the best value for our purposes for the outline and thinning applications. On the other hand, the purpose of the adding algorithms is to find broken skeletons on the image. That is why the best threshold was the value that allowed a maximum of two pixels distance between adjacent ends of broken skeletons. The best threshold value increased to 12 for 4N and 13 for 8N thresholding for the adding application. It removed great deal of noise from the images. The best threshold value was observed for each algorithm, then fiber length and analysis time were recorded for the procedure using this threshold value.

5.4. FIBER ORIENTATION

In the high-resolution images, one fiber fit into five frames. Fibers were oriented lengthwise to fit into the frame and fed to the measurement area in the vertical direction.

In order to determine if the system was sensitive to direction of fiber orientation, an experiment was designed in which we measured individual fibers in different orientations. Here, we arranged the fiber vertically with respect to the camera for the first analysis, then remounted it at approximately 90° to the original orientation for a second length analysis. For a strong comparison, 18 fibers were measured in the horizontal direction using the same threshold value of 29 vertical measurements. Results and single factor ANOVA for the vertical and horizontal directions are given in Appendix B. The outline algorithm was found significantly different for 4N and 8N applications in 95% confidence interval. The other six algorithms measured statistically the same length. All measurements in the horizontal direction had lower average values than those in the vertical direction. The most logical explanation for this is the lighting conditions. The system setup was changed, so the lighting conditions changed as well. If the focus point of the camera is on the bright spots of the beamsplitter, it creates higher contrast in the image. Higher contrast results in more accurate measurement unless saturation occurs.

5.5. IMAGE PROCESSING VARIATION SOURCES

Since polyester fibers have a specific cut length, all fibers should be the same length with some small natural variation. Hand-measurement results showed significant variations in length measurements. However, it is not easy to address whether that variation came from fiber-to-fiber variation or because of human error factors during measurement. Image processing applications also showed natural variation for which it was difficult to determine the source: fiber-to-fiber variation or measurement-to-measurement variation. To address this question, a single fiber was mounted and measured in three unique positions and with four angles with respect to the camera, for

each position using the 37-micron resolution and backlighting technique discussed in the next chapter. A total of twelve images were obtained for this fiber. We stopped with only 3 mountings so as not to deform the fiber as a result of the manual manipulation. Results are given in Appendix C. ANOVA shows the comparison of the twelve same fiber measurements and 29 different fiber measurements. None of the image processing applications produced statistically significant differences for these sets of images. As a conclusion, most of the variation from the hand measurements came from measurement-to-measurement difference rather than fiber-to-fiber.

6. RESULTS AND DISCUSSION

To be an alternative to existing fiber length measurement systems, image-based fiber length measurement must have precise results in a reasonable amount of processing time. The desired time for measurement of a population distribution should be less than 30 seconds (given by industry expectations). However, there is not currently a standard for single fiber length measurement precision. Arguably, the confidence interval was chosen as a precision limit by the following procedure. Cotton length is classified with 0.03-inch intervals equal to 0.762 mm. Our ultimate goal was to be able to measure the length distribution with a 95% confidence interval, which is less than +/-0.4 mm for approximately 1-inch mean length cotton fibers. The confidence interval should be proportional to the mean length so that for the same level of precision, a confidence interval is more than 0.5 mm for 1.5-inch polyester fibers. Therefore a 0.5 mm confidence interval was chosen as the limit of acceptable precision for polyester fiber images in this work.

6.1. HAND-MEASUREMENT

Hand-measurement results show similar characteristics to historical data that have been obtained from North Carolina State University, Physical Testing Laboratory. Table 6.1 shows hand measurement results. All reported measurements were shorter than the given cut length (38.1 mm), and varied between 36-38 mm. Mean length is about 1.5 mm less than the given cut length and the 95% confidence level is about 0.26 mm. Arguably, these numbers show low accuracy and high precision. Using relatively straight cotton fibers might improve this measurement accuracy for hand-measurement. The confidence interval was in the range of our chosen required limit of 0.5 mm as discussed above.

Table 6.1: 30 individual polyester fiber hand-measurement results

38.1 mm Polyester	
Mean	36.66667
Standard Error	0.129839
Median	37
Mode	36
Standard Deviation	0.711159
Sample Variance	0.505747
Kurtosis	-0.75753
Skewness	0.593507
Range	2
Minimum	36
Maximum	38
Sum	1100
Count	30
Confidence Level(95.0%)	0.265551

6.2. IMAGE PROCESSING

In the first step, samples without fiber crossovers were prepared for different lighting techniques and resolutions. In the second step, samples with fiber crossovers were prepared. Applied and discussed algorithms were outline-4N, outline-8N, outline-adding-4N, outline-adding-8N, thinning-4N, thinning-8N, thinning-adding-4N, and thinning-adding-8N.

6.2.1. Without Fiber Crossover-37 micron Resolution-Backlighting

Twenty-nine images were captured and analyzed for 37-micron resolution and backlighting for the best threshold values. In one instance, the adding algorithm connected a fiber to noise at the edge of the image. We necessarily have a decision criteria in the algorithm which eliminates a fiber if it touches the edge of the image since we cannot, as a result, be certain to have an image of the entire fiber. Therefore, no result was obtained for this image as can be observed from Figure 6.1 and Figure 6.2. Figure 6.1 shows the length measurement results that can be divided into three regions. The top

region shows individual fiber length measurements for the outline 4N and 8N thresholding applications. The data points are connected with a line only as a means of denoting that they were all measured with the same algorithm and for ease of viewing and comprehending the data. The middle region shows results of the same images using outline-adding with 4N and 8N thresholding. The bottom region shows results of the thinning applications, again with the same original raw fiber images. Results show that the adding algorithm slightly improved the accuracy of the thinning algorithm while it had an even greater positive effect on the accuracy of the outline algorithms. There are high correlations among the length measurements of the various applied algorithms from sample-to-sample. Each application has some tendency to measure the fiber length either longer or shorter compared to the others. Figure 6.2 shows normalized analysis time of 100 Kbytes images. There is a considerable difference between the outline and thinning applications. The top application in Figure 6.1 becomes the bottom in Figure 6.2 meaning better accuracy requires more analysis time.

The best threshold value was found to be 8 gray levels for the outline-4N algorithm. Table 6.2 shows that the mean length of the outline-4N is 42.8 mm with a range of 3.5, 4.7 mm greater than the given cut length. The confidence interval is 0.33 mm which is greater than the hand-measurement confidence interval of 0.26 mm but lower than our chosen limit of 0.5 mm. The analysis time is 74 ms for 100 Kbytes (Table 6.3), meaning 40 Mbytes of data can be analyzed in 30 seconds.

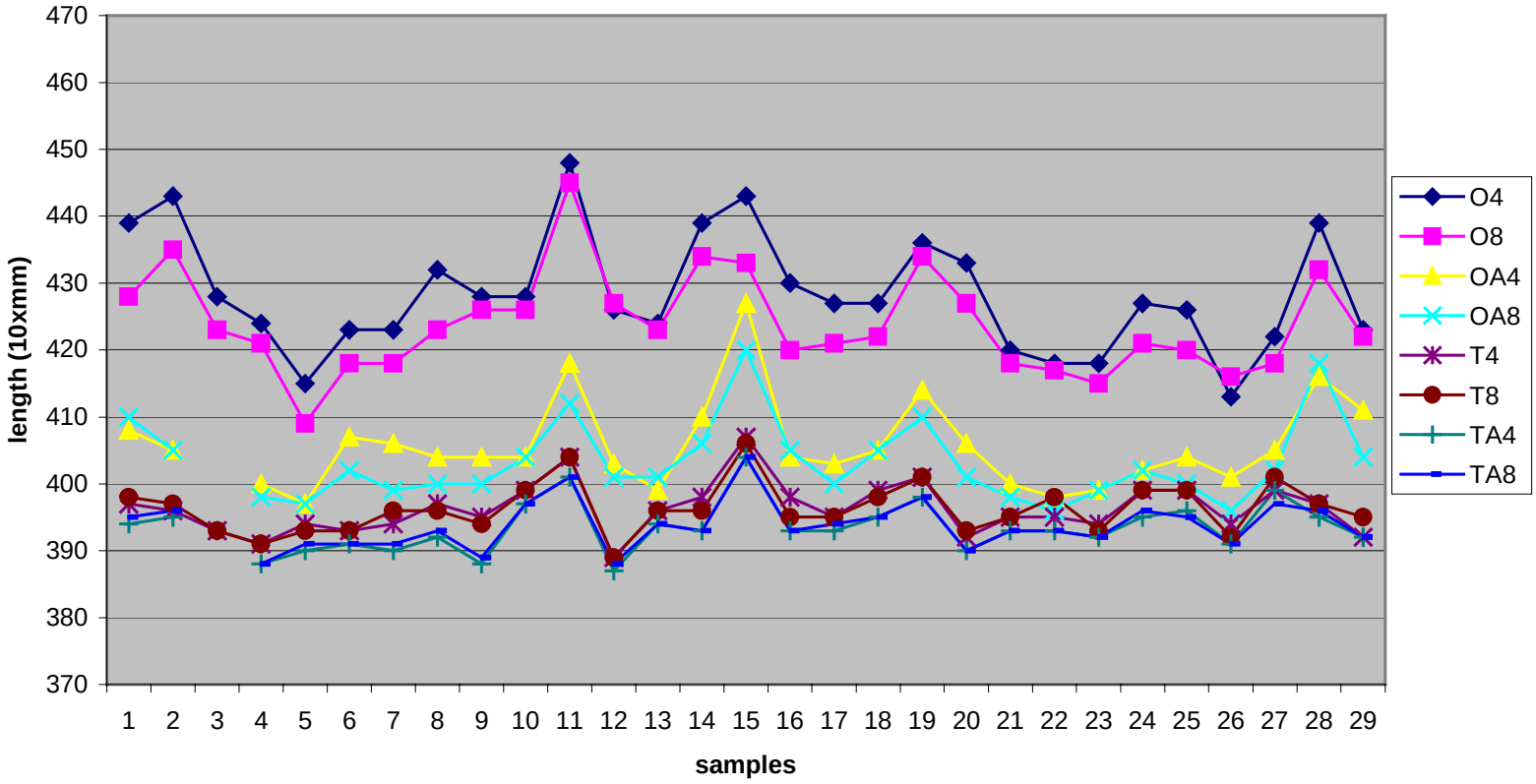

Figure 6.1: Length measurement results of images without crossover-backlighting-37 micron resolution (10xmm)

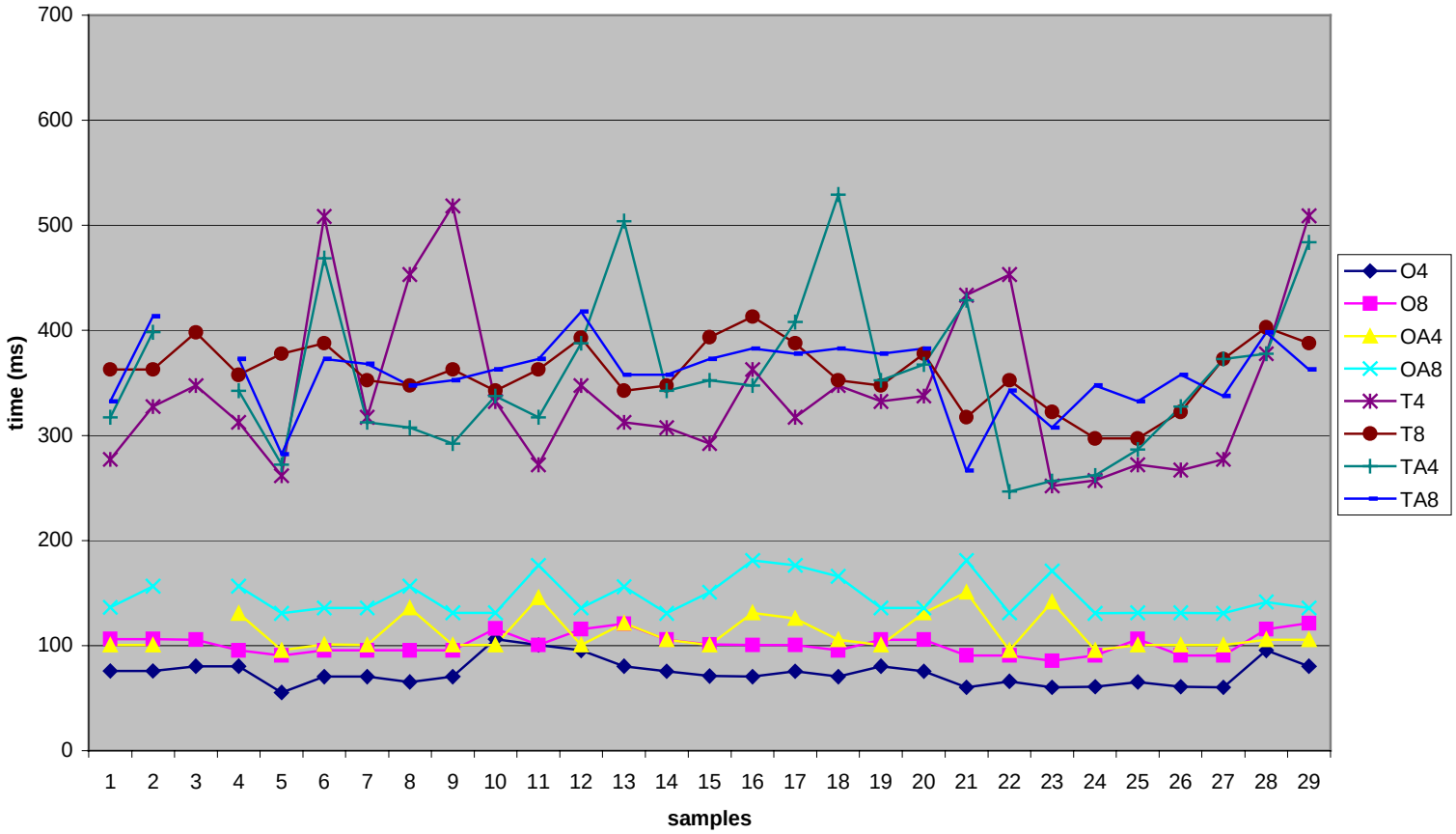

Figure 6.2: Analysis time of 100 Kbytes images without crossover-backlighting-37 micron resolution (ms)

Table 6.2: Length measurement results of images without crossover-backlighting-37 micron resolution (10xmm)

OUT-4N-8 --> OUTLINE-4 NEIGHBORHOOD-Threshold 8
OUT-8N-9 --> OUTLINE-8 NEIGHBORHOOD-Threshold 9
OUT-ADD-4N-12--> OUTLINE-4 NEIGHBORHOOD-Threshold 12
OUT-ADD-8N-13--> OUTLINE-8 NEIGHBORHOOD-Threshold 13

THIN-4N-8 --> THINNING-4 NEIGHBORHOOD-Threshold 8
THIN-8N-9--> THINNING-8 NEIGHBORHOOD-Threshold 9
THIN-ADD-4N-12--> THINNING-4 NEIGHBORHOOD-Threshold 12
THIN-ADD-8N-13--> THINNING-8 NEIGHBORHOOD-Threshold 13

OUT-4N-8	
Mean	428.3448
Standard E	1.619825
Median	427
Mode	439
Standard D	8.723023
Sample Va	76.09113
Kurtosis	-0.261808
Skewness	0.486894
Range	35
Minimum	413
Maximum	448
Sum	12422
Count	29
Confidence	3.318064

OUT-8N-9	
Mean	423.8621
Standard E	1.395563
Median	422
Mode	418
Standard D	7.515337
Sample Va	56.4803
Kurtosis	1.012316
Skewness	0.774525
Range	36
Minimum	409
Maximum	445
Sum	12292
Count	29
Confidence	2.858685

OUT-ADD-4N-12	
Mean	405.7143
Standard E	1.25447
Median	404
Mode	404
Standard D	6.638034
Sample Va	44.06349
Kurtosis	2.865971
Skewness	1.51016
Range	30
Minimum	397
Maximum	427
Sum	11360
Count	28
Confidence	2.573959

OUT-ADD-8N-13	
Mean	403.25
Standard E	1.139276
Median	401.5
Mode	400
Standard D	6.028482
Sample Va	36.34259
Kurtosis	1.746424
Skewness	1.384442
Range	24
Minimum	396
Maximum	420
Sum	11291
Count	28
Confidence	2.3376

THIN-4N-8	
Mean	396.2759
Standard E	0.708667
Median	396
Mode	399
Standard D	3.816286
Sample Va	14.56404
Kurtosis	1.27624
Skewness	0.757738
Range	18
Minimum	389
Maximum	407
Sum	11492
Count	29
Confidence	1.451639

THIN-8N-9	
Mean	396.2759
Standard E	0.698162
Median	396
Mode	393
Standard D	3.759716
Sample Va	14.13547
Kurtosis	0.684279
Skewness	0.622066
Range	17
Minimum	389
Maximum	406
Sum	11492
Count	29
Confidence	1.430121

THIN-ADD-4N-12	
Mean	393.5357
Standard E	0.731893
Median	393
Mode	393
Standard D	3.872813
Sample Va	14.99868
Kurtosis	0.924497
Skewness	0.746989
Range	17
Minimum	387
Maximum	404
Sum	11019
Count	28
Confidence	1.501719

THIN-ADD-8N-13	
Mean	393.7857
Standard E	0.688832
Median	393
Mode	393
Standard D	3.644957
Sample Va	13.28571
Kurtosis	1.205692
Skewness	0.798018
Range	16
Minimum	388
Maximum	404
Sum	11026
Count	28
Confidence	1.413366

Table 6.3: Analysis time of 100 Kbytes images without crossover-backlighting-37 micron resolution (ms)

OUT-4N-8 --> OUTLINE-4 NEIGHBORHOOD-Threshold 8
OUT-8N-9 --> OUTLINE-8 NEIGHBORHOOD-Threshold 9
OUT-ADD-4N-12--> OUTLINE-4 NEIGHBORHOOD-Threshold 12
OUT-ADD-8N-13--> OUTLINE-8 NEIGHBORHOOD-Threshold 13

THIN-4N-8 -->THINNIN(4 N
THIN-8N-9--> THINNING-8 NEIGHBORHOOD-Threshold 9
THIN-ADD-4N-12--> THINNING-4 NEIGHBORHOOD-Threshold 12
THIN-ADD-8N-13--> THINNING-8 NEIGHBORHOOD-Threshold 13

OUT-4N-8		*OUT-8N-9*		*OUT-ADD-4N-12*		*OUT-ADD-8N-13*	
Mean	74.35728	Mean	101.2244	Mean	111.8277	Mean	146.4449
Standard E	2.335795	Standard E	1.822616	Standard E	3.248608	Standard E	3.362076
Median	70.923	Median	100.6	Median	100.8515	Median	135.81
Mode	80.48	Mode	95.57	Mode	100.6	Mode	135.81
Standard D	12.57864	Standard D	9.815089	Standard D	17.19002	Standard D	17.79043
Sample Va	158.2222	Sample Va	96.33598	Sample Va	295.4968	Sample Va	316.4995
Kurtosis	0.605938	Kurtosis	-0.533043	Kurtosis	-0.382586	Kurtosis	-0.748687
Skewness	0.92482	Skewness	0.536669	Skewness	1.04453	Skewness	0.869377
Range	50.803	Range	35.713	Range	55.33	Range	50.3
Minimum	55.33	Minimum	85.51	Minimum	95.57	Minimum	130.78
Maximum	106.133	Maximum	121.223	Maximum	150.9	Maximum	181.08
Sum	2156.361	Sum	2935.508	Sum	3131.175	Sum	4100.456
Count	29	Count	29	Count	28	Count	28
Confidence	4.784665	Confidence	3.733465	Confidence	6.665589	Confidence	6.898405
THIN-4N-8		*THIN-8N-9*		*THIN-ADD-4N-12*		*THIN-ADD-8N-13*	
Mean	344.2948	Mean	360.0786	Mean	357.148	Mean	358.5492
Standard E	14.64774	Standard E	5.566783	Standard E	13.99507	Standard E	6.380102
Median	327.453	Median	362.663	Median	345.058	Median	362.663
Mode	347.573	Mode	362.663	Mode	317.393	Mode	372.723
Standard D	78.88051	Standard D	29.97804	Standard D	74.05497	Standard D	33.76033
Sample Va	6222.135	Sample Va	898.683	Sample Va	5484.138	Sample Va	1139.76
Kurtosis	0.140724	Kurtosis	-0.263301	Kurtosis	0.074741	Kurtosis	1.588506
Skewness	1.047093	Skewness	-0.38218	Skewness	0.730671	Skewness	-0.936308
Range	266.59	Range	115.69	Range	282.686	Range	151.403
Minimum	252.003	Minimum	297.273	Minimum	246.47	Minimum	266.59
Maximum	518.593	Maximum	412.963	Maximum	529.156	Maximum	417.993
Sum	9984.55	Sum	10442.28	Sum	10000.14	Sum	10039.38
Count	29	Count	29	Count	28	Count	28
Confidence	30.00458	Confidence	11.40305	Confidence	28.7155	Confidence	13.09088

The best threshold value was found to be 9 for the outline-8N. Table 6.2 shows that the mean length of the outline-8N is 42.3 mm, and confidence interval is 0.28 mm, both accuracy and precision are better than the outline-4N. For the same threshold value, it is expected that the 8N thresholding would produce longer length measurements and higher variations than the 4N. However, the higher threshold value eliminated a great amount of noise from the images as discussed before which resulted in the improved accuracy and precision. Slightly better length measurement results of the 8N over the 4N were also observed for the adding and thinning algorithm applications as in Table 6.2.

The best threshold values for the adding algorithm were found to be 12 and 13 for the 4N and 8N thresholding respectively. The adding algorithm significantly improved the length measurement of the outline algorithm by means of accuracy and precision while causing about 40% more analysis time. Table 6.2 shows that the confidence interval is reduced after the adding algorithm applications is included and, in fact, results in greater precision than the hand-measurement results.

The thinning algorithm produced superior results to the outline algorithm in terms of both accuracy and precision as in Table 6.2 while the processing time was measured as more than double as in Table 6.3. Average length was measured as less than 40 mm with a maximum of 1.5 mm over the given cut length as in Table 6.2. Hand-measurement results were 1.5 mm lower than the given cut length, therefore, with the given cut length as the reference value, hand-measurement and thinning algorithms provided almost the same accuracy. However, precision of the thinning algorithm was significantly better than hand-measurement precision by comparison of the confidence intervals 0.14 mm and

0.26 mm respectively. On the other hand, the adding algorithm application to the thinned images did not produce a significant difference in accuracy, precision or time.

The most important result was that each application except outline-4N and outline-8N had smaller confidence intervals (better precision) than hand-measurement. Conclusively, image analysis can measure fiber length more precise than hand-measurement in 37-micron resolution with backlighting. On the other hand, each algorithm measured fiber length longer than the hand-measurement results and longer than the producer stated cut length of 38.1 mm.

The 4N and 8N thresholding applications produced small but significantly different results in length measurement for outlining while with all other algorithms, the differences were not significant. However, there was a general tendency that the 8N thresholding produced less measurement variation since we observed all confidence intervals and standard errors were lower than for the 4N. On the other hand, the 8N thresholding caused significantly more analysis time for the outline and outline-adding algorithms as seen in Table 6.3.

Observing Table 6.2, the thinning-adding-8N produced the lowest confidence interval and thinning-adding-4N produced the lowest mean length. As a conclusion, the thinning-adding algorithm had the best results in terms of accuracy and precision. However, this does not necessarily imply that the thinning-adding algorithm is the best image processing application for 37 micron-backlighting images. Since all algorithms are in the range of the predetermined precision limit of 0.5 mm, the fastest algorithm, which is the outline-4N, would be the best choice. It is about 5 times faster than the most precise algorithm: thinning-adding-8N.

6.2.2. Without Fiber Crossover-37 micron Resolution-Frontlighting

Twenty-nine images were captured and analyzed with 37-micron resolution and frontlighting in order to determine the best threshold values. The most interesting result was obtained from the outline-4N. Even the lowest threshold value produced broken skeletons on some images. These results proved the risk involved with the 4N application without the adding algorithm. Figure 6.3 and Figure 6.4 shows that for high resolution, frontlighting results in more accurate and precise length measurement and less processing time than backlighting (Figure 6.1 and Figure 6.2).

The best threshold value was found to be 9 for the outline-8N with frontlighting. Mean length is about 40.6 mm with a 0.174 mm confidence interval which shows that accuracy and precision are much better than with backlighting. Besides, analysis time is much lower with frontlighting. Since the best threshold values are the same for frontlighting and backlighting implying the same contrast level, the most logical explanation for better results would be that less noise is produced with the frontlighting technique.

The best threshold values were observed as 13 with the adding algorithm for both 4N and 8N thresholding. With the adding algorithm, the 4N and 8N thresholding applications did not produce significantly different results in terms of accuracy or precision of length measurements as in Table 6.4, but slightly lower precision for 8N, as expected, since the best threshold value was found to be the same for 4N and 8N. However, Table 6.5 shows that analysis time significantly increased for the 8N applications.

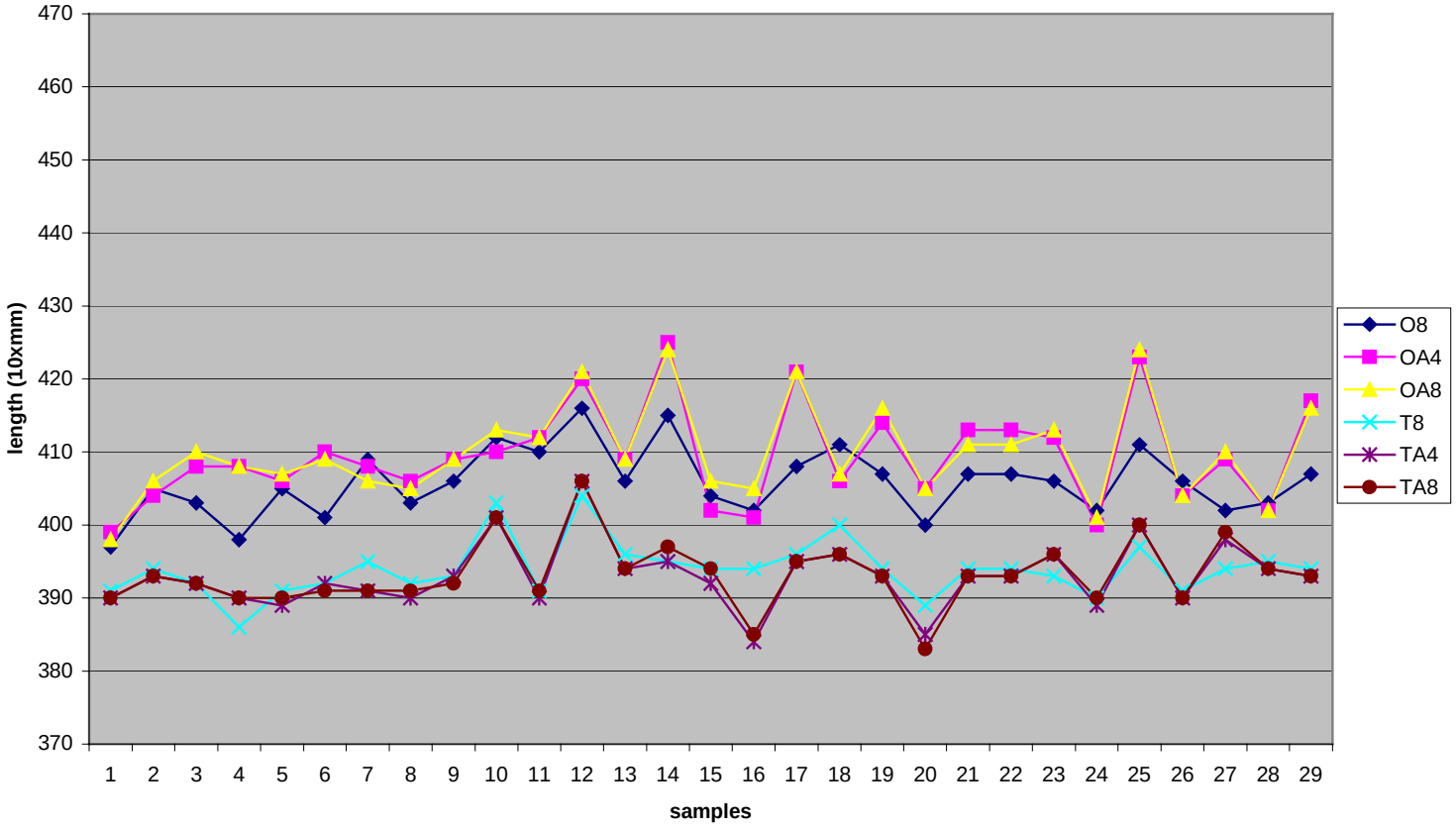

Figure 6.3: Length measurement results of images without crossover-frontlighting-37 micron resolution (10xmm)

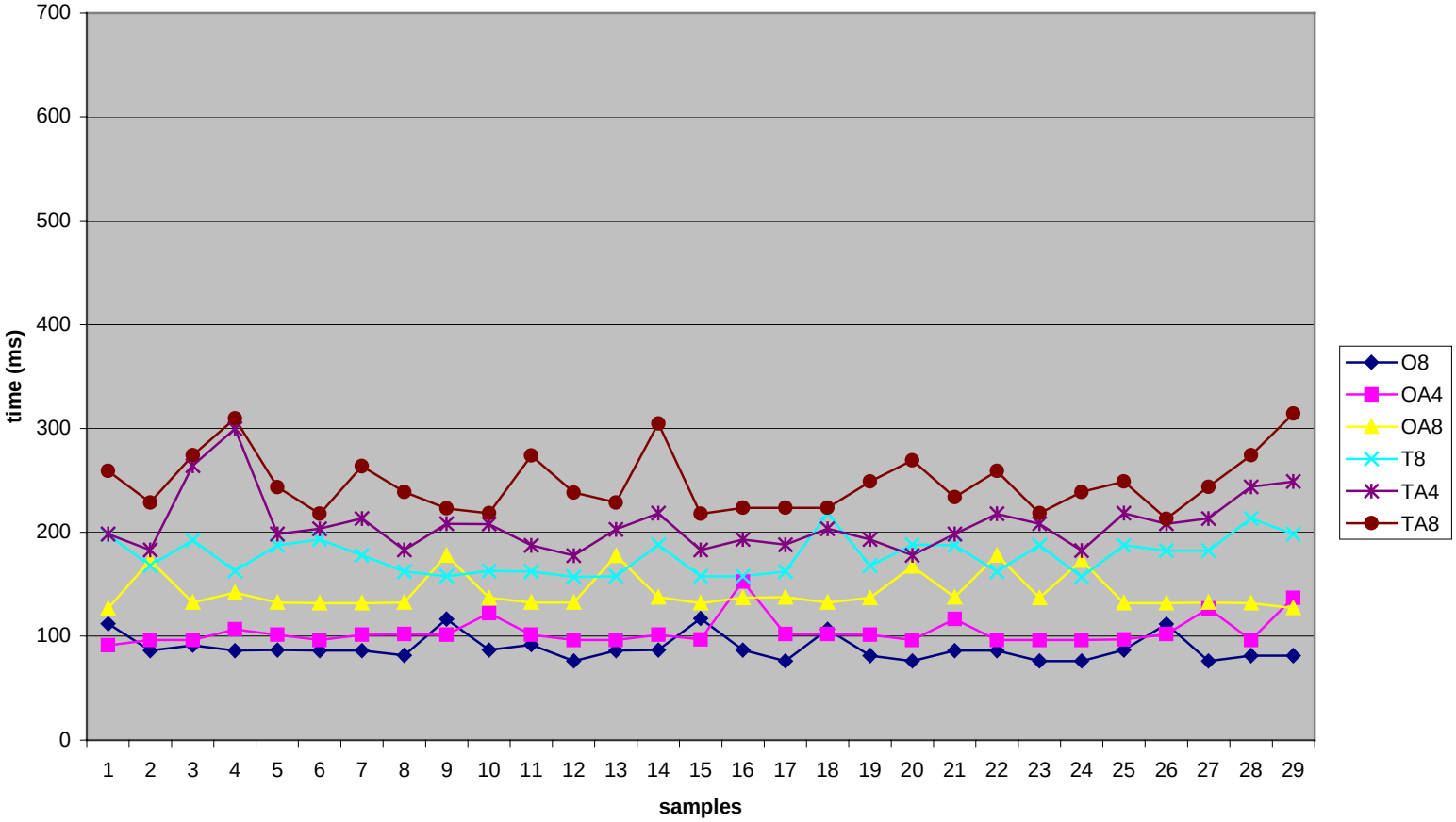

Figure 6.4: Analysis time of 100 Kbytes images without crossover-frontlighting-37 micron resolution (ms)

Table 6.4: Length measurement results of images without crossover-frontlighting-37 micron resolution (10xmm)

OUT-8N-9 --> OUTLINE-8 NEIGHBORHOOD-Threshold 9
OUT-ADD-4N-12--> OUTLINE-4 NEIGHBORHOOD-Threshold 13
OUT-ADD-8N-13--> OUTLINE-8 NEIGHBORHOOD-Threshold 13

THIN-8N-9--> THINNING-8 NEIGHBORHOOD-Threshold 9
THIN-ADD-4N-12--> THINNING-4 NEIGHBORHOOD-Threshold 13
THIN-ADD-8N-13--> THINNING-8 NEIGHBORHOOD-Threshold 13

OUT-8N-9	
Mean	405.8276
Standard E	0.849614
Median	406
Mode	406
Standard D	4.575314
Sample Va	20.9335
Kurtosis	0.03062
Skewness	0.294905
Range	19
Minimum	397
Maximum	416
Sum	11769
Count	29
Confidence	1.740358

OUT-ADD-4N-13	
Mean	409.5172
Standard E	1.260054
Median	409
Mode	408
Standard D	6.785598
Sample Va	46.04433
Kurtosis	-0.036954
Skewness	0.661814
Range	26
Minimum	399
Maximum	425
Sum	11876
Count	29
Confidence	2.581106

OUT-ADD-8N-13	
Mean	409.9655
Standard E	1.217163
Median	409
Mode	406
Standard D	6.554621
Sample Va	42.96305
Kurtosis	0.128316
Skewness	0.674747
Range	26
Minimum	398
Maximum	424
Sum	11889
Count	29
Confidence	2.493247

THIN-8N-9	
Mean	393.931
Standard E	0.694686
Median	394
Mode	394
Standard D	3.740999
Sample Va	13.99507
Kurtosis	1.994968
Skewness	0.906385
Range	18
Minimum	386
Maximum	404
Sum	11424
Count	29
Confidence	1.423002

THIN-ADD-4N-13	
Mean	393
Standard E	0.833415
Median	393
Mode	393
Standard D	4.488079
Sample Va	20.14286
Kurtosis	1.828258
Skewness	0.735773
Range	22
Minimum	384
Maximum	406
Sum	11397
Count	29
Confidence	1.707176

THIN-ADD-8N-13	
Mean	393.2069
Standard E	0.848614
Median	393
Mode	390
Standard D	4.569927
Sample Va	20.88424
Kurtosis	1.7326
Skewness	0.543724
Range	23
Minimum	383
Maximum	406
Sum	11403
Count	29
Confidence	1.738309

Table 6.5: Analysis time of 100 Kbytes images without crossover-frontlighting-37 micron resolution (ms)

OUT-8N-9 --> OUTLINE-8 NEIGHBORHOOD-Threshold 9
OUT-ADD-4N-12--> OUTLINE-4 NEIGHBORHOOD-Threshold 13
OUT-ADD-8N-13--> OUTLINE-8 NEIGHBORHOOD-Threshold 13

THIN-8N-9--> THINNING-8 NEIGHBORHOOD-Threshold 9
THIN-ADD-4N-12--> THINNING-4 NEIGHBORHOOD-Threshold 13
THIN-ADD-8N-13--> THINNING-8 NEIGHBORHOOD-Threshold 13

OUT-8N-9	
Mean	88.44528
Standard E	2.282344
Median	86.19
Mode	86.19
Standard D	12.2908
Sample Va	151.0638
Kurtosis	0.835573
Skewness	1.32767
Range	41.067
Minimum	76.05
Maximum	117.117
Sum	2564.913
Count	29
Confidence	4.675176

OUT-ADD-4N-13	
Mean	104.3371
Standard E	2.570637
Median	101.4
Mode	96.33
Standard D	13.8433
Sample Va	191.637
Kurtosis	5.092844
Skewness	2.275155
Range	61.347
Minimum	91.26
Maximum	152.607
Sum	3025.776
Count	29
Confidence	5.265716

OUT-ADD-8N-13	
Mean	142.0474
Standard E	3.19439
Median	132.327
Mode	132.327
Standard D	17.20232
Sample Va	295.9197
Kurtosis	0.363539
Skewness	1.441198
Range	51.207
Minimum	126.75
Maximum	177.957
Sum	4119.375
Count	29
Confidence	6.543419

THIN-8N-9	
Mean	177.1878
Standard E	3.314668
Median	177.957
Mode	187.59
Standard D	17.85003
Sample Va	318.6236
Kurtosis	-0.550258
Skewness	0.571057
Range	61.347
Minimum	157.17
Maximum	218.517
Sum	5138.445
Count	29
Confidence	6.789797

THIN-ADD-4N-13	
Mean	207.7476
Standard E	5.068167
Median	203.307
Mode	198.237
Standard D	27.29292
Sample Va	744.9033
Kurtosis	3.798312
Skewness	1.76558
Range	122.187
Minimum	177.45
Maximum	299.637
Sum	6024.681
Count	29
Confidence	10.38168

THIN-ADD-8N-13	
Mean	247.381
Standard E	5.303627
Median	238.797
Mode	223.587
Standard D	28.56091
Sample Va	815.7254
Kurtosis	0.229541
Skewness	0.979017
Range	101.4
Minimum	212.94
Maximum	314.34
Sum	7174.05
Count	29
Confidence	10.864

An interesting observation came from the adding algorithm in that it caused less accurate, longer length measurements with increased standard deviation and larger confidence intervals as in Table 6.4. This is the opposite effect compared to backlighting. This was simply because of dust on the glass surface that created strong shiny points on the images due to the directional lighting. The adding algorithm connected some of these shiny points to the fibers. Since these errors were the result of dust, providing a dust free environment would surely remove this source of the error.

The thinning algorithm improved accuracy and precision while causing approximately twice as much analysis time. Mean lengths were found less than 40 mm and confidence intervals were found less than 0.2 mm for each thinning application as in Table 6.4. Only the thinning algorithm application with frontlighting produced accurate and precise results than backlighting. However the adding algorithm lowered the precision of the thinning causing more variation then backlighting applications.

Frontlighting produced better results than backlighting, with the exception of the adding algorithm, when considering length precision. Indeed, adding did not change the results with statistical significance, but slightly higher variations were observed. Average measured lengths with frontlighting were shorter than backlighting for each algorithm so that the results were closer to the given cut length. Confidence interval, standard deviation and standard error results were also had lower values so accuracy and precision were improved. Especially thinning applications produced highly significant results by reducing the analysis time about 30% to 50%.

6.2.3. Without Fiber Crossover-57 micron Resolution-Backlighting

Since 37-micron resolution images produced satisfactory results, lower resolution images were analyzed. At the first attempt, the new resolution was about 64-micron. Unfortunately, backlighting images produced a few broken skeletons using this resolution so we set out to determine the minimum resolution which could be used with our backlighting technique which would not result in broken skeletons. The resolution was determined as about 57-micron since this was the lowest resolution, which did not produce broken skeletons for the best threshold value in twenty-nine images. By choosing 57-micron resolution, we always had an actual resolution between 55 and 60-microns. Conclusively, about 60-microns was the lowest resolution limit of backlighting without producing broken skeletons for length measurement of cotton fibers using our system. Two images for the outline-8N and one image for the adding applications did not produce any results since the fibers touched the edge of the images.

Figures 6.5 and 6.6 show the length and time measurements of applied algorithms to 57 micron-backlighting images, and Tables 6.6 and 6.7 show the respective descriptive statistics. As expected, results were worse for low-resolution images. High variation of length measurements can be observed from Figure 6.5 with some measurements much greater than the given cut length and some which are equal to the given cut length implying the shortest length measurements reported to this point.

The best threshold value without the adding algorithm was reduced to 7 for 4N that formerly (37-micron resolution) was 8, and for 8N that formerly was 9, as a sign of low contrast images. Since the best threshold value was the same for the 4N and 8N, significantly different results were obtained for each algorithm for comparison. The 8N

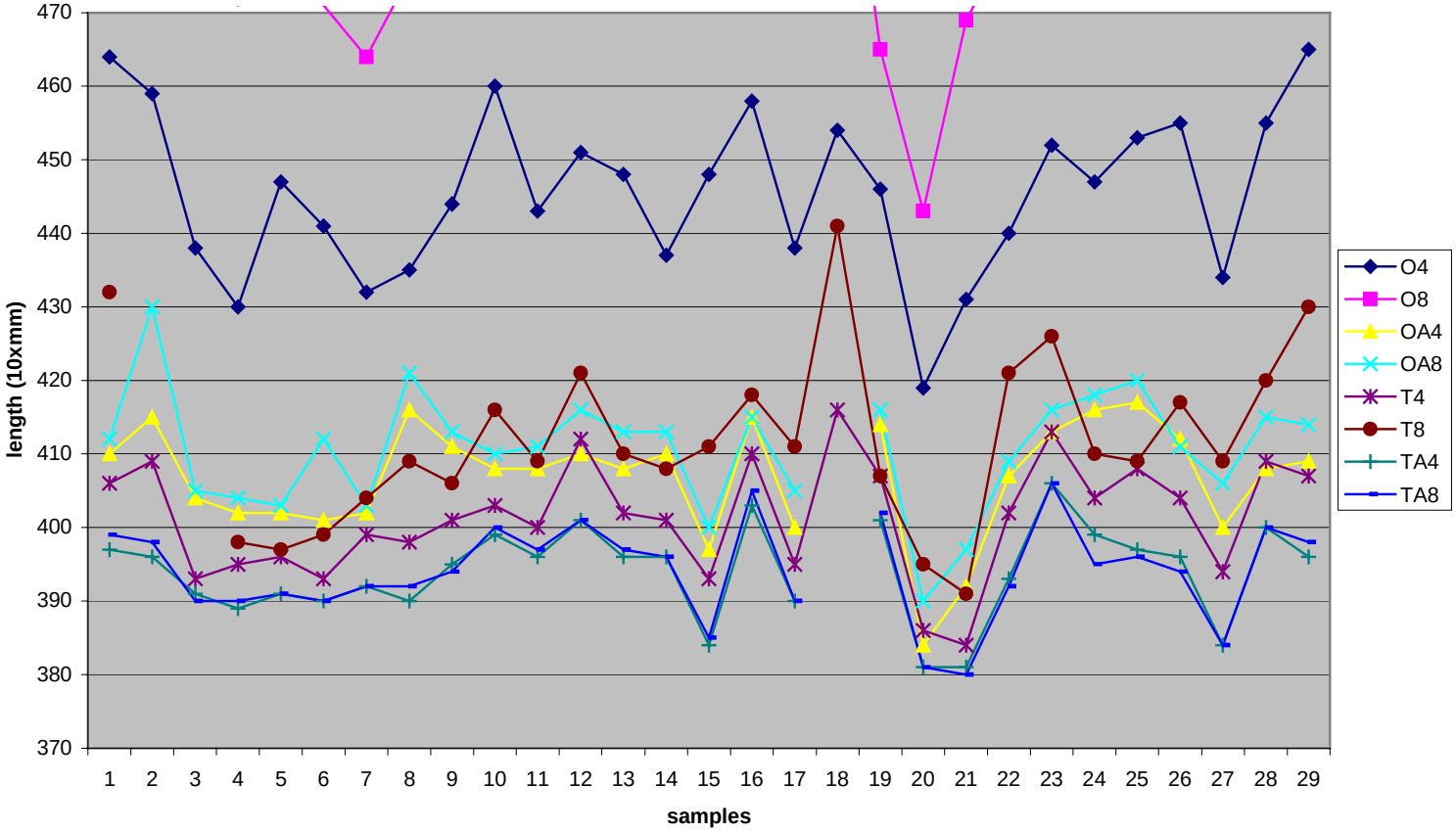

Figure 6.5: Length measurement results of images without crossover-backlighting-57 micron resolution (10xmm)

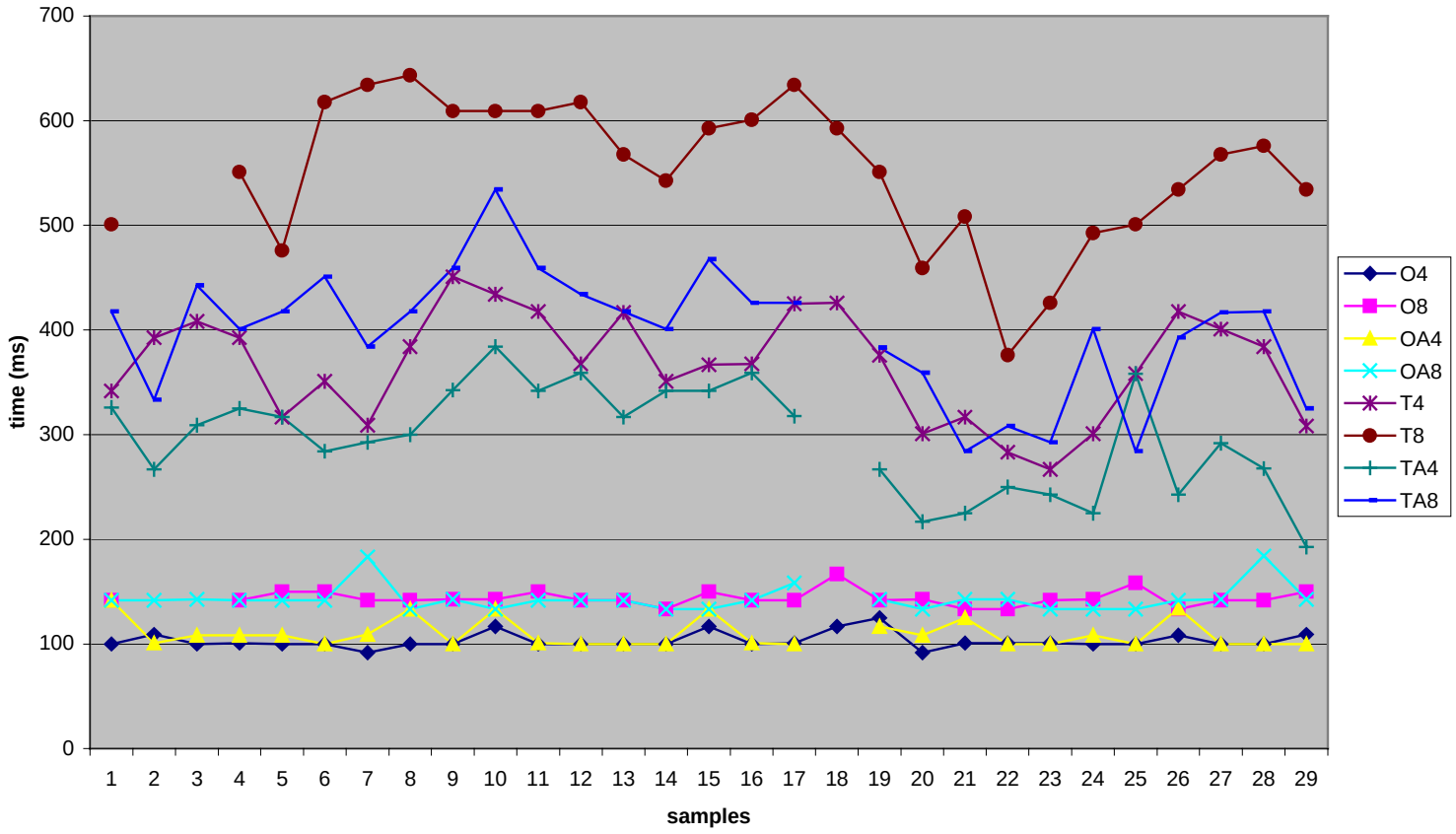

Figure 6.6: Analysis time of 100 Kbytes images without crossover-backlighting-57 micron resolution (ms)

Table 6.6: Length measurement results of images without crossover-backlighting-57 micron resolution (10xmm)

OUT-4N-7 --> OUTLINE-4 NEIGHBORHOOD-Threshold 7
OUT-8N-7 --> OUTLINE-8 NEIGHBORHOOD-Threshold 7
OUT-ADD-4N-13--> OUTLINE-4 NEIGHBORHOOD-Threshold 13
OUT-ADD-8N-13--> OUTLINE-8 NEIGHBORHOOD-Threshold 13

THIN-4N-8 --> THINNING-4 NEIGHBORHOOD-Threshold 7
THIN-8N-10--> THINNING-8 NEIGHBORHOOD-Threshold 7
THIN-ADD-4N-13--> THINNING-4 NEIGHBORHOOD-Threshold 13
THIN-ADD-8N-14--> THINNING-8 NEIGHBORHOOD-Threshold 13

OUT-4N-7	
Mean	445.6552
Standard E	2.073333
Median	447
Mode	438
Standard D	11.16524
Sample Va	124.6626
Kurtosis	-0.310855
Skewness	-0.260214
Range	46
Minimum	419
Maximum	465
Sum	12924
Count	29
Confidence	4.247035

OUT-8N-7	
Mean	484.6667
Standard E	3.035404
Median	484
Mode	471
Standard D	15.77242
Sample Va	248.7692
Kurtosis	0.550123
Skewness	-0.375612
Range	70
Minimum	443
Maximum	513
Sum	13086
Count	27
Confidence	6.239366

OUT-ADD-4N-13	
Mean	406.8214
Standard E	1.464802
Median	408
Mode	408
Standard D	7.751003
Sample Va	60.07804
Kurtosis	1.446615
Skewness	-1.083852
Range	33
Minimum	384
Maximum	417
Sum	11391
Count	28
Confidence	3.005523

OUT-ADD-8N-13	
Mean	410.6429
Standard E	1.523375
Median	412
Mode	413
Standard D	8.060945
Sample Va	64.97884
Kurtosis	1.087111
Skewness	-0.297055
Range	40
Minimum	390
Maximum	430
Sum	11498
Count	28
Confidence	3.125706

THIN-4N-7	
Mean	401.3793
Standard E	1.459987
Median	402
Mode	393
Standard D	7.862269
Sample Va	61.81527
Kurtosis	-0.308185
Skewness	-0.282575
Range	32
Minimum	384
Maximum	416
Sum	11640
Count	29
Confidence	2.99065

THIN-8N-7	
Mean	412.037
Standard E	2.255403
Median	410
Mode	409
Standard D	11.71942
Sample Va	137.3447
Kurtosis	0.2922
Skewness	0.500914
Range	50
Minimum	391
Maximum	441
Sum	11125
Count	27
Confidence	4.63605

THIN-ADD-4N-13	
Mean	393.9286
Standard E	1.198465
Median	396
Mode	396
Standard D	6.341682
Sample Va	40.21693
Kurtosis	-0.139077
Skewness	-0.442474
Range	25
Minimum	381
Maximum	406
Sum	11030
Count	28
Confidence	2.459046

THIN-ADD-8N-13	
Mean	394.1071
Standard E	1.241201
Median	394.5
Mode	390
Standard D	6.567819
Sample Va	43.13624
Kurtosis	-0.093383
Skewness	-0.377501
Range	26
Minimum	380
Maximum	406
Sum	11035
Count	28
Confidence	2.546733

Table 6.7: Analysis time of 100 Kbytes images without crossover-backlighting-57 micron resolution (ms)

OUT-4N-7 --> OUTLINE-4 NEIGHBORHOOD-Threshold 7
OUT-8N-7 --> OUTLINE-8 NEIGHBORHOOD-Threshold 7
OUT-ADD-4N-13--> OUTLINE-4 NEIGHBORHOOD-Threshold 13
OUT-ADD-8N-13--> OUTLINE-8 NEIGHBORHOOD-Threshold 13

THIN-4N-8 --> THINNING-4 NEIGHBORHOOD-Threshold 7
THIN-8N-10--> THINNING-8 NEIGHBORHOOD-Threshold 7
THIN-ADD-4N-13--> THINNING-4 NEIGHBORHOOD-Threshold 13
THIN-ADD-8N-14--> THINNING-8 NEIGHBORHOOD-Threshold 13

OUT-4N-7		*OUT-8N-7*		*OUT-ADD-4N-13*		*OUT-ADD-8N-13*	
Mean	103.0706	Mean	143.6362	Mean	109.6682	Mean	143.0895
Standard E	1.387802	Standard E	1.424797	Standard E	2.559569	Standard E	2.391306
Median	99.996	Median	141.661	Median	100.8293	Median	141.661
Mode	99.996	Mode	141.661	Mode	99.996	Mode	141.661
Standard D	7.473542	Standard D	7.40346	Standard D	13.54397	Standard D	12.6536
Sample Va	55.85384	Sample Va	54.81122	Sample Va	183.439	Sample Va	160.1136
Kurtosis	1.931432	Kurtosis	2.767491	Kurtosis	0.112048	Kurtosis	6.728966
Skewness	1.397457	Skewness	1.246834	Skewness	1.254989	Skewness	2.568783
Range	33.332	Range	33.332	Range	41.665	Range	50.8313
Minimum	91.663	Minimum	133.328	Minimum	99.996	Minimum	133.328
Maximum	124.995	Maximum	166.66	Maximum	141.661	Maximum	184.1593
Sum	2989.047	Sum	3878.178	Sum	3070.711	Sum	4006.506
Count	29	Count	27	Count	28	Count	28
Confidence	2.842787	Confidence	2.928713	Confidence	5.251798	Confidence	4.90655
THIN-4N-7		*THIN-8N-7*		*THIN-ADD-4N-13*		*THIN-ADD-8N-13*	
Mean	366.5945	Mean	552.6631	Mean	296.506	Mean	398.2876
Standard E	9.262165	Standard E	13.05832	Standard E	9.54757	Standard E	11.34411
Median	367.4853	Median	567.4773	Median	304.5712	Median	417.0667
Mode	392.4843	Mode	609.1423	Mode	341.653	Mode	417.4833
Standard D	49.87828	Standard D	67.853	Standard D	50.52099	Standard D	60.02738
Sample Va	2487.843	Sample Va	4604.03	Sample Va	2552.371	Sample Va	3603.286
Kurtosis	-0.912628	Kurtosis	0.305992	Kurtosis	-0.826794	Kurtosis	0.146713
Skewness	-0.292025	Skewness	-0.834065	Skewness	-0.312739	Skewness	-0.363248
Range	184.1593	Range	267.4893	Range	191.659	Range	249.99
Minimum	266.656	Minimum	375.8183	Minimum	192.4923	Minimum	284.1553
Maximum	450.8153	Maximum	643.3076	Maximum	384.1513	Maximum	534.1453
Sum	10631.24	Sum	14921.9	Sum	8302.168	Sum	11152.05
Count	29	Count	27	Count	28	Count	28
Confidence	18.97271	Confidence	26.84177	Confidence	19.58998	Confidence	23.27617

thresholding naturally produced more noise causing longer length measurements and more processing time. Table 6.6 shows that the mean length of outline-8N is 48.5 mm, 10.4 mm higher than the given cut length. The confidence interval is 0.62 mm, which is over the chosen precision limit.

The best threshold values with the adding algorithm were found to be 13 for both the 4N and 8N thresholding. The adding algorithm improved the results as evidenced by the confidence interval of outline-adding-8N algorithm dropping to 0.312 mm (Table 6.6) satisfying the required precision yet higher than hand-measurement. Besides, analysis time was found to be 143 ms for each application meaning in this case, the adding application did not result in increased processing time.

The thinning algorithm significantly improved precision and accuracy while almost tripling the analysis time for each application (Table 6.7). However, only the thinning algorithm combined with the adding algorithm produced better results than hand-measurement. Moreover, the thinning-adding combined algorithm resulted in less processing time than only the thinning algorithm.

All applications produced longer length measurements than 37-micron resolution, evidently causing less accurate measurements (Table 6.6). Precision also was reduced for each application causing higher standard deviation, standard error and confidence intervals. Only the thinning-adding algorithm produced slightly better results than hand-measurement with a confidence interval of 0.25 mm. The main reason was: lower resolution caused lower contrast on the images, as evidenced by the lower best threshold value as compared to 37-micron resolution results.

6.2.4. Without Fiber Crossover-57 micron Resolution-Frontlighting

Thirty images were captured and analyzed for 57-micron resolution and frontlighting to determine the best threshold values. Figures 6.7 and 6.8 show the length and time measurements of the applied algorithms, and Tables 6.8 and 6.9 show the respective statistics. Figure 6.7 shows that a few length measurements are lower than the given cut length implying possible shorter mean length measurements. Remember that hand measurement results were always shorter than the given cut length.

The best threshold values were found to be 8 for the 4N and 11 for the 8N thresholding. This difference significantly improved the 8N applications over the 4N. Mean lengths were found to be 42.2 mm for the outline-4N and 40.9 mm for the outline-8N, while confidence intervals were found to be 0.39 mm and 0.33 mm respectively implying slightly less precision than hand-measurement, but clearly meeting our chosen precision requirements.

The adding algorithm lowered accuracy and precision measuring longer mean lengths and greater confidence intervals while causing about 40% more analysis time. Confidence intervals were found higher than 0.5 mm. These results show agreement with 37-micron resolution that the adding algorithm causes added errors with the frontlighting technique.

Thinning improved the accuracy and precision of length measurements in every case while about doubling the analysis time (Table 6.9). The adding algorithm caused significantly lower precision without affecting accuracy.

Interestingly, 57-micron images produced unbroken skeletons of fibers for outline-4N. For the 8N thresholding, the best threshold value increased to 11 from 9

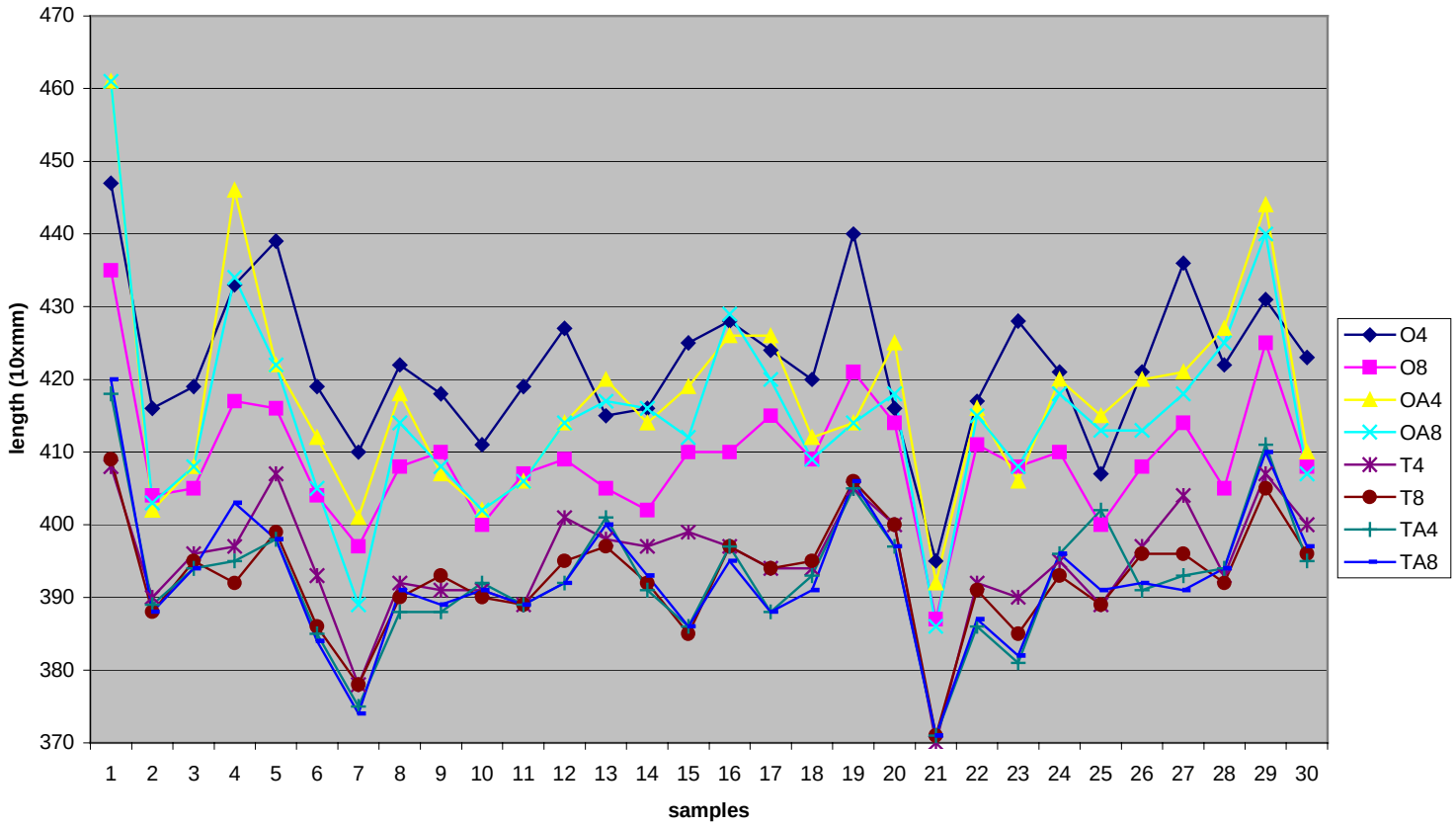

Figure 6.7: Length measurement results of images without crossover-frontlighting-57 micron resolution (10xmm)

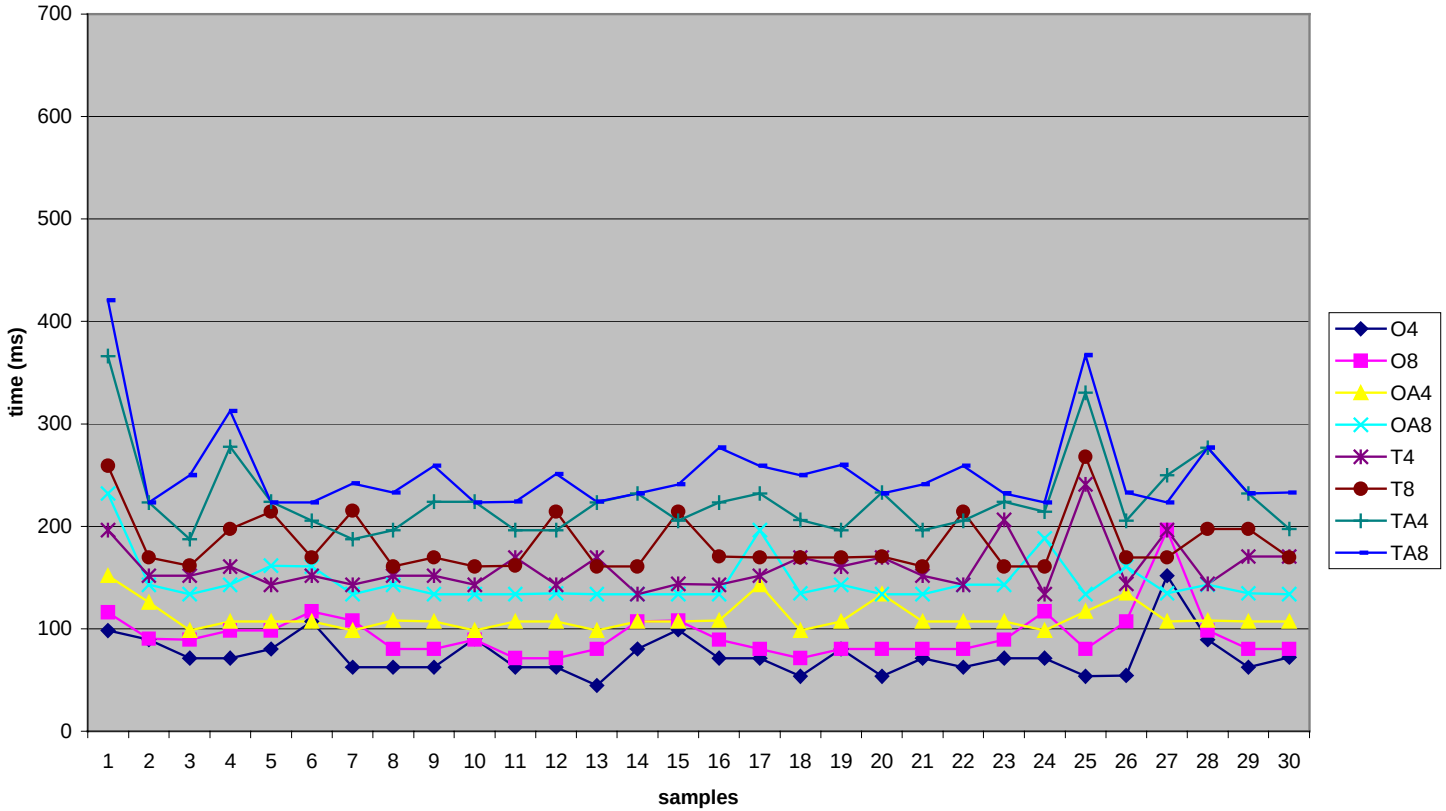

Figure 6.8: Analysis time of 100 Kbytes images without crossover-frontlighting-57 micron resolution (ms)

Table 6.8: Length measurement results of images without crossover-frontlighting-57 micron resolution (10xmm)

OUT-4N-8 --> OUTLINE-4 NEIGHBORHOOD-Threshold 8
OUT-8N-11 --> OUTLINE-8 NEIGHBORHOOD-Threshold 11
OUT-ADD-4N-11--> OUTLINE-4 NEIGHBORHOOD-Threshold 11
OUT-ADD-8N-13--> OUTLINE-8 NEIGHBORHOOD-Threshold 13

THIN-4N-8 --> THINNNING-4 NEIGHBORHOOD-Threshold 8
THIN-8N-11 --> THINNING-8 NEIGHBORHOOD-Threshold 11
THIN-ADD-4N-11--> THINNING-4 NEIGHBORHOOD-Threshold 11
THIN-ADD-8N-13--> THINNING-8 NEIGHBORHOOD-Threshold 13

OUT-4N-8	
Mean	422.1667
Standard E	1.916704
Median	421
Mode	416
Standard D	10.49822
Sample Va	110.2126
Kurtosis	1.078746
Skewness	0.088794
Range	52
Minimum	395
Maximum	447
Sum	12665
Count	30
Confidence	3.920102

OUT-8N-11	
Mean	409.1333
Standard E	1.600096
Median	408.5
Mode	408
Standard D	8.764086
Sample Va	76.8092
Kurtosis	2.556548
Skewness	0.505533
Range	48
Minimum	387
Maximum	435
Sum	12274
Count	30
Confidence	3.272565

OUT-ADD-4N-11	
Mean	417.5333
Standard E	2.57786
Median	415.5
Mode	414
Standard D	14.11952
Sample Va	199.3609
Kurtosis	2.444041
Skewness	1.203646
Range	69
Minimum	392
Maximum	461
Sum	12526
Count	30
Confidence	5.272319

OUT-ADD-8N-13	
Mean	414.8
Standard E	2.577712
Median	414
Mode	408
Standard D	14.11871
Sample Va	199.3379
Kurtosis	3.445916
Skewness	1.026156
Range	75
Minimum	386
Maximum	461
Sum	12444
Count	30
Confidence	5.272015

THIN-4N-8	
Mean	395.1333
Standard E	1.462743
Median	395.5
Mode	397
Standard D	8.011773
Sample Va	64.18851
Kurtosis	2.588895
Skewness	-1.019631
Range	38
Minimum	370
Maximum	408
Sum	11854
Count	30
Confidence	2.991647

THIN-8N-11	
Mean	392.8
Standard E	1.3949
Median	393
Mode	395
Standard D	7.640184
Sample Va	58.37241
Kurtosis	1.779609
Skewness	-0.486955
Range	38
Minimum	371
Maximum	409
Sum	11784
Count	30
Confidence	2.852893

THIN-ADD-4N-11	
Mean	392.7
Standard E	1.70944
Median	392.5
Mode	388
Standard D	9.362987
Sample Va	87.66552
Kurtosis	1.667092
Skewness	0.318945
Range	47
Minimum	371
Maximum	418
Sum	11781
Count	30
Confidence	3.496199

THIN-ADD-8N-13	
Mean	392.6667
Standard E	1.742197
Median	391.5
Mode	391
Standard D	9.542404
Sample Va	91.05747
Kurtosis	2.089504
Skewness	0.447385
Range	49
Minimum	371
Maximum	420
Sum	11780
Count	30
Confidence	3.563194

Table 6.9: Analysis time of 100 Kbytes images without crossover-frontlighting-57 micron resolution (ms)

OUT-4N-8 --> OUTLINE-4 NEIGHBORHOOD-Threshold 8
OUT-8N-11 --> OUTLINE-8 NEIGHBORHOOD-Threshold 11
OUT-ADD-4N-11--> OUTLINE-4 NEIGHBORHOOD-Threshold 11
OUT-ADD-8N-13--> OUTLINE-8 NEIGHBORHOOD-Threshold 13

THIN-4N-8 --> THINNNING-4 NEIGHBORHOOD-Threshold 8
THIN-8N-11 --> THINNING-8 NEIGHBORHOOD-Threshold 11
THIN-ADD-4N-11--> THINNING-4 NEIGHBORHOOD-Threshold 11
THIN-ADD-8N-13--> THINNING-8 NEIGHBORHOOD-Threshold 13

OUT-4N-8	
Mean	74.59498
Standard E	3.950355
Median	71.424
Mode	71.424
Standard D	21.27331
Sample Va	452.5538
Kurtosis	5.108171
Skewness	1.821843
Range	107.136
Minimum	44.64
Maximum	151.776
Sum	2163.254
Count	29
Confidence	8.091944

OUT-8N-11	
Mean	94.35972
Standard E	4.482237
Median	89.28
Mode	80.352
Standard D	24.13759
Sample Va	582.6231
Kurtosis	11.06663
Skewness	2.840718
Range	124.992
Minimum	71.424
Maximum	196.416
Sum	2736.432
Count	29
Confidence	9.181457

OUT-ADD-4N-11	
Mean	124.2
Standard E	2.753639
Median	120
Mode	120
Standard D	15.0823
Sample Va	227.4759
Kurtosis	2.673564
Skewness	1.777302
Range	60
Minimum	110
Maximum	170
Sum	3726
Count	30
Confidence	5.631828

OUT-ADD-8N-13	
Mean	146.4192
Standard E	4.261726
Median	134.8128
Mode	133.92
Standard D	22.9501
Sample Va	526.7069
Kurtosis	6.831066
Skewness	2.563454
Range	98.208
Minimum	133.92
Maximum	232.128
Sum	4246.157
Count	29
Confidence	8.729759

THIN-4N-8	
Mean	159.6265
Standard E	4.470895
Median	151.776
Mode	151.776
Standard D	24.07651
Sample Va	579.6782
Kurtosis	3.758659
Skewness	1.836998
Range	107.136
Minimum	133.92
Maximum	241.056
Sum	4629.168
Count	29
Confidence	9.158224

THIN-8N-11	
Mean	184.0399
Standard E	5.507106
Median	169.632
Mode	169.632
Standard D	29.65667
Sample Va	879.5182
Kurtosis	1.690941
Skewness	1.493382
Range	107.136
Minimum	160.704
Maximum	267.84
Sum	5337.158
Count	29
Confidence	11.28081

THIN-ADD-4N-11	
Mean	227.4177
Standard E	7.529896
Median	223.2
Mode	196.416
Standard D	40.54973
Sample Va	1644.281
Kurtosis	4.916706
Skewness	2.118287
Range	178.56
Minimum	187.488
Maximum	366.048
Sum	6595.114
Count	29
Confidence	15.42431

THIN-ADD-8N-13	
Mean	253.3397
Standard E	8.291767
Median	241.056
Mode	223.2
Standard D	44.65253
Sample Va	1993.849
Kurtosis	7.426599
Skewness	2.626745
Range	197.3088
Minimum	223.2
Maximum	420.5088
Sum	7346.851
Count	29
Confidence	16.98493

(versus 37-micron) because of the light intensity. The 37-micron resolution images were captured in dimmer light conditions so as not to add error due to glare. Even though the outline algorithm with 57-micron resolution produced longer fiber measurements than the same algorithm with 37-micron resolution, the thinning algorithm with 57-micron resolution produced slightly shorter measurements than the same algorithm with 37-micron resolution probably caused by insensitivity to fine curves of fibers. Since the outline algorithm of 57-micron resolution images produced satisfactory precision with lower analysis time over 37-micron resolution images, it would be the logical selection for the best image processing application.

The outline and thinning applications were superior with frontlighting, as compared to backlighting in both precision and processing time. Thinning generated remarkable results with frontlighting, improving the precision and accuracy as compared to backlighting while the analysis time was reduced to less than one third of backlighting. The adding algorithm produced the reverse results in that with backlighting, it resulted in improved precision and accuracy whereas with frontlighting added error due to the dust as we discussed earlier. In a dust free environment the frontlighting condition may have given superior results.

6.2.5. Without Fiber Crossover-106 micron Resolution-Frontlighting

Only frontlighting responded with workable images with 106-micron resolution fitting one fiber to one frame. Figures 6.9 and 6.10 show length and time measurements of applied algorithms, and Table 6.10 and 6.11 show respective descriptive statistics. A few fiber lengths were found to be shorter than the given cut length meaning that either

fine curves were not detected or close points of crimps were connected causing small loops on the images, or, perhaps, some fibers actually were shorter than the cut length.

The best threshold values of the adding algorithm were found to be 19 for the 4N and 21 for the 8N thresholding showing strong contrast. The mean lengths and confidence intervals of the adding algorithm of the 4N and 8N produced quite similar results while causing significantly more analysis time for the 8N. The thinning algorithm combined with the adding algorithm resulted in mean lengths only 0.3 mm over the given cut length implying the best accuracy yet for any reported system to date. However, the confidence intervals were found about 0.4 mm, less precise than hand-measurement, but still in the range of our chosen precision.

Results surprisingly improved in every aspect of the measurements, with the exception of the case of the adding algorithm, as compared to 57-micron resolution-frontlighting results. The only possible explanation is the new set up of camera and lighting conditions.

Since one frame could capture the entire fiber, the frame construction algorithm was unnecessary. This eliminated error sources from frame connections. Moreover, one more light source was projected on the surface smoothing the entire image and promoting higher contrast on the fiber surface. This resulted in reduced noise and less analysis time. However, foreign materials were measured as significantly larger because of the resolution. A shiny point (glare) might cause several pixels to illuminate which, with the longer pixel dimensions, lead to larger foreign objects being seen by the system as short fibers. In some instances they created longer than 1 mm fiber length measurements.

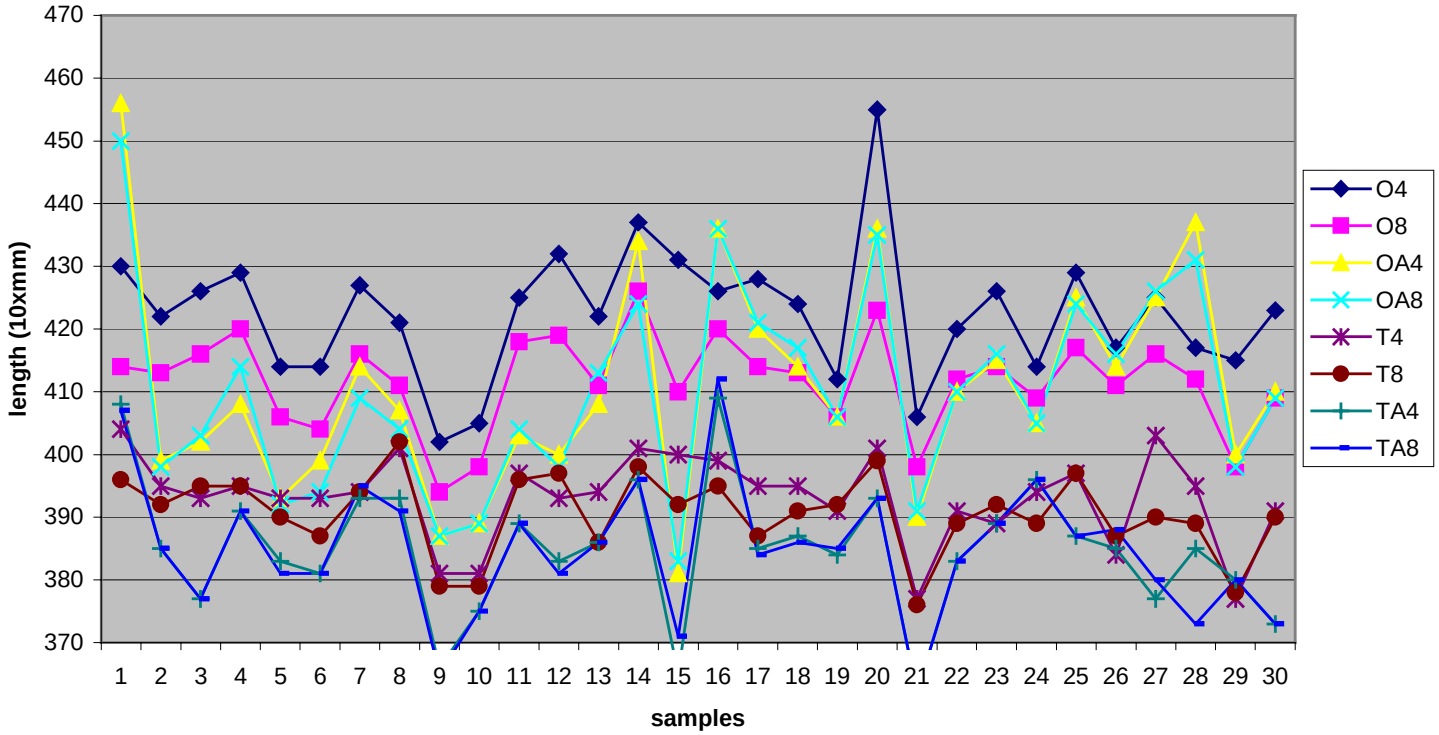

Figure 6.9: Length measurement results of images without crossover-frontlighting-106 micron resolution (10xmm)

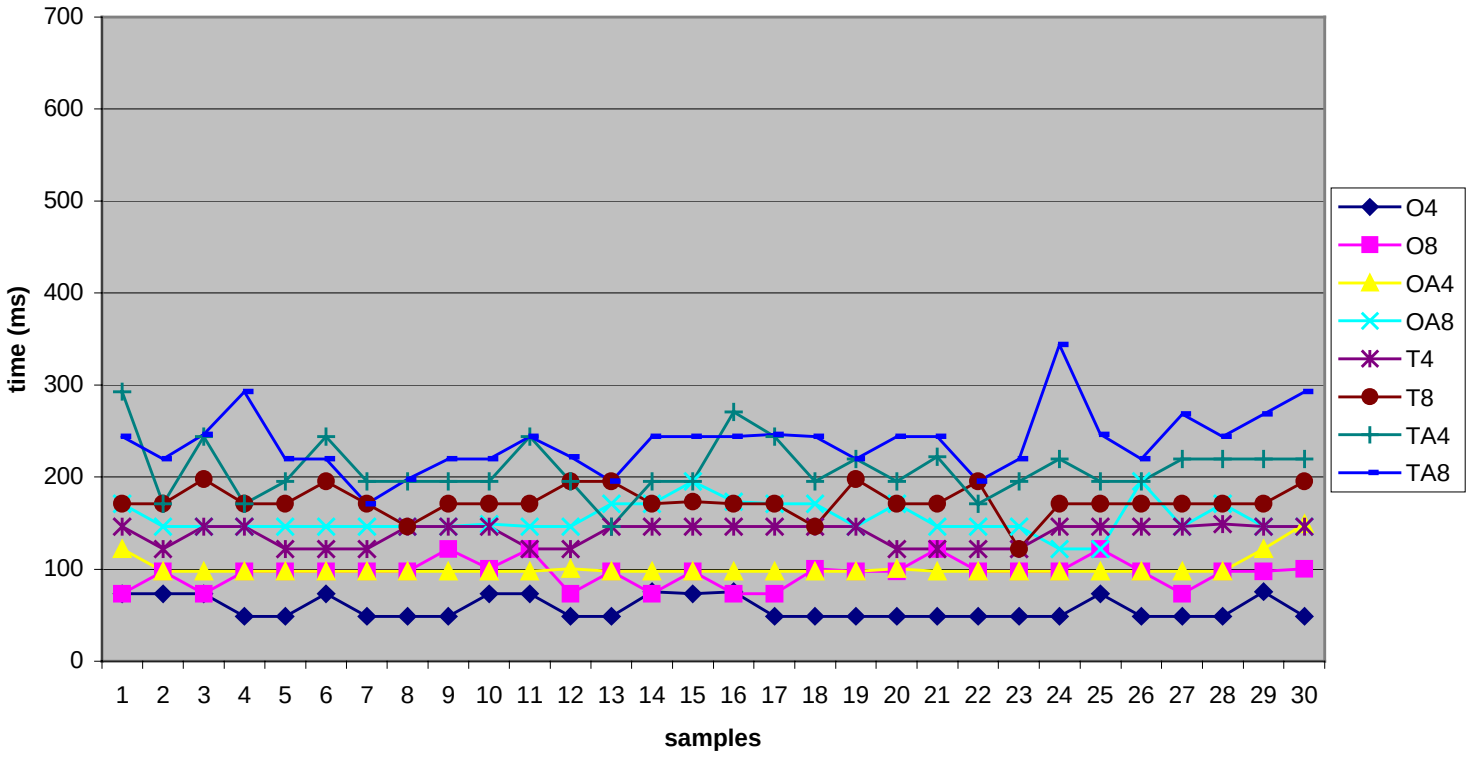

Figure 6.10: Analysis time of 100 Kbytes images without crossover-frontlighting-106 micron resolution (ms)

Table 6.10: Length measurement results of images without crossover-frontlighting-106 micron resolution (10xmm)

OUT-4N-8 --> OUTLINE-4 NEIGHBORHOOD-Threshold 8
OUT-8N-11 --> OUTLINE-8 NEIGHBORHOOD-Threshold 11
OUT-ADD-4N-19--> OUTLINE-4 NEIGHBORHOOD-Threshold 19
OUT-ADD-8N-21--> OUTLINE-8 NEIGHBORHOOD-Threshold 21

THIN-4N-8 --> THINNING-4 NEIGHBORHOOD-Threshold 8
THIN-8N-11 --> THINNING-8 NEIGHBORHOOD-Threshold 11
THIN-ADD-4N-19--> THINNING-4 NEIGHBORHOOD-Threshold 19
THIN-ADD-8N-21--> THINNING-8 NEIGHBORHOOD-Threshold 21

OUT-4N-8		*OUT-8N-11*		*OUT-ADD-4N-19*		*OUT-ADD-8N-21*	
Mean	422.4667	Mean	411.6	Mean	410.4333	Mean	410.1
Standard E	1.89478	Standard E	1.391766	Standard E	3.044378	Standard E	2.934672
Median	423.5	Median	412.5	Median	408	Median	409
Mode	426	Mode	414	Mode	414	Mode	398
Standard D	10.37814	Standard D	7.623014	Standard D	16.67475	Standard D	16.07386
Sample Va	107.7057	Sample Va	58.11034	Sample Va	278.0471	Sample Va	258.369
Kurtosis	2.373025	Kurtosis	0.18741	Kurtosis	0.638494	Kurtosis	-0.085141
Skewness	0.605264	Skewness	-0.587816	Skewness	0.671986	Skewness	0.462133
Range	53	Range	32	Range	75	Range	67
Minimum	402	Minimum	394	Minimum	381	Minimum	383
Maximum	455	Maximum	426	Maximum	456	Maximum	450
Sum	12674	Sum	12348	Sum	12313	Sum	12303
Count	30	Count	30	Count	30	Count	30
Confidence	3.875263	Confidence	2.846482	Confidence	6.226456	Confidence	6.002081
THIN-4N-8		*THIN-8N-11*		*THIN-ADD-4N-19*		*THIN-ADD-8N-21*	
Mean	393.1333	Mean	390.6333	Mean	384.8667	Mean	384.7333
Standard E	1.296089	Standard E	1.166075	Standard E	1.956853	Standard E	1.981485
Median	394	Median	391.5	Median	385	Median	385
Mode	395	Mode	392	Mode	385	Mode	381
Standard D	7.098972	Standard D	6.386858	Standard D	10.71812	Standard D	10.85304
Sample Va	50.3954	Sample Va	40.79195	Sample Va	114.8782	Sample Va	117.7885
Kurtosis	0.420462	Kurtosis	0.223473	Kurtosis	0.729344	Kurtosis	0.811086
Skewness	-0.872915	Skewness	-0.705961	Skewness	0.026725	Skewness	0.27471
Range	27	Range	26	Range	47	Range	50
Minimum	377	Minimum	376	Minimum	362	Minimum	362
Maximum	404	Maximum	402	Maximum	409	Maximum	412
Sum	11794	Sum	11719	Sum	11546	Sum	11542
Count	30	Count	30	Count	30	Count	30
Confidence	2.650801	Confidence	2.384893	Confidence	4.002215	Confidence	4.052594

Table 6.11: Analysis time of 100 Kbytes images without crossover-frontlighting-106 micron resolution (ms)

OUT-4N-8 --> OUTLINE-4 NEIGHBORHOOD-Threshold 8
OUT-8N-11 --> OUTLINE-8 NEIGHBORHOOD-Threshold 11
OUT-ADD-4N-19--> OUTLINE-4 NEIGHBORHOOD-Threshold 19
OUT-ADD-8N-21--> OUTLINE-8 NEIGHBORHOOD-Threshold 21

THIN-4N-8 --> THINNING-4 NEIGHBORHOOD-Threshold 8
THIN-8N-11 --> THINNING-8 NEIGHBORHOOD-Threshold 11
THIN-ADD-4N-19--> THINNING-4 NEIGHBORHOOD-Threshold 19
THIN-ADD-8N-21--> THINNING-8 NEIGHBORHOOD-Threshold 21

OUT-4N-8		*OUT-8N-11*		*OUT-ADD-4N-19*		*OUT-ADD-8N-21*	
Mean	57.99067	Mean	95.404	Mean	101.0973	Mean	154.696
Standard E	2.246322	Standard E	2.716943	Standard E	1.994597	Standard E	3.177281
Median	48.8	Median	97.6	Median	97.6	Median	146.4
Mode	48.8	Mode	97.6	Mode	97.6	Mode	146.4
Standard D	12.30361	Standard D	14.88131	Standard D	10.92486	Standard D	17.40269
Sample Va	151.3788	Sample Va	221.4534	Sample Va	119.3526	Sample Va	302.8535
Kurtosis	-1.755075	Kurtosis	-0.132967	Kurtosis	13.28206	Kurtosis	0.51953
Skewness	0.592905	Skewness	-0.010201	Skewness	3.570636	Skewness	0.621772
Range	26.84	Range	48.8	Range	51.24	Range	73.2
Minimum	48.8	Minimum	73.2	Minimum	97.6	Minimum	122
Maximum	75.64	Maximum	122	Maximum	148.84	Maximum	195.2
Sum	1739.72	Sum	2862.12	Sum	3032.92	Sum	4640.88
Count	30	Count	30	Count	30	Count	30
Confidence	4.594246	Confidence	5.556776	Confidence	4.079412	Confidence	6.498273
THIN-4N-8		*THIN-8N-11*		*THIN-ADD-4N-19*		*THIN-ADD-8N-21*	
Mean	138.348	Mean	173.484	Mean	209.1893	Mean	237.9813
Standard E	2.148111	Standard E	2.990323	Standard E	5.608076	Standard E	6.103346
Median	146.4	Median	170.8	Median	195.2	Median	244
Mode	146.4	Mode	170.8	Mode	195.2	Mode	244
Standard D	11.76569	Standard D	16.37868	Standard D	30.7167	Standard D	33.4294
Sample Va	138.4315	Sample Va	268.261	Sample Va	943.5156	Sample Va	1117.525
Kurtosis	-1.552612	Kurtosis	2.495782	Kurtosis	1.039132	Kurtosis	2.675559
Skewness	-0.739879	Skewness	-0.817075	Skewness	0.692957	Skewness	0.992259
Range	26.84	Range	75.64	Range	146.4	Range	173.24
Minimum	122	Minimum	122	Minimum	146.4	Minimum	170.8
Maximum	148.84	Maximum	197.64	Maximum	292.8	Maximum	344.04
Sum	4150.44	Sum	5204.52	Sum	6275.68	Sum	7139.44
Count	30	Count	30	Count	30	Count	30
Confidence	4.393383	Confidence	6.115901	Confidence	11.46981	Confidence	12.48275

Some of these were connected to fibers with the adding algorithm resulting in reduced accuracy and precision.

6.2.6. Without Fiber Crossover-185 micron Resolution-Frontlighting

Fifteen images were captured and analyzed for 185-micron resolution and frontlighting for the best threshold values. Two polyester fibers fit into one frame easily. Figures 6.11 and 6.12 show the length and time measurement of applied algorithms, and Tables 6.12 and 6.13 show the respective descriptive statistics.

The best threshold values without the adding algorithm were found to be 8 for the 4N and 10 for the 8N thresholding. With the adding algorithm, they were found to be 17 for the 4N and 18 for the 8N thresholding. Compared to the previous threshold values, these numbers still show high contrast implying adequate image quality. However, analysis time sharply increased for all algorithms compared to 106-micron resolution.

The thinning algorithm produced the best accuracy for all measurements when compared to the reference of cut length. The 4N thresholding measured the average length to be 38.4 mm while 8N thresholding measured slightly lower than 38.4 mm as seen in Table 6.12. The confidence interval was only slightly lower than 0.4 mm showing that the precision still satisfies our requirements. It seems that noise connected to fibers causes longer length measurement. On the other hand, lower resolution causes shorter length measurements by missing fine curves on the fibers. If this is true, these two effects effectively cancel each other causing the best accuracy in length measurements. However, dust makes invalid the length measurements of 185-micron resolution images since it creates more than 4 mm non-existing fiber lengths on some images.

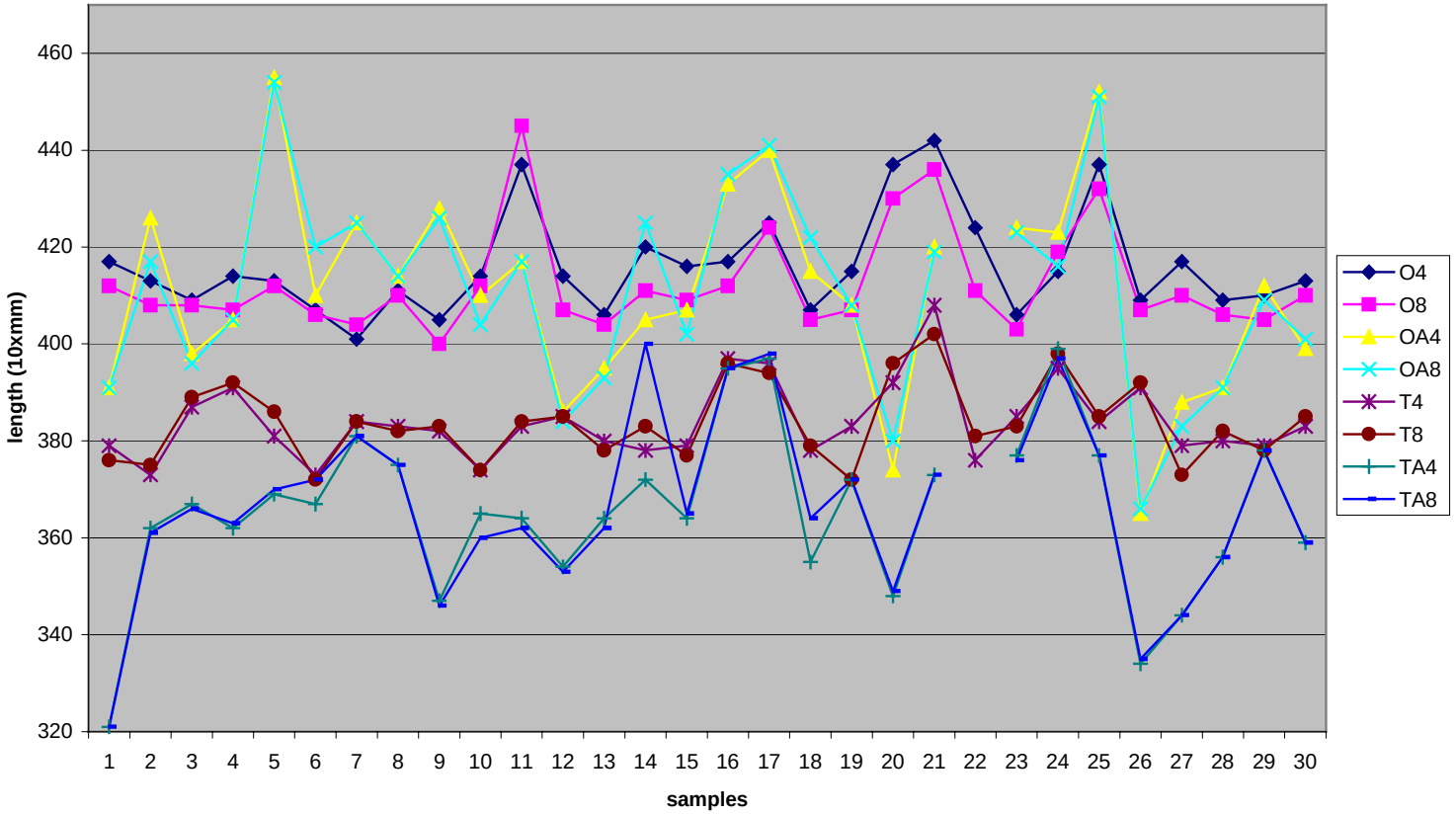

Figure 6.11: Length measurement results of images without crossover-frontlighting-185 micron resolution (10xmm)

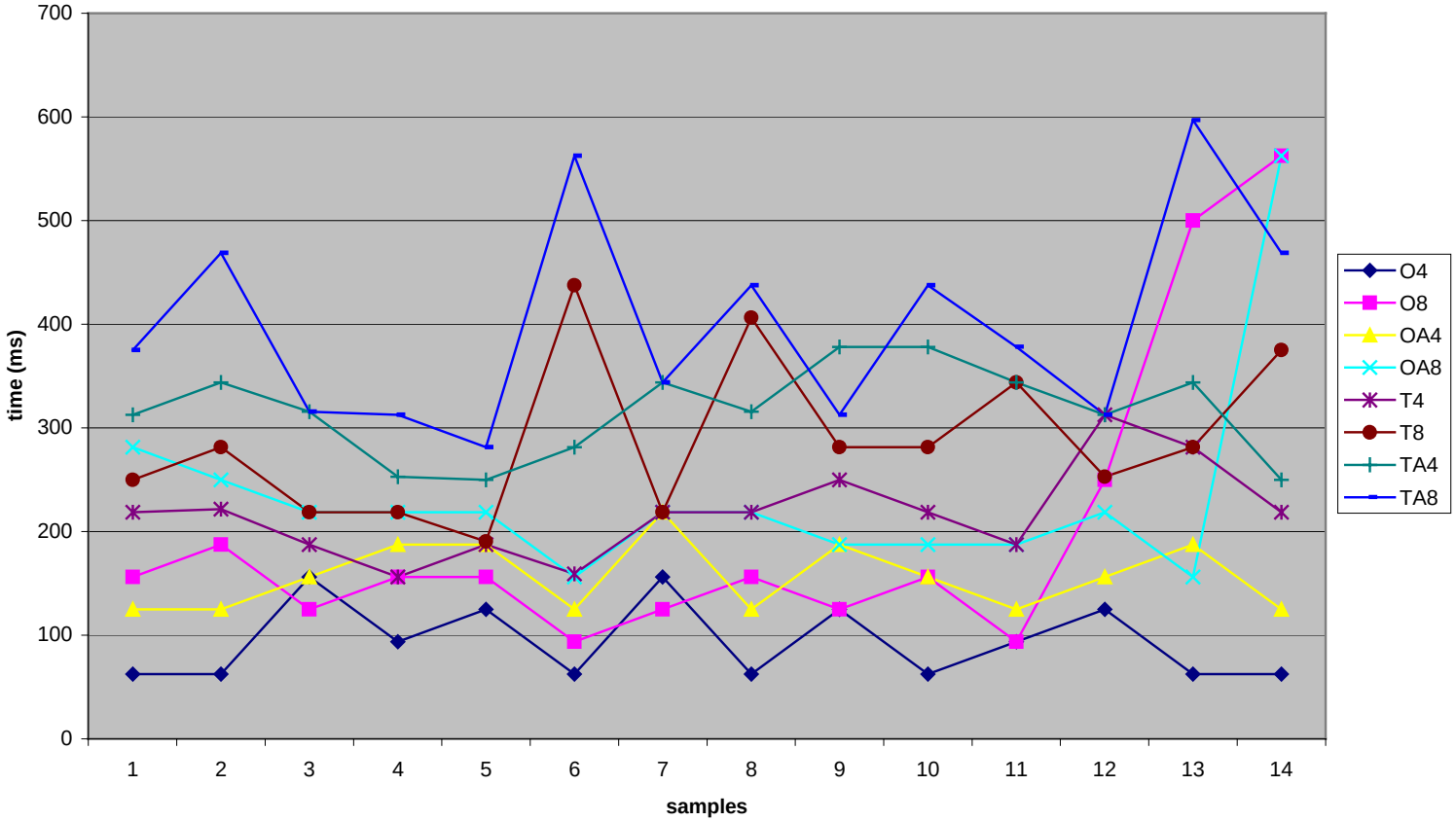

Figure 6.12: Analysis time of 100 Kbytes images without crossover-frontlighting-185 micron resolution (ms)

Table 6.12: Length measurement results of images without crossover-frontlighting-185 micron resolution (10xmm)

OUT-4N-8 --> OUTLINE-4 NEIGHBORHOOD-Threshold 8
OUT-8N-11 --> OUTLINE-8 NEIGHBORHOOD-Threshold 10
OUT-ADD-4N-19--> OUTLINE-4 NEIGHBORHOOD-Threshold 17
OUT-ADD-8N-21--> OUTLINE-8 NEIGHBORHOOD-Threshold 18

THIN-4N-8 --> THINNING-4 NEIGHBORHOOD-Threshold 8
THIN-8N-11 --> THINNING-8 NEIGHBORHOOD-Threshold 10
THIN-ADD-4N-19--> THINNING-4 NEIGHBORHOOD-Threshold 17
THIN-ADD-8N-21--> THINNING-8 NEIGHBORHOOD-Threshold 18

OUT-4N-8		*OUT-8N-10*		*OUT-ADD-4N-17*		*OUT-ADD-8N-18*	
Mean	416	Mean	412.4	Mean	410.8966	Mean	410.9655
Standard E	1.893728	Standard E	1.934324	Standard E	3.878495	Standard E	3.873773
Median	414	Median	409.5	Median	410	Median	414
Mode	417	Mode	412	Mode	391	Mode	391
Standard D	10.37238	Standard D	10.59473	Standard D	20.88633	Standard D	20.8609
Sample Va	107.5862	Sample Va	112.2483	Sample Va	436.2389	Sample Va	435.1773
Kurtosis	0.910712	Kurtosis	2.582523	Kurtosis	0.186689	Kurtosis	-0.086617
Skewness	1.225849	Skewness	1.75452	Skewness	0.036206	Skewness	0.039118
Range	41	Range	45	Range	90	Range	88
Minimum	401	Minimum	400	Minimum	365	Minimum	366
Maximum	442	Maximum	445	Maximum	455	Maximum	454
Sum	12480	Sum	12372	Sum	11916	Sum	11918
Count	30	Count	30	Count	29	Count	29
Confidence	3.873111	Confidence	3.956139	Confidence	7.944745	Confidence	7.935073
THIN-4N-8		*THIN-8N-10*		*THIN-ADD-4N-17*		*THIN-ADD-8N-18*	
Mean	383.9333	Mean	383.8667	Mean	365.4483	Mean	366.5517
Standard E	1.442327	Standard E	1.472923	Standard E	3.213114	Standard E	3.396095
Median	383	Median	383	Median	365	Median	365
Mode	379	Mode	383	Mode	364	Mode	372
Standard D	7.899949	Standard D	8.067531	Standard D	17.30315	Standard D	18.28853
Sample Va	62.4092	Sample Va	65.08506	Sample Va	299.399	Sample Va	334.4704
Kurtosis	1.648963	Kurtosis	-0.436076	Kurtosis	0.844549	Kurtosis	0.493423
Skewness	1.153718	Skewness	0.490644	Skewness	-0.285014	Skewness	-0.180442
Range	35	Range	30	Range	78	Range	79
Minimum	373	Minimum	372	Minimum	321	Minimum	321
Maximum	408	Maximum	402	Maximum	399	Maximum	400
Sum	11518	Sum	11516	Sum	10598	Sum	10630
Count	30	Count	30	Count	29	Count	29
Confidence	2.949891	Confidence	3.012467	Confidence	6.581774	Confidence	6.956594

Table 6.13: Analysis time of 100 Kbytes images without crossover-frontlighting-185 micron resolution (ms)

OUT-4N-8 --> OUTLINE-4 NEIGHBORHOOD-Threshold 8
OUT-8N-11 --> OUTLINE-8 NEIGHBORHOOD-Threshold 10
OUT-ADD-4N-19--> OUTLINE-4 NEIGHBORHOOD-Threshold 17
OUT-ADD-8N-21--> OUTLINE-8 NEIGHBORHOOD-Threshold 18

THIN-4N-8 --> THINNING-4 NEIGHBORHOOD-Threshold 8
THIN-8N-11 --> THINNING-4 NEIGHBORHOOD-Threshold 10
THIN-ADD-4N-19--> THINNING-4 NEIGHBORHOOD-Threshold 17
THIN-ADD-8N-21--> THINNING-8 NEIGHBORHOOD-Threshold 18

OUT-4N-8		*OUT-8N-10*		*OUT-ADD-4N-17*		*OUT-ADD-8N-18*	
Mean	93.75	Mean	203.125	Mean	156.25	Mean	234.375
Standard E	9.82767	Standard E	38.72623	Standard E	8.667191	Standard E	26.76424
Median	78.125	Median	156.25	Median	156.25	Median	218.75
Mode	62.5	Mode	156.25	Mode	125	Mode	218.75
Standard D	36.77178	Standard D	144.9003	Standard D	32.42966	Standard D	100.1426
Sample Va	1352.163	Sample Va	20996.09	Sample Va	1051.683	Sample Va	10028.55
Kurtosis	-1.159933	Kurtosis	3.064359	Kurtosis	-1.097403	Kurtosis	10.37909
Skewness	0.660984	Skewness	2.009278	Skewness	0.481812	Skewness	3.051593
Range	93.75	Range	468.75	Range	93.75	Range	406.25
Minimum	62.5	Minimum	93.75	Minimum	125	Minimum	156.25
Maximum	156.25	Maximum	562.5	Maximum	218.75	Maximum	562.5
Sum	1312.5	Sum	2843.75	Sum	2187.5	Sum	3281.25
Count	14	Count	14	Count	14	Count	14
Confidence	21.23139	Confidence	83.66292	Confidence	18.72432	Confidence	57.82062
THIN-4N-8		*THIN-8N-10*		*THIN-ADD-4N-17*		*THIN-ADD-8N-18*	
Mean	216.9643	Mean	288.3929	Mean	315.8482	Mean	400.2232
Standard E	11.48298	Standard E	20.12588	Standard E	11.64884	Standard E	26.30004
Median	218.75	Median	281.25	Median	315.625	Median	376.5625
Mode	218.75	Mode	281.25	Mode	343.75	Mode	312.5
Standard D	42.96539	Standard D	75.30416	Standard D	43.58596	Standard D	98.40574
Sample Va	1846.025	Sample Va	5670.716	Sample Va	1899.736	Sample Va	9683.69
Kurtosis	0.770867	Kurtosis	-0.345196	Kurtosis	-0.890113	Kurtosis	-0.347354
Skewness	0.772	Skewness	0.782137	Skewness	-0.313591	Skewness	0.763191
Range	156.25	Range	246.875	Range	128.125	Range	315.625
Minimum	156.25	Minimum	190.625	Minimum	250	Minimum	281.25
Maximum	312.5	Maximum	437.5	Maximum	378.125	Maximum	596.875
Sum	3037.5	Sum	4037.5	Sum	4421.875	Sum	5603.125
Count	14	Count	14	Count	14	Count	14
Confidence	24.80748	Confidence	43.47932	Confidence	25.16578	Confidence	56.81777

The thinning algorithm produced satisfactory precision and the best accuracy for all length measurements for 185-micron resolution and frontlighting images. Thinning-adding measured the mean length less than hand-measurement with the values of 36.5 for the 4N and 36.6 mm for the 8N thresholding. Many sharp curves on the fiber connected to each other by the adding algorithm creating short cut between the pixels. All adding algorithms reduced precision creating higher confidence intervals than the required value. There is an opportunity to satisfy the required precision even in lower resolution images than 185-micron with a dust free environment. However, in this work the lowest satisfactory resolution was found to be 106-micron since it created less than 2 mm non-existing fiber measurements.

6.2.7. With Fiber Crossover-37 micron Resolution-Backlighting

Analysis of previous results showed that the maximum resolution was about 60-micron for backlighting and about 100-micron for frontlighting. However, as discussed before, the crossover algorithm was very noise sensitive creating misreading or eliminating many fibers so that inefficiency becomes a factor. Instead of using only the maximum resolution, one lower resolution data set was added to each lighting technique. The sample preparation procedure was the same as without fiber crossovers while adding one cotton fiber which cut through the polyester fiber creating a crossover and hit to at least one edge of frame so that the cotton fiber could be eliminated from measurement. Edge connections of cotton helped the inspection of images visually and literally.

Figures 6.13 and 14 show the length and time measurement of applied algorithms, and Table 14 and 15 show the respective descriptive statistics. As mentioned before, the crossover algorithm was very noise sensitive in that two out of twenty-nine images, for 6

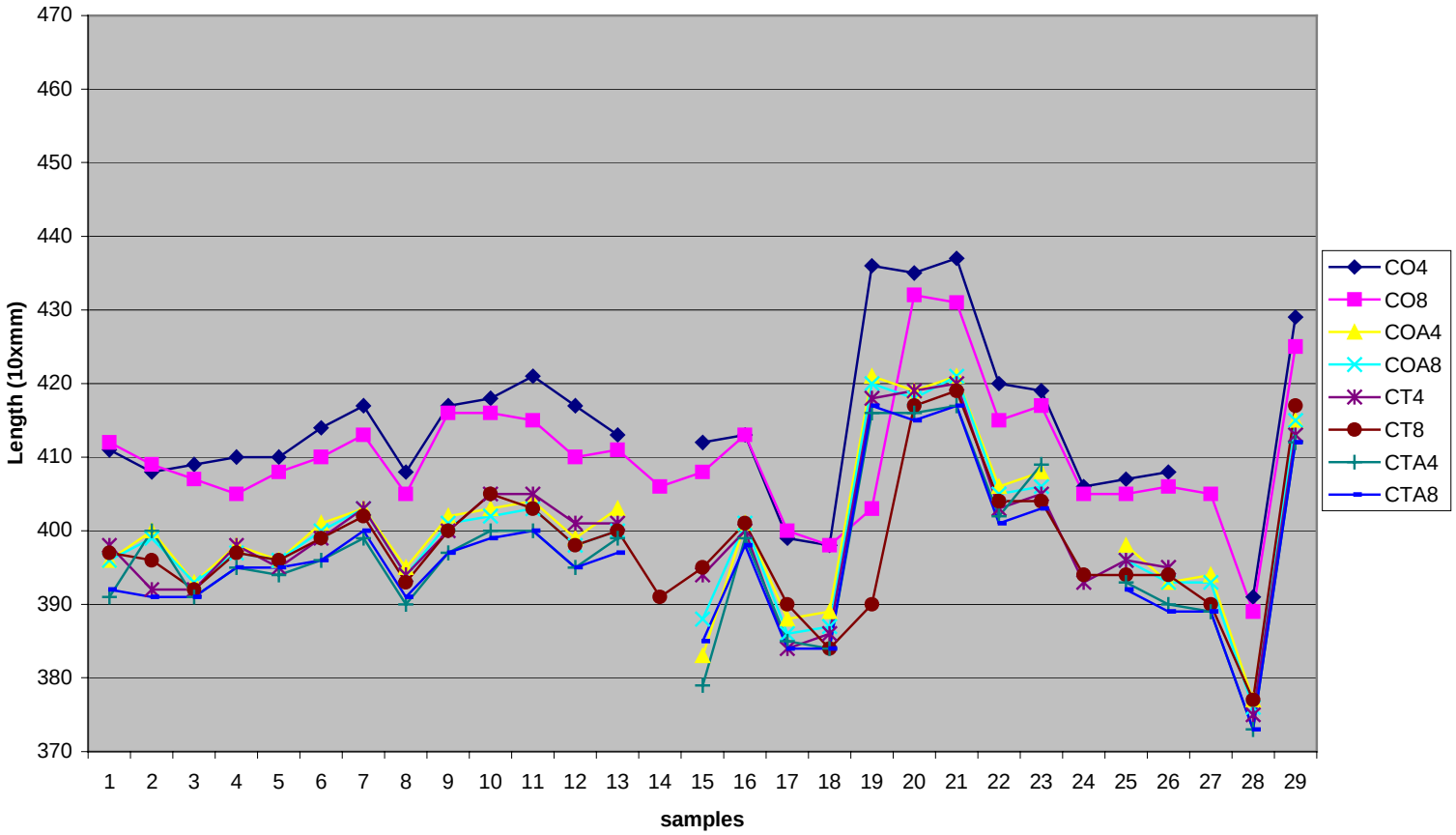

Figure 6.13: Length measurement results of images with crossover-backlighting-37 micron resolution (10xmm)

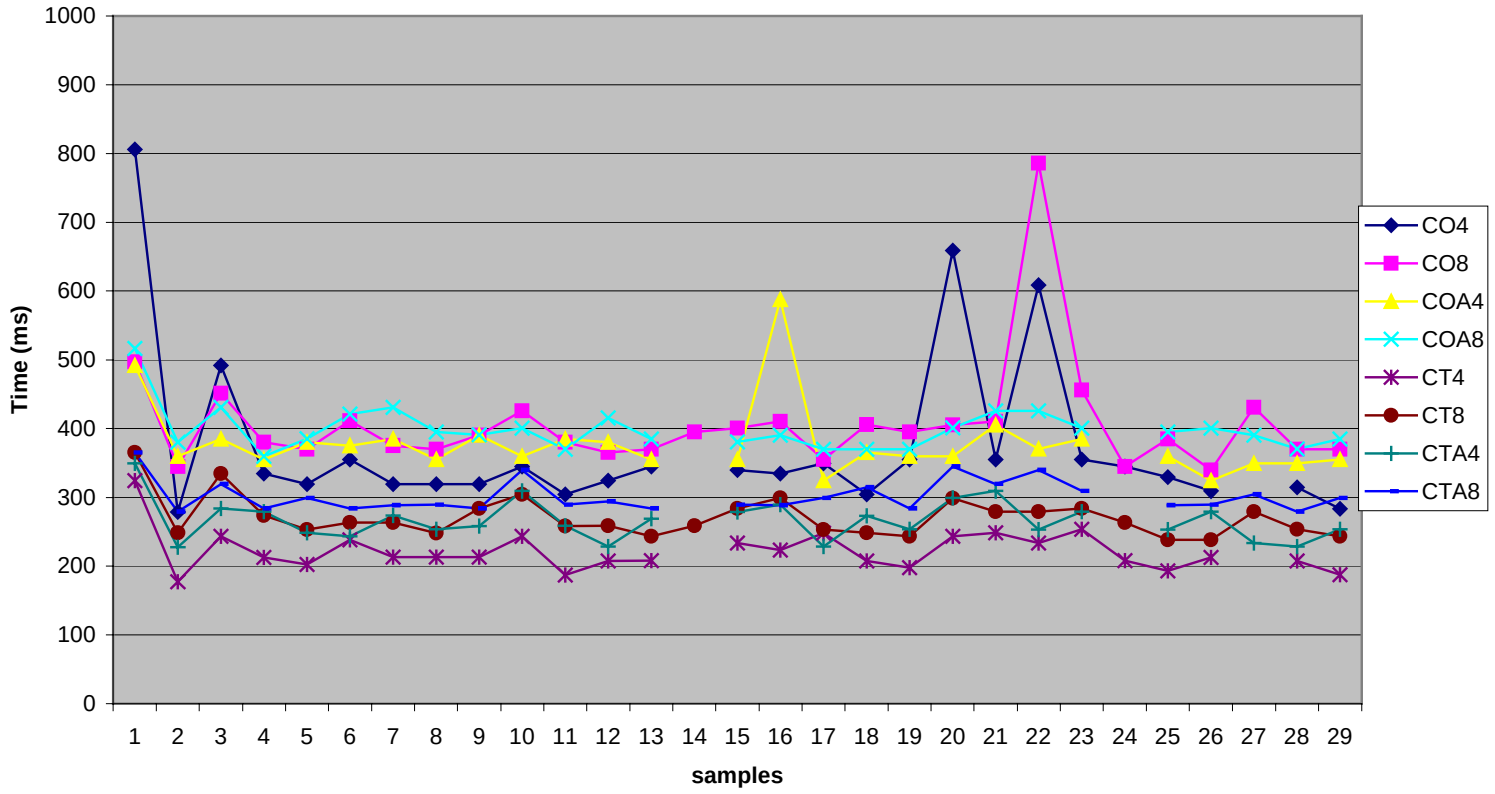

Figure 6.14: Analysis time of 100 Kbytes images with crossover-backlighting-37 micron resolution (ms)

Table 6.14: Length measurement results of images with crossover-backlighting-37 micron resolution (10xmm)

OUT-4N-8 --> OUTLINE-4 NEIGHBORHOOD-Threshold 8
OUT-8N-9 --> OUTLINE-8 NEIGHBORHOOD-Threshold 9
OUT-ADD-4N-12--> OUTLINE-4 NEIGHBORHOOD-Threshold 12
OUT-ADD-8N-13--> OUTLINE-8 NEIGHBORHOOD-Threshold 13

THIN-4N-8 --> THINNING-4 NEIGHBORHOOD-Threshold 8
THIN-8N-9--> THINNING-8 NEIGHBORHOOD-Threshold 9
THIN-ADD-4N-12--> THINNING-4 NEIGHBORHOOD-Threshold 12
THIN-ADD-8N-13--> THINNING-8 NEIGHBORHOOD-Threshold 13

OUT-4N-8		*OUT-8N-9*		*OUT-ADD-4N-12*		*OUT-ADD-8N-13*	
Mean	414.1852	Mean	410.1724	Mean	400.2222	Mean	399.5185
Standard E	2.112935	Standard E	1.665404	Standard E	2.032032	Standard E	1.9967
Median	413	Median	409	Median	400	Median	399
Mode	408	Mode	405	Mode	403	Mode	396
Standard D	10.97913	Standard D	8.968472	Standard D	10.55875	Standard D	10.37516
Sample Va	120.5413	Sample Va	80.4335	Sample Va	111.4872	Sample Va	107.6439
Kurtosis	0.493175	Kurtosis	1.505663	Kurtosis	0.422567	Kurtosis	0.611554
Skewness	0.411408	Skewness	0.535911	Skewness	0.225669	Skewness	0.33298
Range	46	Range	43	Range	44	Range	45
Minimum	391	Minimum	389	Minimum	377	Minimum	376
Maximum	437	Maximum	432	Maximum	421	Maximum	421
Sum	11183	Sum	11895	Sum	10806	Sum	10787
Count	27	Count	29	Count	27	Count	27
Confidence	4.343202	Confidence	3.411428	Confidence	4.176905	Confidence	4.104278
THIN-4N-8		*THIN-8N-9*		*THIN-ADD-4N-12*		*THIN-ADD-8N-13*	
Mean	399.4074	Mean	397.8966	Mean	396.7037	Mean	396.2222
Standard E	1.975822	Standard E	1.700728	Standard E	2.0788	Standard E	1.984508
Median	399	Median	397	Median	396	Median	395
Mode	405	Mode	390	Mode	400	Mode	391
Standard D	10.26667	Standard D	9.158699	Standard D	10.80176	Standard D	10.31181
Sample Va	105.4046	Sample Va	83.88177	Sample Va	116.6781	Sample Va	106.3333
Kurtosis	0.711303	Kurtosis	1.15105	Kurtosis	0.160092	Kurtosis	0.570834
Skewness	0.138249	Skewness	0.511995	Skewness	0.145982	Skewness	0.3834
Range	45	Range	42	Range	44	Range	44
Minimum	375	Minimum	377	Minimum	373	Minimum	373
Maximum	420	Maximum	419	Maximum	417	Maximum	417
Sum	10784	Sum	11539	Sum	10711	Sum	10698
Count	27	Count	29	Count	27	Count	27
Confidence	4.061363	Confidence	3.483787	Confidence	4.273038	Confidence	4.079217

Table 6.15: Analysis time of 100 Kbytes images
with crossover-frontlighting-37 micron resolution (ms)

OUT-4N-8 --> OUTLINE-4 NEIGHBORHOOD-Threshold 8
OUT-8N-9 --> OUTLINE-8 NEIGHBORHOOD-Threshold 9
OUT-ADD-4N-12--> OUTLINE-4 NEIGHBORHOOD-Threshold 12
OUT-ADD-8N-13--> OUTLINE-8 NEIGHBORHOOD-Threshold 13

THIN-4N-8 --> THINNING-4 NEIGHBORHOOD-Threshold 8
THIN-8N-9--> THINNING-8 NEIGHBORHOOD-Threshold 9
THIN-ADD-4N-12--> THINNING-4 NEIGHBORHOOD-Threshold 12
THIN-ADD-8N-13--> THINNING-8 NEIGHBORHOOD-Threshold 13

OUT-4N-8		*OUT-8N-9*		*OUT-ADD-4N-12*		*OUT-ADD-8N-13*	
Mean	374.0464	Mean	406.4576	Mean	377.982	Mean	398.297
Standard E	23.76392	Standard E	15.06132	Standard E	9.979734	Standard E	5.999408
Median	334.466	Median	390.126	Median	359.766	Median	390.632
Mode	319.286	Mode	369.886	Mode	359.766	Mode	369.886
Standard D	123.4809	Standard D	81.1077	Standard D	51.85622	Standard D	31.17384
Sample Va	15247.54	Sample Va	6578.459	Sample Va	2689.067	Sample Va	971.8083
Kurtosis	5.943864	Kurtosis	17.98395	Kurtosis	10.7894	Kurtosis	7.160486
Skewness	2.514273	Skewness	3.900456	Skewness	3.050966	Skewness	2.181172
Range	527.252	Range	446.292	Range	263.12	Range	156.86
Minimum	278.3	Minimum	339.526	Minimum	324.346	Minimum	359.766
Maximum	805.552	Maximum	785.818	Maximum	587.466	Maximum	516.626
Sum	10099.25	Sum	11787.27	Sum	10205.51	Sum	10754.02
Count	27	Count	29	Count	27	Count	27
Confidence	48.84746	Confidence	30.85175	Confidence	20.51365	Confidence	12.33197
THIN-4N-8		*THIN-8N-9*		*THIN-ADD-4N-12*		*THIN-ADD-8N-13*	
Mean	221.4593	Mean	270.3436	Mean	266.3059	Mean	301.6135
Standard E	5.645635	Standard E	5.403938	Standard E	5.599568	Standard E	4.372834
Median	213.026	Median	263.626	Median	258.566	Median	288.926
Mode	213.026	Mode	263.626	Mode	278.806	Mode	283.866
Standard D	29.33558	Standard D	29.1011	Standard D	29.09621	Standard D	22.72191
Sample Va	860.5764	Sample Va	846.8738	Sample Va	846.5892	Sample Va	516.2853
Kurtosis	4.655267	Kurtosis	3.070867	Kurtosis	1.142451	Kurtosis	1.159364
Skewness	1.601637	Skewness	1.59232	Skewness	0.854349	Skewness	1.371002
Range	147.246	Range	126.5	Range	121.946	Range	86.02
Minimum	177.1	Minimum	238.326	Minimum	227.7	Minimum	278.806
Maximum	324.346	Maximum	364.826	Maximum	349.646	Maximum	364.826
Sum	5979.402	Sum	7839.964	Sum	7190.26	Sum	8143.564
Count	27	Count	29	Count	27	Count	27
Confidence	11.60478	Confidence	11.06948	Confidence	11.51008	Confidence	8.988495

applications, were eliminated from the measurements. The best threshold values were chosen to be the same as without fiber crossover-37 micron resolution-backlighting images. Confidence intervals were in the precision limit for each application between 0.34 mm and 0.43 mm as in Table 6.14, however, they were significantly greater than non-crossover applications. 8N thresholding produced slightly better precision than 4N thresholding as in without fiber crossover-37 micron-backlighting applications, while causing slightly more analysis time. However, the adding algorithm lowered precision which is an opposite result compared to previous backlighting results. Interestingly, the thinning algorithm did not significantly improve the precision of any application. Accuracy was improved without the thinning algorithm, most probably because of the new lighting conditions which produced images with less noise. The outline analysis time was increased about five times over the non-crossover algorithms because this crossover algorithm requires thinning to determine the point of crossover. Since the outline algorithm requires one more step than the thinning algorithm for crossover applications, it becomes the most time consuming algorithm.

6.2.8. With Fiber Crossover-57 micron Resolution-Backlighting

Twenty-nine images were captured and analyzed for 57-micron resolution and backlighting for the best threshold values. The outline-8N algorithm did not produce error free measurements. The outline-4N produced results for only 17 out of twenty-nine images. The other data were eliminated because of undetermined points on the images. Figure 6.15 and Figure 6.16 shows the length and time measurement of applied algorithms, and Table 6.16 and Table 6.17 shows respective descriptive statistics.

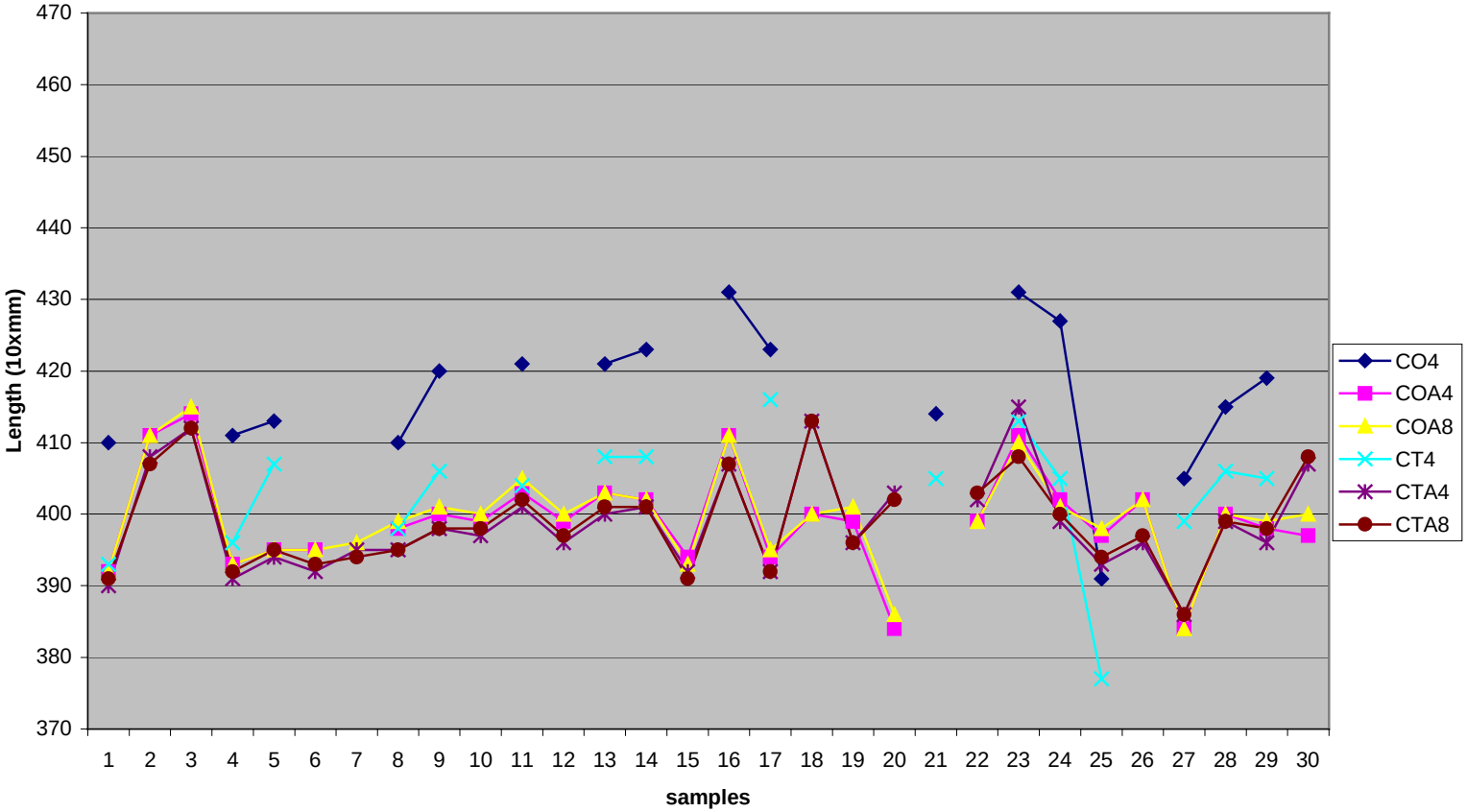

Figure 6.15: Length measurement results of images with crossover-backlighting-57 micron resolution (10xmm)

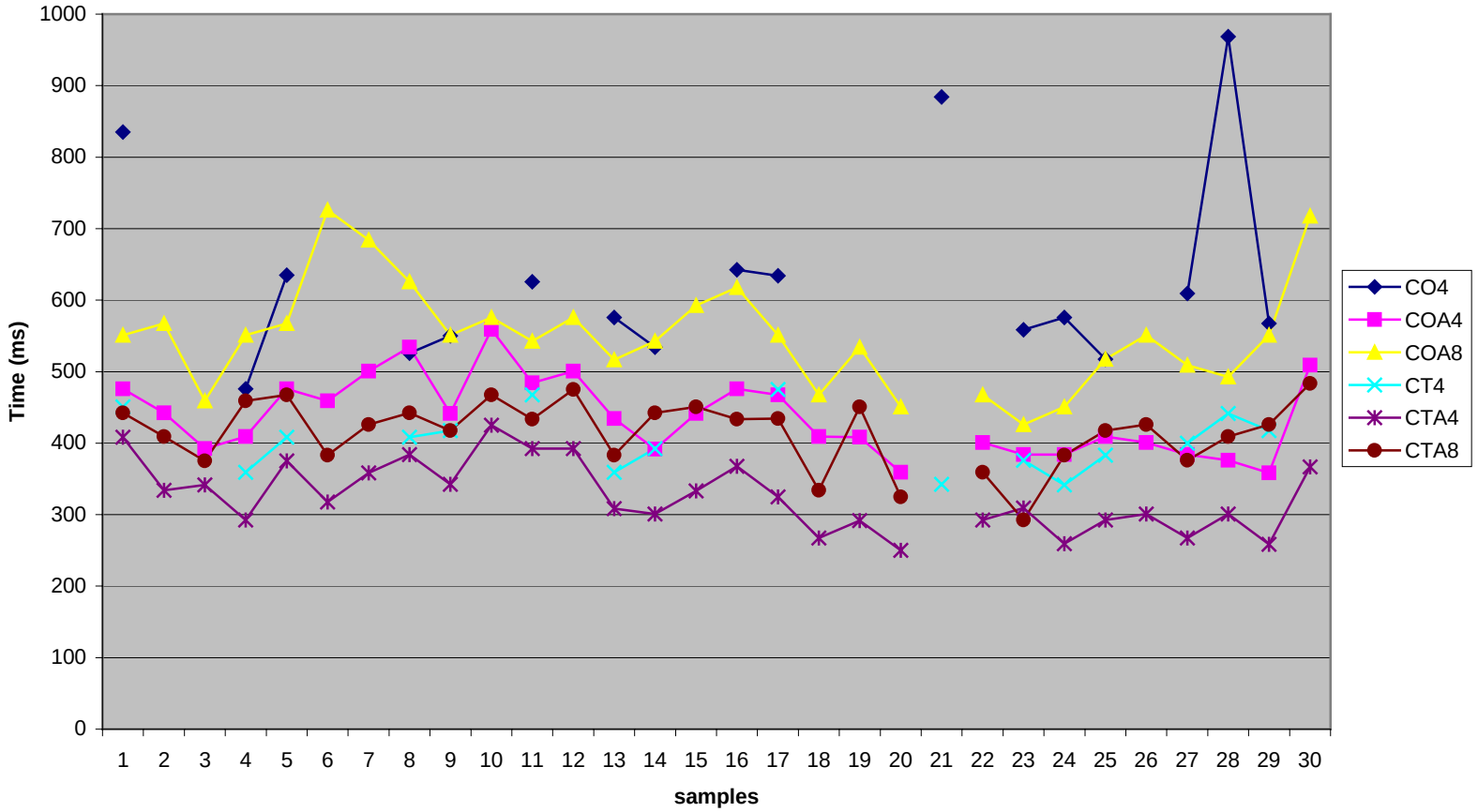

Figure 6.16: Analysis time of 100 Kbytes images with crossover-backlighting-57 micron resolution (ms)

Table 6.16: Length measurement results of images with crossover-backlighting-57 micron resolution (10xmm)

OUT-4N-7 --> OUTLINE-4 NEIGHBORHOOD-Threshold 7
OUT-ADD-4N-13--> OUTLINE-4 NEIGHBORHOOD-Threshold 13
OUT-ADD-8N-13--> OUTLINE-8 NEIGHBORHOOD-Threshold 13

THIN-4N-8 --> THINNING-4 NEIGHBORHOOD-Threshold 8
THIN-ADD-4N-13--> THINNING-4 NEIGHBORHOOD-Threshold 13
THIN-ADD-8N-13--> THINNING-8 NEIGHBORHOOD-Threshold 13

OUT-4N-7	
Mean	416.7647
Standard E	2.41857
Median	419
Mode	410
Standard D	9.97202
Sample Va	99.44118
Kurtosis	1.521341
Skewness	-0.864224
Range	40
Minimum	391
Maximum	431
Sum	7085
Count	17
Confidence	5.127138

OUT-ADD-4N-13	
Mean	399.1429
Standard E	1.334042
Median	399
Mode	399
Standard D	7.059085
Sample Va	49.83069
Kurtosis	0.732611
Skewness	0.055483
Range	30
Minimum	384
Maximum	414
Sum	11176
Count	28
Confidence	2.737226

OUT-ADD-8N-13	
Mean	399.5172
Standard E	1.273663
Median	400
Mode	400
Standard D	6.858887
Sample Va	47.04433
Kurtosis	0.749838
Skewness	0.075013
Range	31
Minimum	384
Maximum	415
Sum	11586
Count	29
Confidence	2.608984

THIN-4N-7	
Mean	402.875
Standard E	2.265456
Median	405
Mode	405
Standard D	9.061825
Sample Va	82.11667
Kurtosis	3.721722
Skewness	-1.541577
Range	39
Minimum	377
Maximum	416
Sum	6446
Count	16
Confidence	4.828708

THIN-ADD-4N-13	
Mean	398.8276
Standard E	1.340051
Median	397
Mode	396
Standard D	7.216395
Sample Va	52.07635
Kurtosis	-0.067941
Skewness	0.673623
Range	29
Minimum	386
Maximum	415
Sum	11566
Count	29
Confidence	2.744973

THIN-ADD-8N-13	
Mean	398.9655
Standard E	1.231246
Median	398
Mode	398
Standard D	6.630464
Sample Va	43.96305
Kurtosis	-0.284139
Skewness	0.412995
Range	27
Minimum	386
Maximum	413
Sum	11570
Count	29
Confidence	2.522096

Table 6.17: Analysis time of 100 Kbytes images with crossover-backlighting-57 micron resolution (ms)

OUT-4N-7 --> OUTLINE-4 NEIGHBORHOOD-Threshold 7
OUT-ADD-4N-13--> OUTLINE-4 NEIGHBORHOOD-Threshold 13
OUT-ADD-8N-13--> OUTLINE-8 NEIGHBORHOOD-Threshold 13

THIN-4N-8 --> THINNING-4 NEIGHBORHOOD-Threshold 8
THIN-ADD-4N-13--> THINNING-4 NEIGHBORHOOD-Threshold 13
THIN-ADD-8N-13--> THINNING-8 NEIGHBORHOOD-Threshold 13

OUT-4N-7	
Mean	630.2941
Standard E	33.18356
Median	575.8333
Mode	575.8333
Standard D	136.8193
Sample Va	18719.53
Kurtosis	1.541986
Skewness	1.519762
Range	492.5
Minimum	475.8333
Maximum	968.3333
Sum	10715
Count	17
Confidence	70.34599

OUT-ADD-4N-13	
Mean	436.8966
Standard E	9.934179
Median	434.1667
Mode	475.8333
Standard D	53.49719
Sample Va	2861.949
Kurtosis	-0.581916
Skewness	0.498098
Range	200.8333
Minimum	358.3333
Maximum	559.1667
Sum	12670
Count	29
Confidence	20.34927

OUT-ADD-8N-13	
Mean	549.3678
Standard E	13.83755
Median	550.8333
Mode	550.8333
Standard D	74.51751
Sample Va	5552.86
Kurtosis	0.600162
Skewness	0.708238
Range	300
Minimum	425.8333
Maximum	725.8333
Sum	15931.67
Count	29
Confidence	28.34498

THIN-4N-7	
Mean	402.5521
Standard E	10.4304
Median	404.1667
Mode	359.1667
Standard D	41.7216
Sample Va	1740.692
Kurtosis	-0.824726
Skewness	0.210743
Range	133.3333
Minimum	341.6667
Maximum	475
Sum	6440.833
Count	16
Confidence	22.23188

THIN-ADD-4N-13	
Mean	326.0632
Standard E	8.95036
Median	317.5
Mode	292.5
Standard D	48.19917
Sample Va	2323.16
Kurtosis	-0.813954
Skewness	0.322291
Range	175
Minimum	250
Maximum	425
Sum	9455.833
Count	29
Confidence	18.334

THIN-ADD-8N-13	
Mean	414.6552
Standard E	8.662971
Median	425.8333
Mode	442.5
Standard D	46.65153
Sample Va	2176.365
Kurtosis	0.453304
Skewness	-0.883302
Range	190.8333
Minimum	292.5
Maximum	483.3333
Sum	12025
Count	29
Confidence	17.74531

Table 6.16 shows that the outline-4N produced slightly lower precision than the required value with a 0.51 mm confidence interval and the slowest analysis time with 630 ms for 100 Kbytes images. The adding algorithm significantly improved precision dropping the confidence interval to almost hand-measurement precision while reducing analysis time. The thinning algorithm did not significantly change precision and accuracy but reduced analysis time. Conclusively, the thinning algorithm combined with the adding algorithm produced the best results for every aspect. The thinning-adding-4N had a slightly higher confidence interval and slightly lowers analysis time than the thinning-adding-8N meaning either thresholding method could be justified.

6.2.9. With Fiber Crossover-57 micron Resolution-Frontlighting

The outline algorithm could not make error free measurements for 57-micron resolution with frontlighting. Only the thinning-8N, the thinning-adding-4N and thinning-adding-8N produced error free measurements while eliminating about 30% of data as can be seen from Figures 6.17 and 6.18. Table 6.18 shows that confidence intervals are in the required range. The adding algorithm significantly improved accuracy and precision contrary to previous frontlighting results.

There was not a significant difference between backlighting and frontlighting in terms of precision. Analysis time was between 25-45% higher for frontlighting, however, frontlighting eliminated about 30% of data while backlighting collected 100% of the data for thinning applications. As a result, neither of these two lighting techniques can be considered superior with respect to precision and processing time, for this resolution. However, backlighting seems more reliable since all the images produced

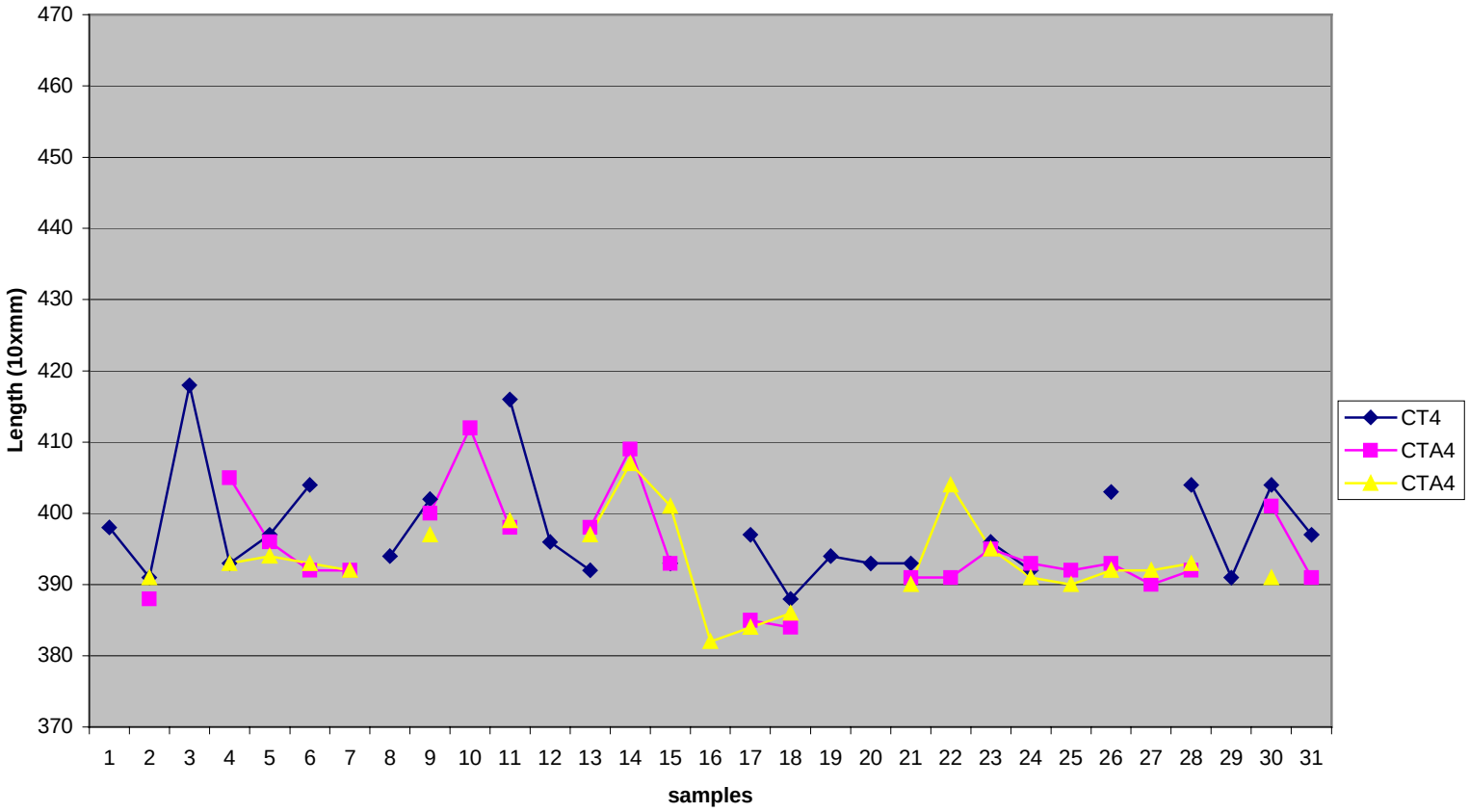

Figure 6.17: Length measurement results of images with crossover-frontlighting-57 micron resolution (10xmm)

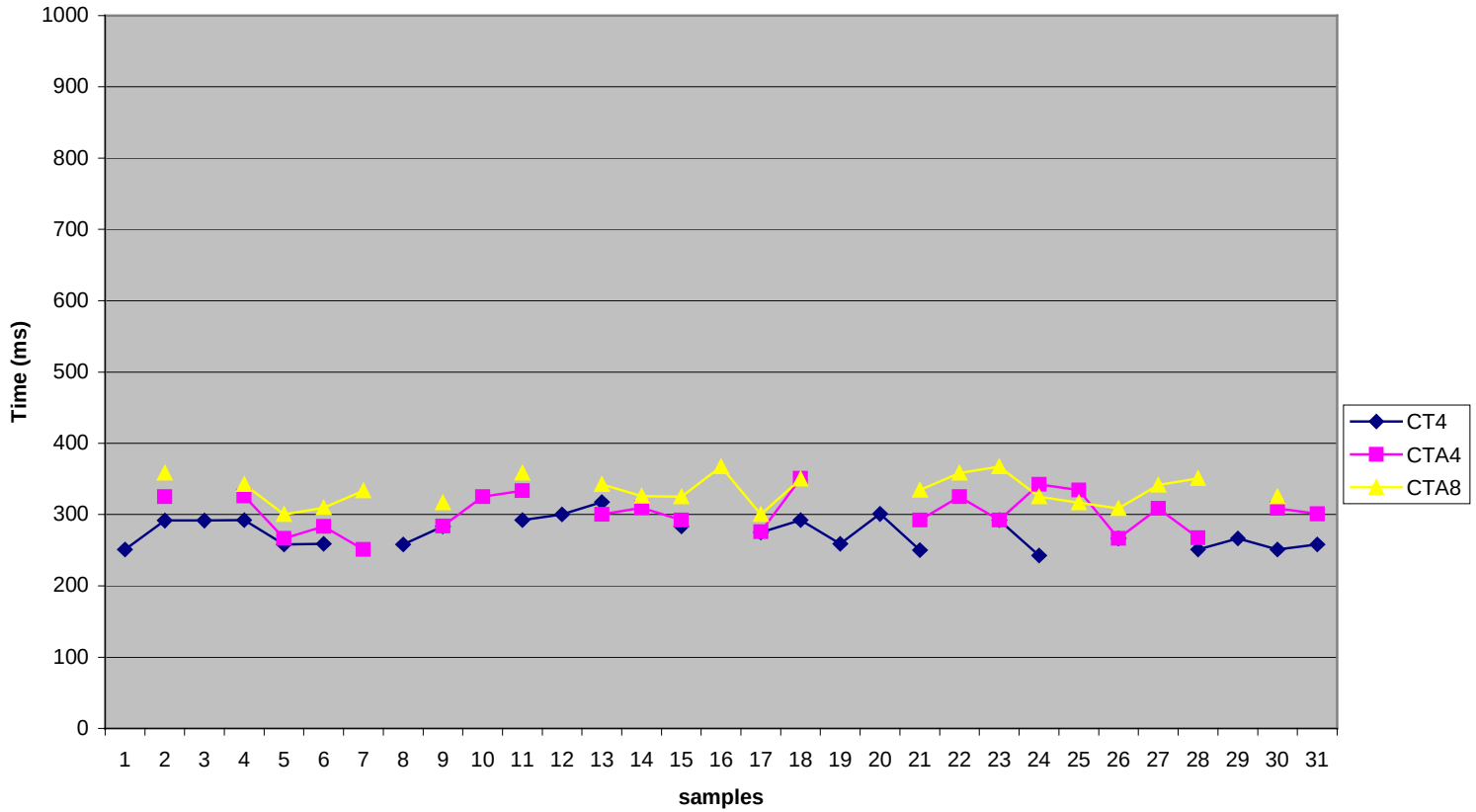

Figure 6.18: Analysis time of 100 Kbytes images with crossover-frontlighting-57 micron resolution (ms)

Table 6.18: Length measurement results of images with crossover-frontlighting-57 micron resolution (10xmm)

THIN-4N-8 -->THINNING-4 NEIGHBORHOOD-Threshold 8
THIN-ADD-4N-11 -->THINNING-4 NEIGHBORHOOD-Threshold 11
THIN-ADD-8N-11 -->THINNING-8 NEIGHBORHOOD-Threshold 13

THIN-4N-8	
Mean	397.75
Standard E	1.525448
Median	396
Mode	393
Standard D	7.47314
Sample Va	55.84783
Kurtosis	2.042627
Skewness	1.462359
Range	30
Minimum	388
Maximum	418
Sum	9546
Count	24
Confidence	3.155626

THIN-ADD-4N-11	
Mean	394.8261
Standard E	1.444154
Median	393
Mode	392
Standard D	6.925921
Sample Va	47.96838
Kurtosis	0.882459
Skewness	0.971127
Range	28
Minimum	384
Maximum	412
Sum	9081
Count	23
Confidence	2.994996

THIN-ADD-8N-13	
Mean	393.3636
Standard E	1.26139
Median	392.5
Mode	391
Standard D	5.916446
Sample Va	35.00433
Kurtosis	0.648322
Skewness	0.41809
Range	25
Minimum	382
Maximum	407
Sum	8654
Count	22
Confidence	2.623205

Table 6.19: Analysis time of 100 Kbytes images with crossover-frontlighting-57 micron resolution (ms)

THIN-4N-8 -->THINNING-4 NEIGHBORHOOD-Threshold 8
THIN-ADD-4N-11 -->THINNING-4 NEIGHBORHOOD-Threshold 11
THIN-ADD-8N-11 -->THINNING-8 NEIGHBORHOOD-Threshold 13

THIN-4N-8	
Mean	274.375
Standard E	4.238288
Median	270.8333
Mode	292.5
Standard D	20.76329
Sample Va	431.1141
Kurtosis	-1.119211
Skewness	0.237397
Range	75
Minimum	242.5
Maximum	317.5
Sum	6585
Count	24
Confidence	8.767556

THIN-ADD-4N-11	
Mean	302.6449
Standard E	5.667135
Median	300.8333
Mode	325
Standard D	27.17862
Sample Va	738.6775
Kurtosis	-0.86024
Skewness	-0.073206
Range	100
Minimum	250.8333
Maximum	350.8333
Sum	6960.833
Count	23
Confidence	11.75293

THIN-ADD-8N-13	
Mean	334.3939
Standard E	4.476631
Median	333.75
Mode	358.3333
Standard D	20.99726
Sample Va	440.885
Kurtosis	-1.060185
Skewness	-0.033736
Range	67.5
Minimum	300
Maximum	367.5
Sum	7356.667
Count	22
Confidence	9.309666

satisfactory results. Frontlighting could not repeat the superior results of without fiber crossover applications.

Finally, one set of data was collected for 106-micron resolution-frontlighting images. However, results showed that error free measurements could not be obtained for any algorithm in this resolution.

6.3. HVI AND AFIS

A total of ten mean length measurements were collected from two sets of HVI data as seen in Table 6.20. Average mean length was found to be 34.925 mm, 3.175 mm lower than the given cut length. The confidence interval was calculated as 0.65 mm, higher than our requirement. These numbers are expected to be much worse for SFC measurements, since SFC measurement is the weakest point of HVI. On the other hand, it should be remembered that cotton most likely produces better results, since these fibers are straighter. Uniformity ratio was found to be 100 implying all the fibers were the same length. However, this number must be an adjusted value since even the mean length measurement showed a range of 3.05 mm.

Table 6.20: HVI Length Measurement Results

Rep	I			II		
	ML(mm)	UHML(mm)	Uniformity	ML(mm)	UHML(mm)	Uniformity
1	35.56	35.56	100	35.31	35.31	100
2	34.04	34.04	100	36.58	36.58	100
3	34.80	34.80	100	33.53	33.53	100
4	35.31	35.31	100	35.56	35.56	100
5	34.04	34.04	100	34.54	34.54	100
Mean	34.80	34.80	100	35.05	35.05	100
SD	0.70	0.70	0	1.14	1.14	0

Table 6.21 shows AFIS length measurement results. Average mean length was found to be 34.04 mm, lower than HVI. 2.5% span length was found to be 42.16 mm

implying longer single fiber length measurements. SFC(n) was found to be 0.5 meaning only fifteen out of 3000 fibers were measured shorter than 12.7 mm. Arguably, these numbers show the ability of AFIS to measure fiber length, since AFIS was designed specifically for cotton length measurement. It is expected to give significantly more accurate and precise results for cotton. On the other hand, these numbers also show the need for better measurement techniques.

Table 6.21: AFIS Length Measurement Results

Rep	ML(w)	%CV	SFC(w)	UQL(w)	ML(n)	%CV	SFC(n)	5%(n)	2.5%(n)	D(μ)
1	33.53	18.8	0.1	37.08	32.00	21.1	0.3	39.88	41.66	11.7
2	34.29	18.2	0.1	37.59	32.77	21.0	0.6	40.64	42.42	11.0
3	34.04	18.8	0.2	37.59	32.51	22.0	0.7	40.89	42.67	11.0
Mean	34.04	18.6	0.1	37.34	32.51	21.4	0.5	40.39	42.16	11.2
SD	0.38	0.30	0.1	0.35	0.39	0.60	0.2	0.52	0.52	0.4
%CV	1.1	1.9	43.3	0.80	1.2	2.6	39.0	1.3	1.3	3.6

6.4. SUMMARY

Each of these systems measured the mean fiber length significantly different than the others. On the other hand, each system resulted in a confidence interval relatively small compared to the differences in mean length. There are consistent error sources for each system and HVI and AFIS error sources have been discussed. Hand-measurement tends to measure the mean length shorter than the actual length. Since the fiber length is measured between two catching points of a pair of tweezers, any miscatch results in a negative bias, unless stretching occurs. Figure 6.19 shows normal probability distribution functions of the measurement methods.

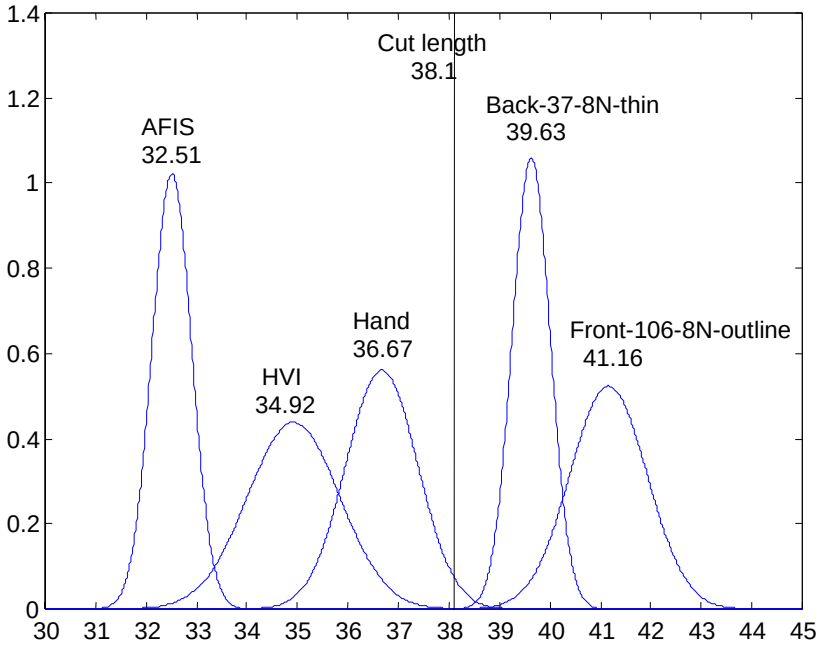

Figure 6.19: Normal probability distribution functions of the measurement methods

It is believed that the given cut length is the best representation of the real mean length. Variation is very low for man-made fibers. With our system, the lowest confidence interval was found to be only +/-0.141 mm, and it is expected to be lower for high-resolution images. The highest hand-measurement value was 38 mm which is an evidence that the given cut length is correct since all fibers should be cut at approximately the same length, and it should be impossible to measure by hand a length greater than the fiber length, without stretching. It is assumed that the given cut length is the true representation of the fiber length for the following discussions.

All image processing algorithms measured the fiber length as being greater than the given cut length with the exception of 185 micron resolution-thinning-adding algorithms. In another words, the image processing algorithms produced inaccurately longer length measurements. There are several reasons for this, which are discussed below.

The first reason for the positive bias in the length data is random noise because of poor performance of the camera. As we mentioned before, in a completely black image, randomly distributed pixels were detected with a gray level of between '0' and '10', ideally, all pixels should produce '0' gray level. Any positive bias pixel higher than the threshold value creates a white point on the image representing a fiber. Most of the best threshold values for the outline algorithm were found to be less than '10' gray level, therefore, many white pixels caused by noise should be expected in the images. Figure 6.20 shows a preprocessed backlighting-57 micron resolution and threshold 7 image. There are two fibers on the image crossing over that all other white pixels are noise. Logically, some of this noise is connected to fibers. Any noise connected to the fiber causes longer fiber length measurement. As we discussed in preprocessing in section 4.4, higher threshold values eliminate many noises from the images. Appendix A proves that higher threshold value results in lower length measurement because of noise elimination.

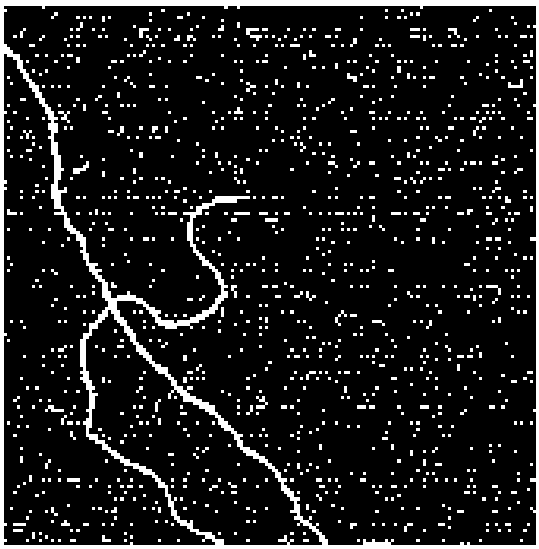

Figure 6.20: Random noise on the images

The second reason for the positive bias in fiber length measurement is lighting conditions. The maximum gray level in our camera is 255. To escape from saturation,

the brightest point on the images was held to about 230 gray levels for backlighting images. Uneven lighting created gradually decreasing contrast so that the lowest gray level value dropped to about 190 in an empty image as in Figure 2.16. The polyester fiber diameter is about 11 micron, which is about one-fifth the pixel with at 57-micron resolution. Considering the case of without crossover-backlighting-57 micron resolution, for a fiber to be resolved by one pixel, it should have created at least a 38 gray levels (190 gray levels x 1/5 pixel per fiber width = 38 gray levels) difference from a neighboring empty pixel in the lowest contrast area. In the worst condition, when a fiber is split between two pixels, it should create an 19 gray level difference from a neighboring empty pixel and a maximum width of two-pixels. However, the best threshold value was found to be only 7 and a combination of lighting and poor camera performance created more than two-pixel width in some cases.

Especially in low resolution conditions for frontlighting, light intensity was increased in order to detect fibers, the diameters of which, were relatively very small compared to pixel size. This resulted in most of the fiber diameter being represented as a few pixels in width due to glinting highlights as in Figure 4.5. Also, foreign particles in the air become a factor since the dust was out of focus, it appeared larger than reality as in Figure 4.6. Increasing light intensity made these particles much bigger in size on the images and sometimes they were connected to the fiber images. Conclusively, these effects created longer fiber length measurements in the same manner as added noise discussed above; that is, they result in a positive bias in the fiber length measurements.

Finally, digitization caused longer fiber length measurements. Discrete representation of continuous lines tend to be measured longer than their real lengths with

chain code algorithm unless the pixel size is large relative to curvature detail. Studying this effect, Dorst and Smeulders [29] consistently found a positive bias of 6.6% in arc length measurements. These researchers presented the following formula to correct for this effect in the case of an arc where n_e is the number of even and n_o is the number of odd connections:

$$L = 0.948n_e + 1.343n_o \qquad \textbf{Equation 6.1}$$

In the case of our measurements, we used the following formula:

$$L = 1.00n_e + 1.41n_o \qquad \textbf{Equation 6.2}$$

Proffitt and Rosen [84] found 5.3% positive bias in the measurement of straight lines with chain code compared to the real length. In Figure 6.21, the real length of the given circle is 28.26-unit length. If the chain code algorithm is applied, the measured length is found to be 31.31-unit length. Our applications fit the Dorst and Smeulders [29] criteria in that the fibers deviate from straight lines because of an imposed 2-D shape (crimp) which is large relative to the pixel size.

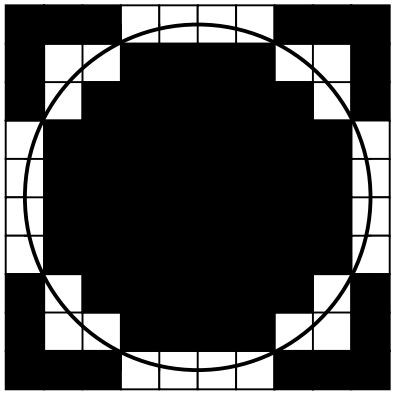

Figure 6.21: Measurement of a circle with discrete units

The outline algorithm contains all these error sources so that the length measurement results were found to be 6 to 27% higher than the given cut length. The thinning algorithm tends to minimize error sources caused by poor camera performance and lighting conditions while retaining the discretization error. Length measurement results with the thinning algorithm were found to be consistently higher than the given cut length: between 3 to 5% for 37-micron and 57-micron resolutions. A correction factor of 5.3 to 6.6% for discretization error will cause the length measurement results to be slightly shorter than the given cut length. This negative bias might attributable to over-smoothing characteristics of the thinning algorithm. Another explanation would be that the true fiber length was actually shorter than the given cut length due to viscoelastic effects. Figure 6.22 shows the new fiber length distribution (using the Dorst and Smeulders coefficients for Back-37 micron-8N-thinning and Front-106 micron-8N outline as compared to the other distributions from Figure 6.19).

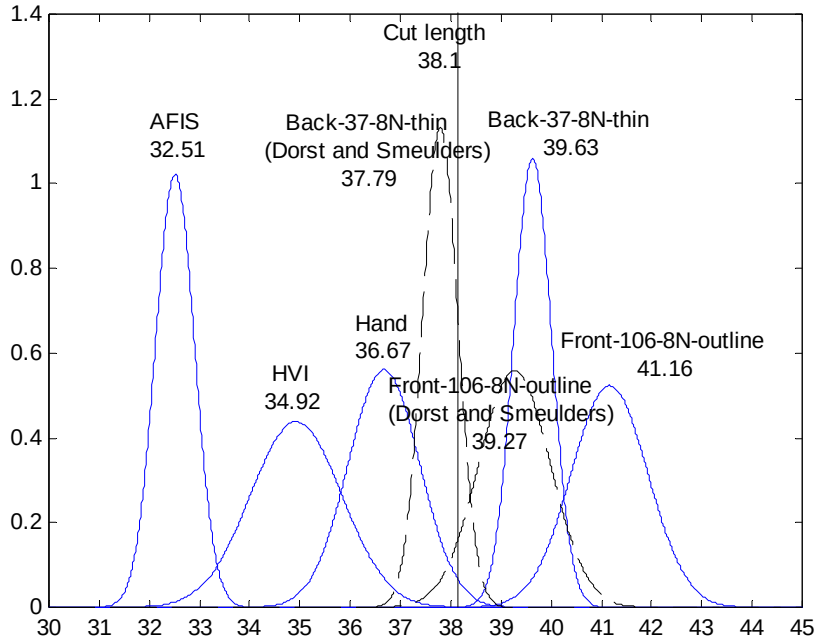

Figure 6.22: Dorst and Smeulders' coefficient applied normal distribution functions

The adding algorithm sometimes causes negative bias with low resolution images. If the closest points of crimp are within a two-pixel distance, the dilation algorithm connects these points creating a shortcut and causing shorter fiber length measurements as in Figure 6.22. Sometimes added noise, dust, or glare causes 2 discontinuous points on a fiber image to appear to be within the two-pixel distance and the errant connection is made. This connection is resulted in a shorter length measurement in the case of length measurements by thinning algorithm. The average fiber length from thinning combined with adding algorithms applied to 185-micron resolution images was found to be shorter than the given cut length because of this inaccuracy.

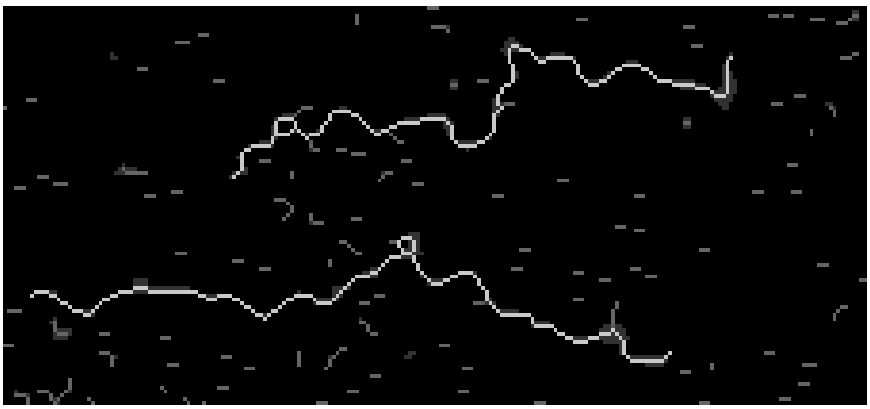

Figure 6.23: 185-micron resolution, thinning-adding algorithm applied image.